MULTIPLE BEAM INTERVAL SCANNER

SCIENTIFIC REPORT SR485-1

SEPTEMBER 11,1963

CONTRACT NO. AF19(604)-7385
PROJECT 4600
TASK 460007

SYLVANIA ELECTRONIC SYSTEMS
Government Systems Management
for GENERAL TELEPHONE & ELECTRONICS

Requests for additional copies
by Agencies of the Department of
Defense, their contractors, and
other government agencies should
be directed to the:

DEFENSE DOCUMENTATION CENTER (DDC)
CAMERON STATION
ALEXANDRIA, VIRGINIA

All other persons and organizations
should apply to the:

UNITED STATES DEPARTMENT OF COMMERCE
OFFICE OF TECHNICAL SERVICES
WASHINGTON 25, D. C.

AFCRL-63-535

MULTIPLE BEAM INTERVAL SCANNER

Francis J. LaRussa

SYLVANIA ELECTRONIC SYSTEMS – EAST
SYLVANIA ELECTRONIC SYSTEMS
A Division of Sylvania Electric Products Inc.
100 First Ave., Waltham 54, Mass.

Contract No. AF19(604) – 7385
Project 4600
Task 460007

Scientific Report SR485-1

September 11, 1963

Prepared
for

AIR FORCE CAMBRIDGE RESEARCH LABORATORIES
OFFICE OF AEROSPACE RESEARCH
UNITED STATES AIR FORCE
BEDFORD, MASSACHUSETTS

ACKNOWLEDGMENT

The author wishes to acknowledge with gratitude the encouragements and suggestions extended throughout the course of this investigation by Walter Rotman and Philipp Blacksmith, Jr. of the Air Force Cambridge Research Laboratories.

TECHNICAL PERSONNEL

R. RUBIN	DR. L. LECHTRECK
L. BLAISDELL	Dr. D. BRICK
F. LA RUSSA	R. SULLIVAN

CONTENTS

ILLUSTRATIONS

ILLUSTRATIONS (Continued)

SUMMARY

An experimental program to demonstrate the feasibility of eombining a eoaxial probe monopulse organ pipe seanner with a wide angle two-dimensional "eonstrained" lens is deseribed in this report. The antenna system whieh was built and tested to prove this feasibility operates in the 5250 Mes to 5750 Mes range. It produees a half power beamwidth of 2 degrees in azimuth by 4 degrees in elevation whieh ean be seanned ±36 degrees from broadside in the azimuth plane. Variations of the measured radiation eharaeteristics with frequency and angle of sean are summarized in graphieal form. Design data and typieal monopulse sum and differenee patterns are presented. The test results show that sueh a lens-seanner antenna system is praeticable for wide angle scanning in one plane.

SECTION 1

PURPOSE OF MUBIS PROGRAM

MUBIS is an acronym which stands for Multiple Beam Interval Scanner. The MUBIS program at Sylvania was carried on under contract with Air Force Cambridge Research Laboratory and represented an extension of the work done there by Mr. Walter Rotman and Mr. Richard Turner on a wide angle microwave lens. The purpose of the program was to demonstrate the feasibility of scanning a monopulse beam over a wide angular sector by combining the constrained lens with a coaxial monopulse organ pipe scanner developed by Sylvania. A feasibility test model was designed and constructed and experimental data taken which adequately proved the practicability of this technique.

SECTION 2

THE MUBIS CONCEPT

2.1 THE CONSTRAINED LENS

In the MUBIS concept, separate beams are generated by each scanner. They may then be independently scanned simultaneously using a single line source fed by a two-dimensional constrained lens. A brief qualitative description of the lens design is given here in the interest of continuity. A detailed explanation of the design of this lens may be found in Reference 1.

The MUBIS lens, Figure 2-1, is a two-dimensional constrained lens with a straight front surface Σ_2 suitable for use with a line source. It has three points of perfect focus: one "on axis", point G, and two "off axis" points F_1 and F_2, which are symmetrically located about the central axis. A TEM mode parallel plate transmission line connects the focal arc with the rear lens surface Σ_1. Energy appearing at this rear surface is coupled out by means of coaxial probes. The lens elements are the coaxial cables which connect these probes to a straight line of radiators which form the line source. These cables are the "constraining" elements of the lens, since energy impinging on a particular point on the surface Σ_1 is "constrained" to follow the same path length, through a particular cable to surface Σ_2 regardless of the angle at which the radiation strikes the surface. In this respect, the "constrained" lens differs from the usual dielectric lens in which Snell's law applies and the path length through the lens is a function of the angle of incidence.

Sources of radiation located at the three focal points of the lens produce fixed collimated beams in space with the direction of each beam determined by the position of the source which generates it. Beam motion can be produced by moving the source along an arc, thereby changing the angle that it makes with the central axis. However, since the lens has only three points of perfect focus, the motion of the radiating sources results in defocussed beams at all points along the focal arc except those three. It has been shown in Reference 1 that these aberrations can be minimized by proper selection of the "on axis" focal point G.

---

1. (AFCRL 62-18) "Wide-Angle Microwave Lens for Line Source Applications". W. Rotman and R.F. Turner, AFCRL, Office of Aerospace Research, USAF, Bedford, Mass., January 1962.

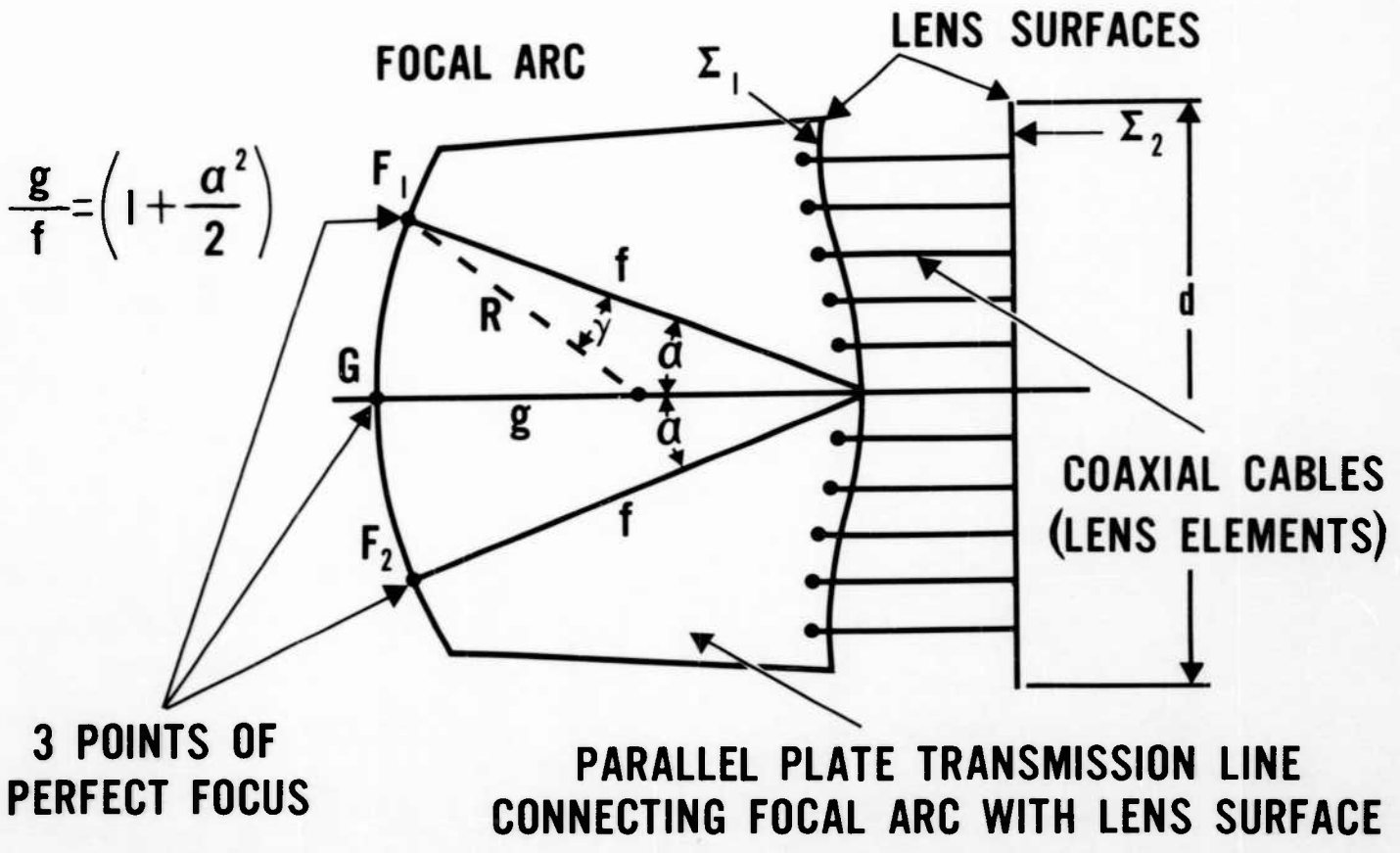

Figure 2-1. Two-dimensional Constrained Lens

The "on axis" focal distance g as measured from the origin of the lens surface Σ_1, which results in minimum "off focus" aberrations, can be defined in the following relation:

$$g' = \frac{g}{f} = (1 + \frac{\alpha^2}{2})$$

where α = the angle that the "off axis" focal line makes with the axis of the lens at origin of the rear surface Σ_1 f = the "off axis" focal distance as measured from the origin of the lens surface Σ_1. The focal arc determined by these three points F_1, F_2 and G minimizes the "off focus" aberrations over the widest excursions of the radiating sources from the focal points. Calculations indicate that in a lens having an angle α of 30 degrees and an $\frac{f}{d}$ ratio of 0.833, the maximum path length error for a scan angle of ±35 degrees is only about 0.0006 f or in terms of the aperture dimension d, only about 0.0005 d. This means that for an aperture of 100 λ the maximum theoretical phase error to be expected when scanning ±35 degrees is 0.05 λ.

2.2 SCANNING TECHNIQUES

Since the lens focuses well over a wide "off-focus" range, scanning can be accomplished by moving a radiating source back and forth along the focal arc. By placing a number of independent sources along this arc and moving them back and forth, each along a sector of the focal arc, a number of beams can be produced each of which scans a sector proportional to its excursion along the focal arc. (See Figure 2-2).

A more desirable method of scanning, which was studied in this program by Sylvania, consists of replacing the moving sources of radiation by a complete focal arc of fixed sources and sequentially energizing one or a group of these by means of an organ pipe scanner. Further, when these sources are coaxial probes placed along the focal arc, the scanning can be accomplished by a coaxial probe monopulse organ-pipe scanner, the concept of which was originated by R. Rubin and D. Ferrante under contract DA36-039-AMC00140(E). (See Figure 2-3.) This last method has greater design flexibility over the conventional waveguide organ pipe scanner and reduces the magnitude of the "cogging errors" because the closer positioning of the probes more nearly approaches a continuous distribution regardless of the scanner horn position. A more detailed discussion of these points is given in Section 8.

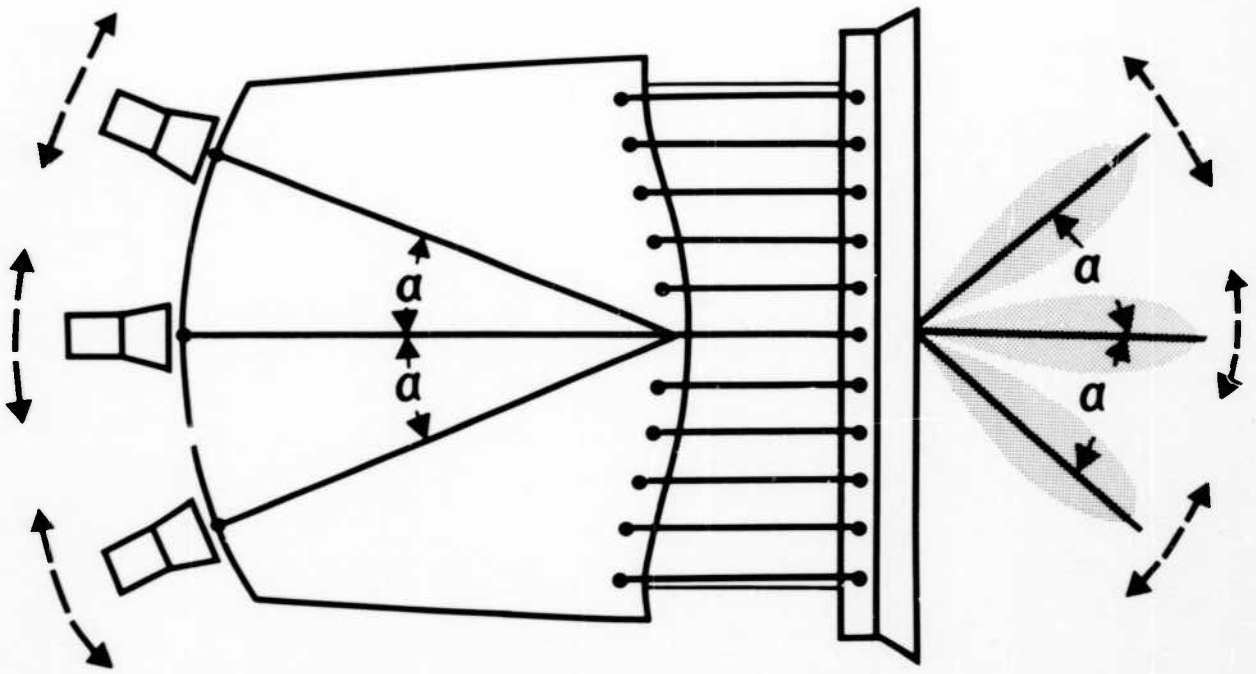

S188-266

Figure 2-2. Two Dimensional Lens with Movable Sources of Radiation

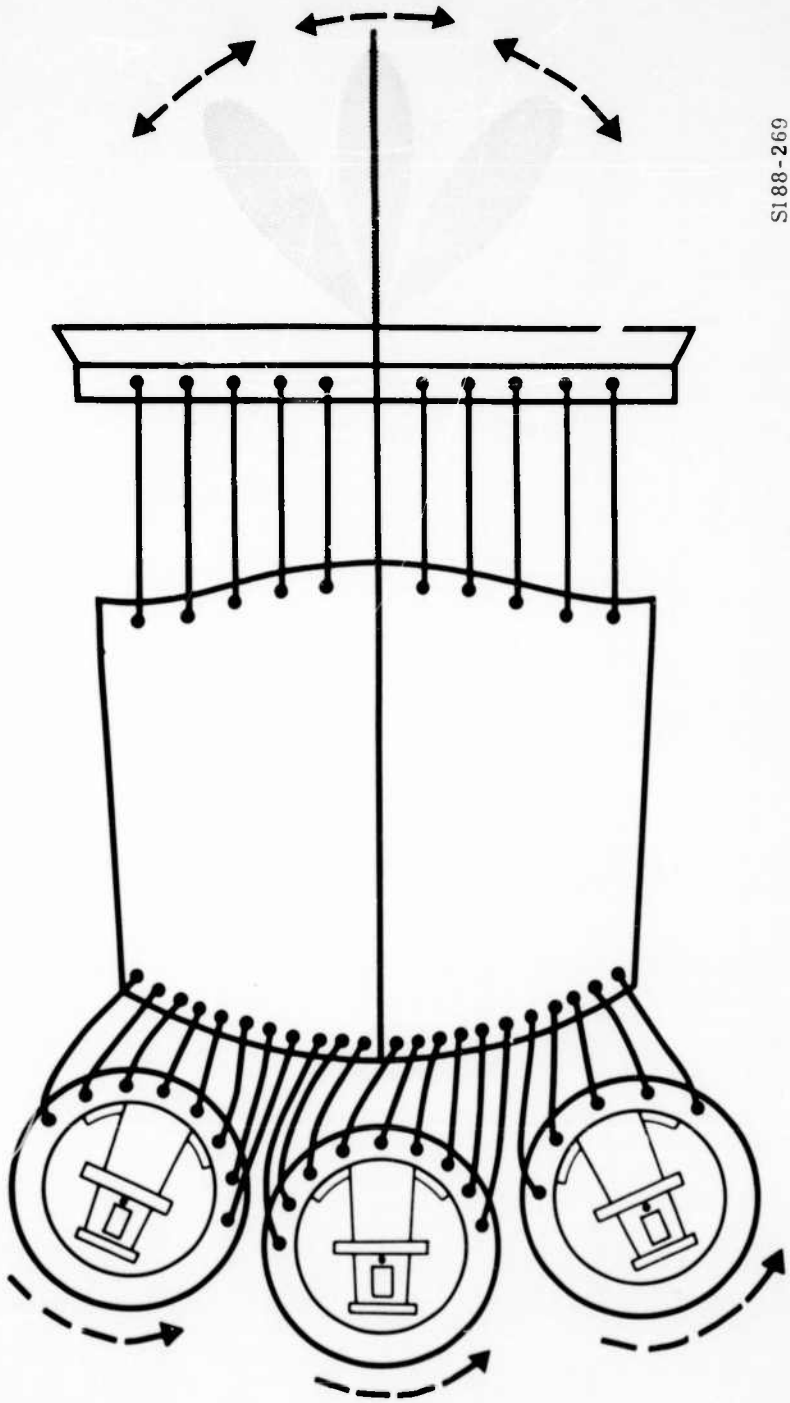

S188-269

Figure 2-3. Two Dimensional Lens with Coaxial Organ Pipe Scanner

SECTION 3

SYSTEM CONSIDERATIONS

3.1 DESIGN OBJECTIVES

MUBIS had the following system design objectives:

1)	Frequency	C-Band 5250 MCS to 5750 MCS
2)	Beamwidth	2° in azimuth by 4° in elevation at the -3 db points
3)	Side Lobes	Azimuth -25 db or greater
4)	Polarization	Vertical
5)	Azimuth Scan	±36° amplitude comparison monopulse
6)	Beam Registry	±0.5°

In view of the foregoing specifications an antenna system consisting of the following components was designed:

1) A parallel plate transmission line having a probe fed focal arc and a probe fed lens surface Σ_1.

2) A probe fed line source which comprises the front lens surface Σ_2.

3) The lens elements which consist of coaxial cables each cut to a specific length connecting the rear lens surface Σ_1 to the line source (lens surface Σ_2).

4) A coaxial probe monopulse organ pipe scanner.

5) Input cable assemblies connecting the focal arc to the organ pipe scanner.

6) Coaxial probes for the organ pipe scanner, the focal arc, the lens surface Σ_1, and the line source Σ_2.

7) A parabolic cylinder reflector.

8) A support structure.

The main effort was centered about the design of the lens and the scanner. In this report, the design philosophy and the problems associated in the development of these components is discussed in detail. The other items which were considered routine are mentioned briefly for the sake of completeness and are discussed only to the extent that they affected the system design.

3.2 PRELIMINARY SYSTEM DESIGN

The system requirement of a 2-degree half power beamwidth was assumed to apply to the broadside (center of scan) position. At the extreme angles of scan ±36 degrees from broadside the beamwidth broadens to 2.5 degrees due to the reduction of the effective aperture which occurs when scanning. Since the antenna was a feasibility test model it was decided to design a 2-degree beamwidth for the broadside condition and to accept whatever beam spreading might occur due to scanning.

The side lobe requirements of greater than 25 db below the peak of the main lobe indicated that the aperture width should be designed assuming a $\cos^2$ distribution. It was anticipated that an aperture distribution approaching a $\cos^2$ function could be obtained by properly designing the monopulse scanner horn. This problem is discussed at length in Section 8.

Assuming a $\cos^2$ distribution the aperture required for a 2-degree beamwidth is approximately 40λ. At the center frequency of 5500 MCS, this results in an aperture width of 86 inches. This aperture dimension is the basis of the lens dimensions.

The lens design was partially fixed by the desirability expressed by AFCRL personnel that the lens have the two "off axis" focal points placed at angles of ±30 degrees from the axis and that the "on axis" focal length g be optimized so that the relationship $g = \frac{g}{f} = (1 + \frac{\alpha^2}{2})$ applied. The only parameter not specified was the focal length of the lens.

In general the selection of a the focal length is governed by the magnitude of the allowable "off focus" aberrations. Curves which relate path length error through the lens as a function of the normalized aperture N′ for a number of different scan angles and different lens designs are contained in Reference 1. These curves indicate that a value of $N' = 0.60$ would keep the path length errors small over a wide scan angle and yet maintain a reasonable $\frac{f}{d}$ ratio ($\frac{f}{d} = \frac{1}{2N'}$). Under these conditions ($N' = 0.60$) the calculated maximum path length error for a scanning capability of ±35 degrees is approximately 0.0006 f. For the 40λ aperture this results in a calculated path length error of 0.02λ maximum for the lens system being designed.

---

1. (AFCRL 62-18) "Wide-Angle Microwave Lens for Line Source Applications". W. Rotman and R.F. Turner, AFCRL, Office of Aerospace Research, USAF, Bedford, Mass., January 1962.

In summary therefore, the antenna-lens system had the following design parameters:

aperture = 40λ = 86"

$\frac{f}{d}$ ratio = 0.833 (i.e., N' = 0.60)

off axis focal length $f = 0.833d = 33.32\lambda$ = 71.63"

on axis focal length $g = 1.137f = 37.88\lambda$ = 81.44"

For collimation in the vertical plane a parabolic cylinder was used. Assuming a cos distribution in the vertical plane, a 4 degree half power beamwidth resulted in an aperture of about 17λ or about 36 inches. The additional requirement that the model be adaptable to height finding studies necessitated the inclusion of a three-position line source holder in the elevation plane to displace the beam from +2 degrees to +18 degrees in 8 degree increments. To minimize the defocussing effects in the elevation plane the vertical axis of the reflector was tilted back 10 degrees. This raised the focussed beam 10 degrees above the horizontal and allowed only two beamwidths of defocussing for each of the remaining two positions (that is, one beam at 2 degrees and the other beam at 18 degrees symmetrically located the feeds two beamwidths either side of focus).

SECTION 4

SYSTEM SUPPORT STRUCTURE, LINE SOURCE, AND REFLECTOR

The support structure and design of the line source reflector of the system represented a very small portion of the development effort. Furthermore, since their design was straightforward, they are discussed only briefly.

4.1 SUPPORT STRUCTURE

The beamwidth and scan angle requirements necessary to adequately demonstrate function resulted in rather larger structures.

The parallel plate transmission line dimensions of 7 feet by 8 feet together with dimensions of 7 feet for the line source and 11 feet by 3 feet for the parabolic cylinder reflector indicated that a rather substantial support structure would be required. It was also desirable to have the components rigid so that any mechanical problems such as sag and vibration would be kept at a minimum. Therefore the three fore-mentioned major components were integrated into a structure capable of adequately supporting them. Figure 4-1 shows the antenna test model and its support structure.

4.2 LINE SOURCE

The line source forms the straight front surface Σ_2 of the lens. It consists of an array of probes feeding a TEM parallel plate transmission line whose plates are flared to form a radiating aperture. The flare is such that the vertical beam characteristics measured on a small test section at 5500 MCS were as follows:

-3 db beam width 23°

-10 db beam width 42°

beam width to first null 51°

Since the reflector subtended angle of 45 degrees at its focus, the elevation radiation pattern of the line source appeared to be adequate in providing a satisfactory illumination of the reflector. The probes used in the line source were of the same design as those used in the parallel plate transmission line. Their design is treated in another section of this report. However, their impedance match was checked on the small test section shown in Figure 4-2.

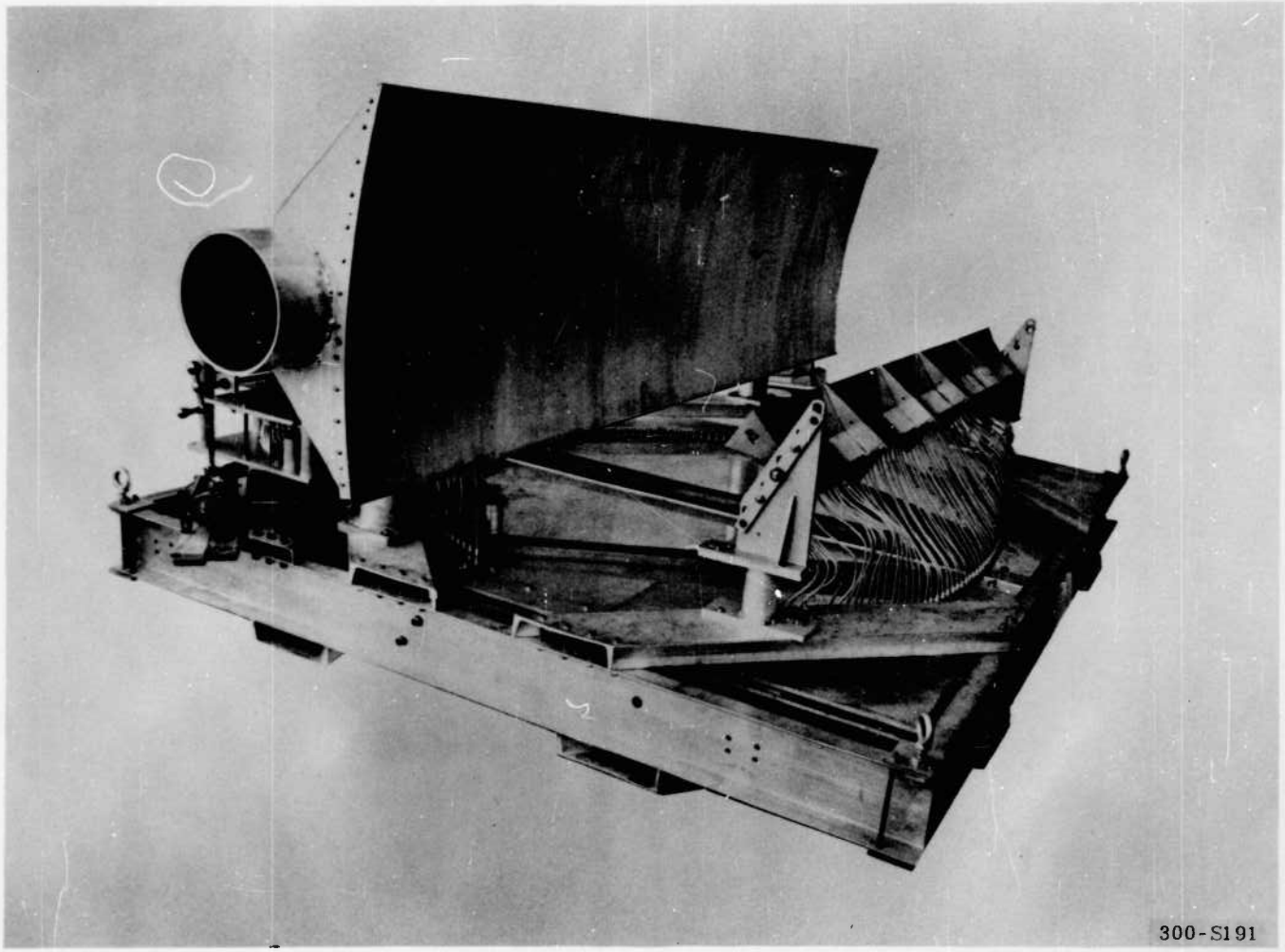

Figure 4-1. Antenna Test Model

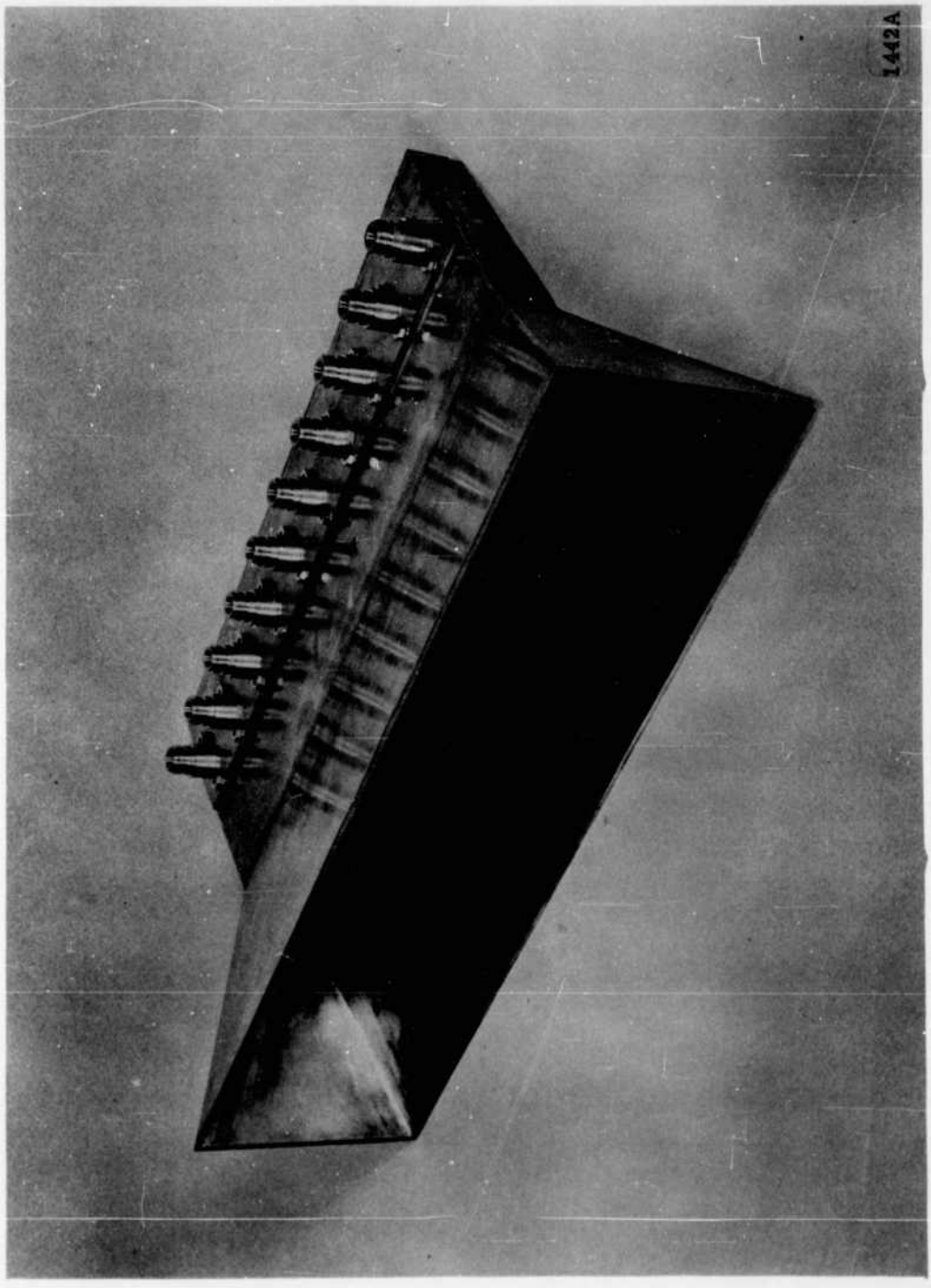

Figure 4-2. Test Section of Line Source

4.3 REFLECTOR

Since the lens output results in a line source, a half parabolic cylinder was used as the reflector. The coaxial cables and the line source would constitute a severe aperture blocking problem if a full parabolic section were used. By using a half section, the cable assemblies are below the aperture and the blocking problem is considerably reduced. The half parabolic section which provided beam collimation in the elevation plane had a focal length of 3 feet. The aperture height was 3 feet which produces a -3 db beamwidth of 4 degrees assuming a cos aperture distribution.

The length of the reflector was 11 feet, which is an extension of 23 inches beyond each end of the line source. This additional length on each end was necessary due to the original requirement for scanning the beam ±30 degrees from broadside. After the reflector had been built, the scanning limits were changed to ±36 degrees. Since the additional length required would have been only 3 inches on each side, the reflector length was not changed.

A unique feature of the reflector was the mechanical design which used a 12-inch diameter aluminum pipe to provide the rigidity required without the use of an expensive back up structure. A number of ribs were welded to the outside of the pipe which provided the stiffness along the axis of the cylinder. The parabolic contour was obtained by attaching precisely machined rib sections to the welded ribs. These sections were accurately positioned, doweled and bolted in place, and a thin aluminum sheet was attached to them. Inspection of the completed reflector indicated that the surface was everywhere within ±0.015 inch' of the true contour.

SECTION 5

PARALLEL PLATE TRANSMISSION LINE AND LENS SURFACE Σ_1

5.1 SOURCE TILT

In the MUBIS lens system energy is conducted from the focal arc to the rear lens surface Σ_1 by means of a parallel plate transmission line operating in the TEM mode. The rear lens surface Σ_1 was calculated with the data supplied in Ref. 1 as indicated in the section on Systems Considerations. The two "off axis" focal points were selected so that $\alpha = \pm 30$ degrees, and the aperture was selected such that $N' = 0.60$. The "on axis" focal distance g was optimized in accordance with the relation $g' = \frac{g}{f} = 1 + \frac{\alpha^2}{2}$. However, the focal arc defined by these three focal points has a center which is not coincident with the origin of the rear lens suface Σ_1. This occurs because of the optimization of the "on axis" focal point. In this case, ($\alpha = \pm 30$ degrees) $g = 1.137f$ where f is the focal distance. The focal arc is merely the arc drawn through these three points. Therefore, since the center of this arc is not coincident with the origin of the rear lens surface Σ_1, directive sources of radiation placed along this focal arc have to be tilted through an angle γ in order to properly illuminate the lens. (See Figure 2-1.) Furthermore this tilt angle varies as a function of scan angle. This variation is shown in Figure 5-1. Note that if $R = a$ then $\gamma = \theta$, i.e., tilt angle equals scan angle.

When designing the input cable assemblies to be used in connecting the coaxial organ pipe scanner probes to the lens input probes along the focal arc, this tilt angle γ must be taken into account. In the coaxial probe scanner more than one probe is excited simultaneously. In MUBIS ten or eleven probes are so excited. These must be phased to point the resultant primary illumination at 0 rather than at 0'. Instead of using equal length cables as is usually done with an organ pipe scanner, cables of increasing length are used in order to effect a delay and thereby tilt the beam by an angle γ from broadside. In the interests of making this system broad band the delay introduced at each probe position was a time delay which is not sensitive to frequency changes. This was accomplished by adding an incremental length Δ to each cable such that the path length from the origin of the lens surface Σ_1 through the parallel plate line to the point on the

---

1. (AFCRL 62-18) "Wide-Angle Microwave lens for Line Source Applications", W. Rotman and R.F. Turner, AFCRL, Office of Aerospace Research, USAF, Bedford, Mass., January 1962.

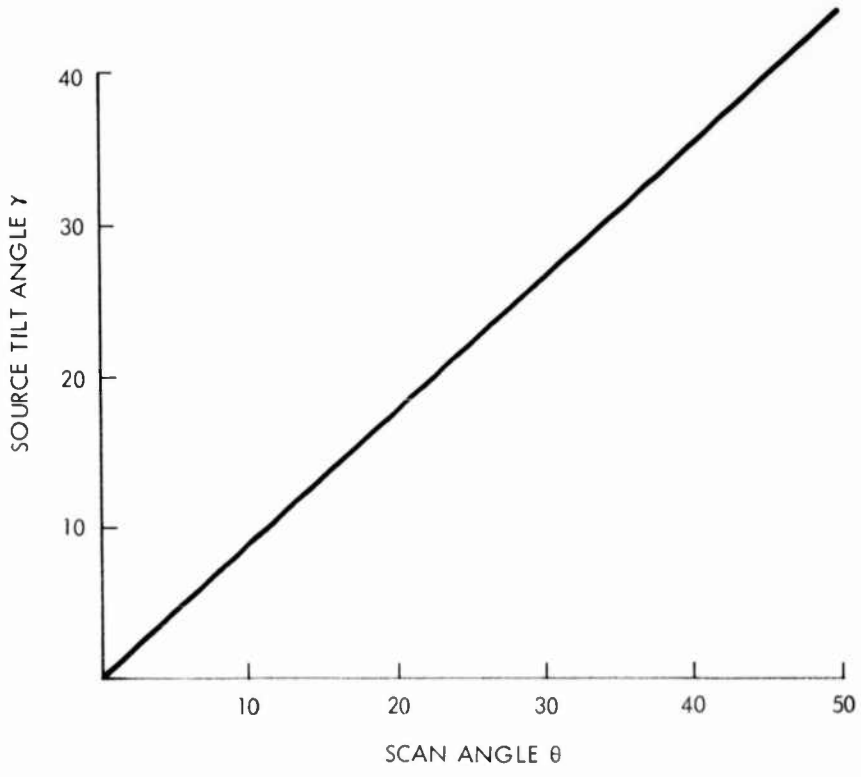

Figure 5-1. Variation of Source Tilt Angle with Scan Angle

focal arc and from the focal arc through the cable to the scanner was constant for each cable. This is the equivalent of determining the path length difference between the focal arc and an arc having a radius g' and the origin of the surface Σ_1 as its center. Figure 5-2 illustrates this procedure. Figure 5-3 shows a plot of this normalized (with respect to the focal length f, that is, $\Delta' = \frac{\Delta}{f}$) path length difference as a function of scan angle. This path length changes very rapidly at large scan angles. This fact almost demands that a path length type of delay be used if any reasonable system bandwidth is desired.

5.2 SHAPING FACTOR

The lens surface contour as indicated in the previous section is computed such that the path length for all rays radiating from a single point on the focal arc passing through the parallel plate region and through the lens cable elements to the equiphase surface is constant (neglecting the small differences in path length when radiating from the "off focus" positions). However, from Figure 5-4, it can be seen that the part of these path lengths in the parallel plate region is not constant for all rays emanating from a particular point on the focal arc. Since cylindrical spreading of the wave front occurs only in the parallel plate region, the attenuation due to "spreading" will differ for each ray. The "shaping factor" can therefore be defined as the variation in attenuation appearing across the aperture due to the variation in spreading loss in the parallel plate region. This variation in attenuation due to these path length differences becomes greater as the radiating point is moved out along the focal arc away from the central axis. At large angles of scan therefore appreciable amplitude asymmetries could occur in the lens aperture.

In order to determine the magnitude of these asymmetries, calculations were made of the spreading loss in the parallel plate region. Variations in attenuation caused by spreading, appearing at the aperture is shown in Figure 5-5 for several positions along the focal arc. Distance along the aperture is normalized to the focal length f.

As can be seen from this figure at extreme angles of scan, the total variation across the aperture is greater than 3 db. Cable length attenuation is neglected since the maximum output cable length variation is only 1.25" maximum over the aperture.

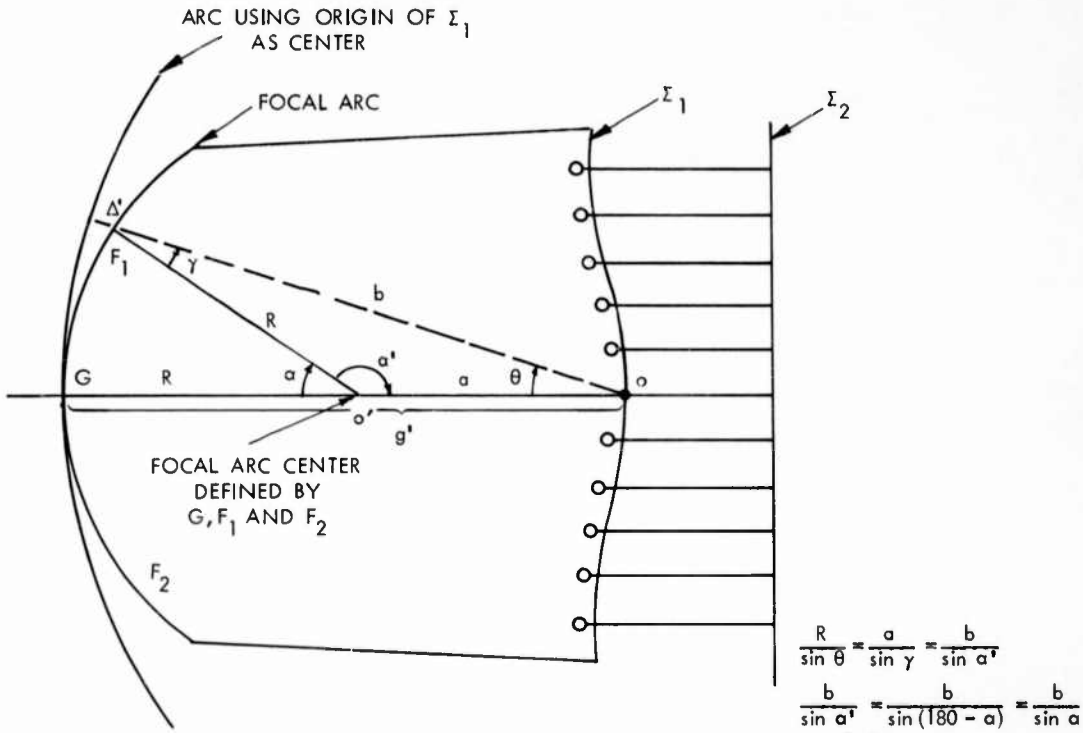

Figure 5-2. Procedure for Obtaining Input Cable Length Characteristics

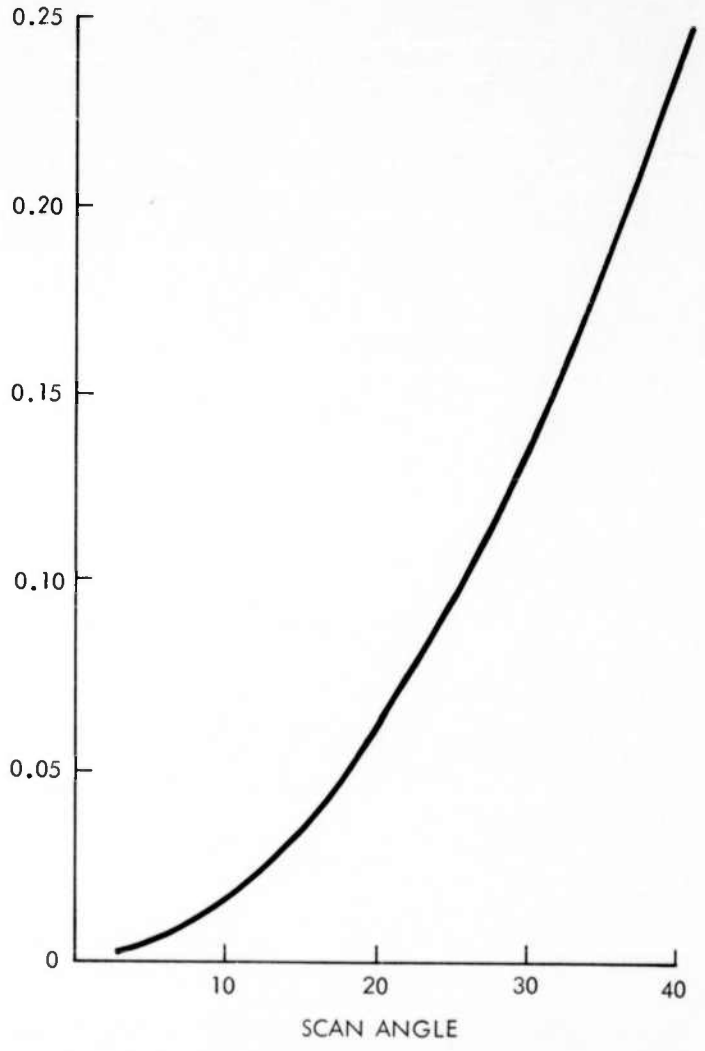

Figure 5-3. Input Cable Length Differences versus Scan Angle

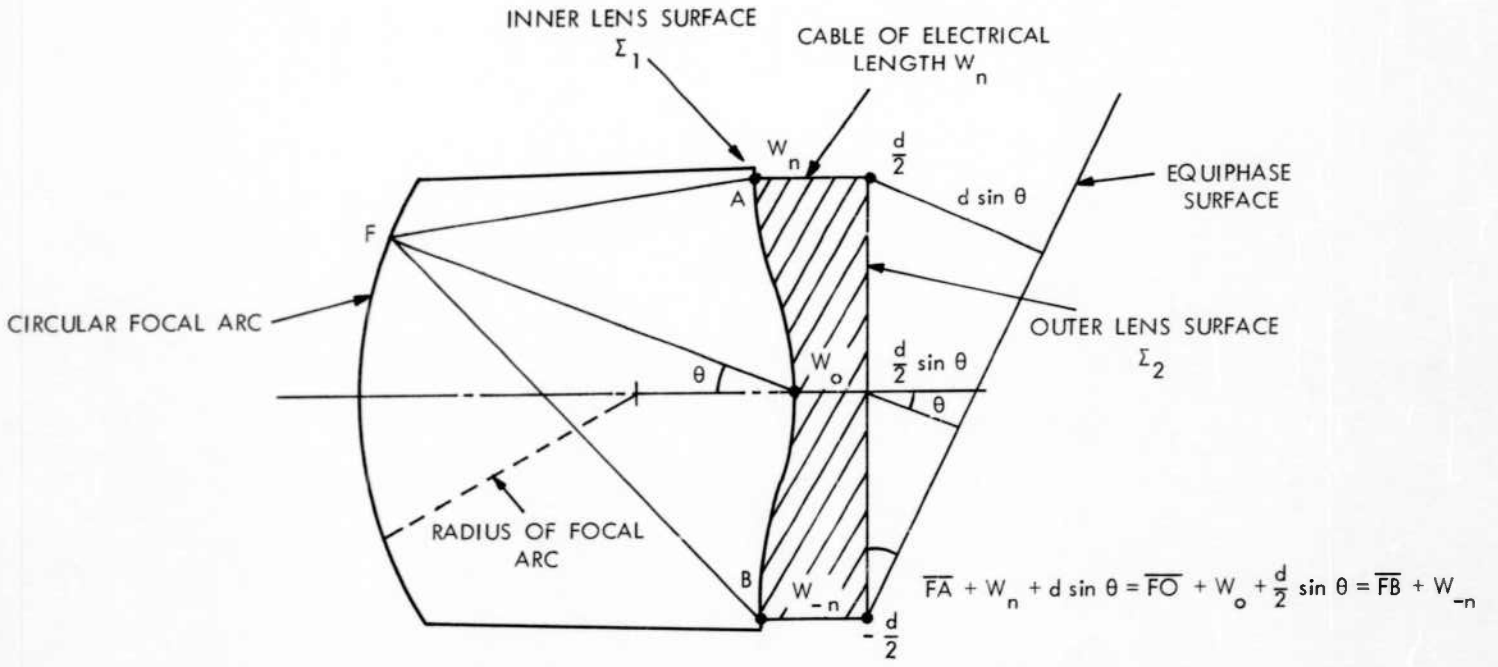

Figure 5-4. Procedure for Calculating Lens Parameters

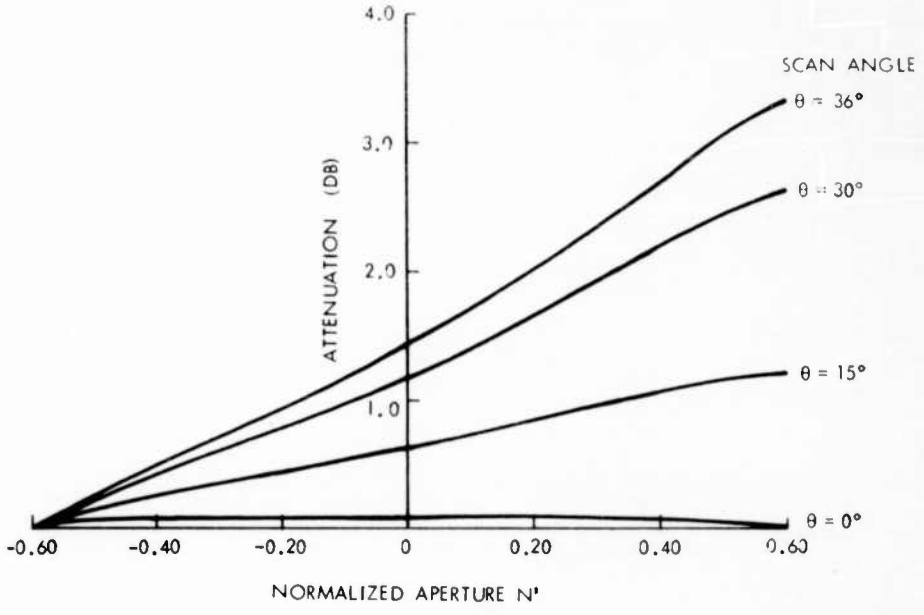

Figure 5-5. Attenuation Across Aperture Due to Cylindrical Spreading in the Parallel Plate Transmission Line

During the experimental part of the program, the effects of this "shaping factor" were not observed. Although asymmetrical far field difference patterns were observed at various points along the focal arc, they occurred randomly even at points near the central axis where the "shaping factor" would have **little**, if any, effect. Consequently it was felt that these asymmetries were attributable to other causes. They were of such magnitude so as to obscure the effects of the "shaping factor" and are discussed in Section 9.

The effect of this "shaping factor" on the resultant amplitude distribution was therefore calculated for both the sum and difference modes at the extreme scan angle of 36°. The normal amplitude distribution and the "shaped" distribution for both the sum mode and the difference mode are shown in Figures 5-6 and 5-7 respectively. It was felt that the effect of this perturbation on the far field sum pattern would be small. However, since its effect might be appreciable in difference patterns, an attempt was made to calculate the error or "boresight shift" that might be expected from the 1.6 db amplitude variation in the peaks of the difference distribution. Based on the assumption that the amplitude asymmetry in the aperture resulted in a similar amplitude asymmetry of the far field radiation patterns, a "boresight shift" of about 0.02° was calculated. This calculation was also based on the simplification assumed in Reference 2.

---

2. "Amplitude- and Phase-Sensing Monopulse System Parameters", William Cohen and C. Martin Steinmetz, Microwave Journal, October and November 1959.

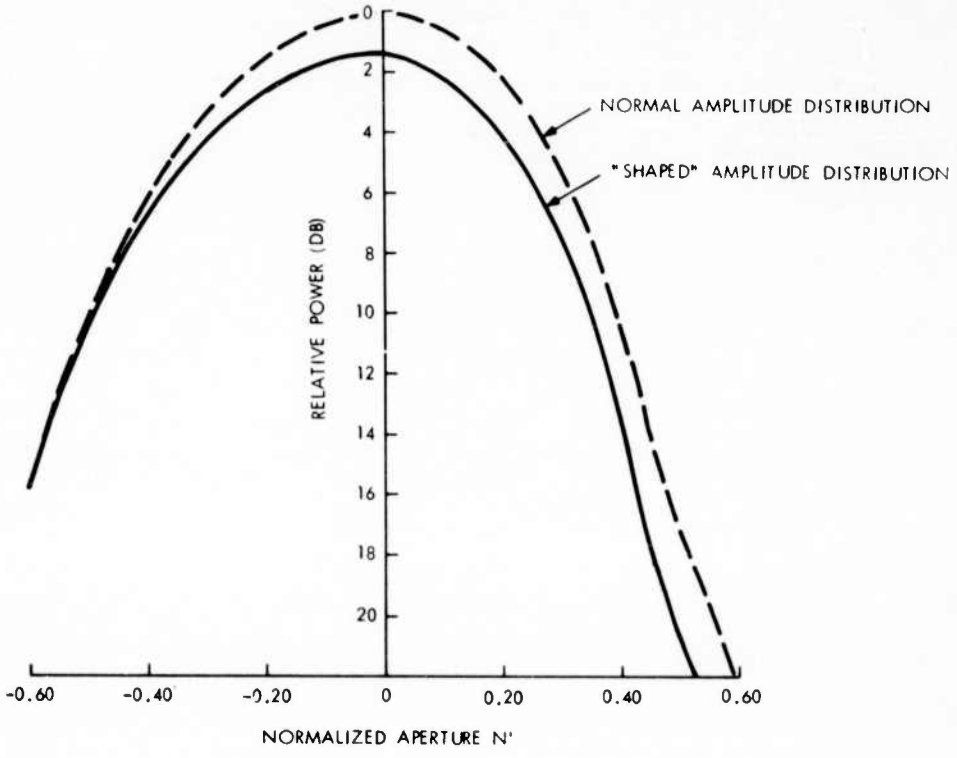

Figure 5-6. Sum Mode Aperture Distribution at $\theta = 36°$

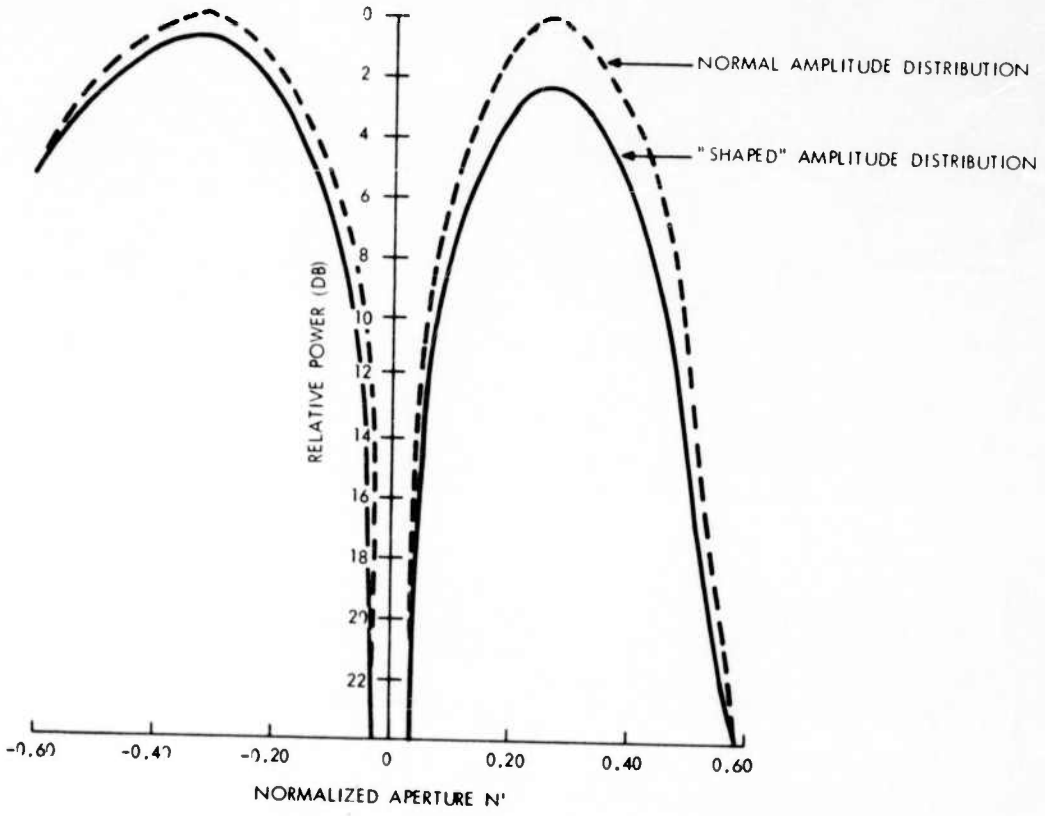

Figure 5-7. Difference Mode Aperture Distribution at $\theta = 36°$

SECTION 6

PROBE DESIGN

The performance of the MUBIS antenna depends to a great extent on the coaxial probes which are used extensively throughout the system. These probes which form the transitions from the parallel plate transmission line to the coaxial cables must be matched in their mutual coupling environment. Furthermore, since this is a wide angle scanning system, this match should not change appreciably as the angle of the incident radiation changes.

In the early stages of this program, the effect of probe mismatch variations was not fully appreciated. This choice of a probe-to-probe spacing of 0.6λ to be used throughout the system was governed by the "grating lobe" considerations at extreme angles of scan. However, during the course of the program this probe spacing was changed to 0.3λ when the variation of probe match as a function of scan angle was thought to be a contributing cause of poor far field radiation patterns. Although no thorough investigation of this variation of probe impedance was made, the basis for reducing the probe to probe spacing was as follows.

In an array of radiating probes, the impedance appearing at the terminals of one probe is made up of the self impedance and the mutual impedance. The mutual impedance component appearing at the terminals of one probe due to the presence of the other probes may form an appreciable fraction of the total impedance if the probes are in close proximity to each other. This mutual impedance component is a function not only of the probe spacing but also of the phase angle of the voltages appearing on the adjacent probes. As the beam is scanned the relative phase of these voltages on the output probes changes. This change is accompanied by a corresponding change in the phase of the mutual impedance component and a consequent change in probe impedance. Decreasing the probe-to-probe spacing results in a smaller phase difference between probes for a given scan angle. This means that as the beam is scanned from broadside to the limit of scan the change in phase required to accomplish this is less for the closer probe spacing. This smaller variation in phase results in a small variation in the mutual impedance as a function of scan angle. Although the actual value of mutual impedance may be greater, its percentage variation as a function of scan is less for a closer probe spacing.

The reason for going to a smaller probe-to-probe spacing for the input probes was the success obtained on another program in which a 0.3λ probe spacing was used. Moreover, the closer probe spacing on the focal arc tended to reduce the "cogging error" (see Section 8) by increasing the number of probes intercepted by the scanner horn.

Prior to installing these probes into the parallel plate line, the variation of VSWR with scan angle was checked experimentally in a test set-up which duplicated closely the actual operating conditions. In this procedure, the reflection coefficient of an array of probes terminating in matched loads was determined for different angles of incidence. The array of terminated probes were installed in a small section of double width C-Band waveguide and the VSWR of the array was measured "looking in" from the waveguide end by means of a special double width slotted line. (See Figure 6-1.) The use of double width C-Band waveguide for simulating the TEM mode in the parallel plate transmission line was justified as follows:

As the width dimension of TE_{10} rectangular waveguide is increased the guide wavelength for a given frequency decreases until it is equal to the TEM mode wavelength. However, it is not recommended that this width be increased indefinitely since the higher order TE_{mo} modes can be propagated. A width of 3.50 inches was used since the ratio of the TE_{10} mode wavelength to the TEM wavelength was 1.05 at the system center frequency of 5500 MCS. At this frequency the TE_{20} and TE_{30} modes could be propagated in the double width C-Band guide. It was felt that the probability of generating the TE_{20} mode was slight since this mode is asymmetrical. However, since the generation of the TE_{30} mode was a distinct possibility, precautions were taken to insure that the reflection coefficient measured was of the TE_{10} mode only. The slot in the special slotted line was positioned one third of the distance across the width of the guide where the null of the TE_{30} mode occurs. The VSWR probe therefore sampled only the TE_{10} mode standing wave. If the slot had been milled along the waveguide center line as is done in the usual slotted lines, both the TE_{10} and TE_{30} standing waves would have been sampled.

The probes were matched for normal incidence and then subsequently checked at angles of incidence of 0, 15, 30, and 45 degrees. Figure 6-2 shows the waveguide test sections for simulating these angles of incidence. The variation of VSWR for all these cases over the frequency range 5250 MCS to 5750 MCS is shown in Figure 6-3.

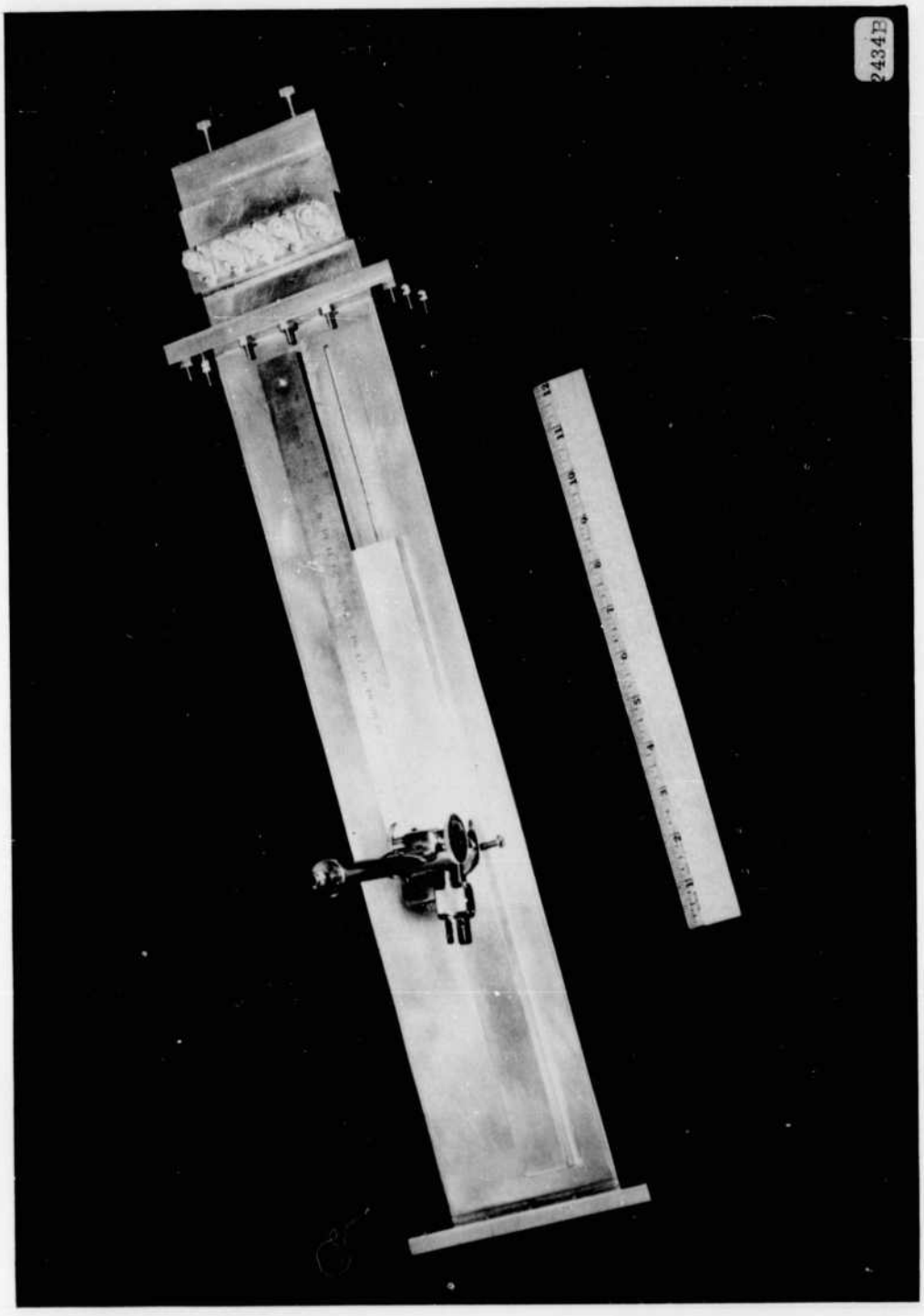

Figure 6-1. Special Double Width C-Band Slotted Line Showing Offset Slot

Figure 6-2. Waveguide Test Sections for Simulating Incidence Angles of 0°, 15°, 30°, and 45°

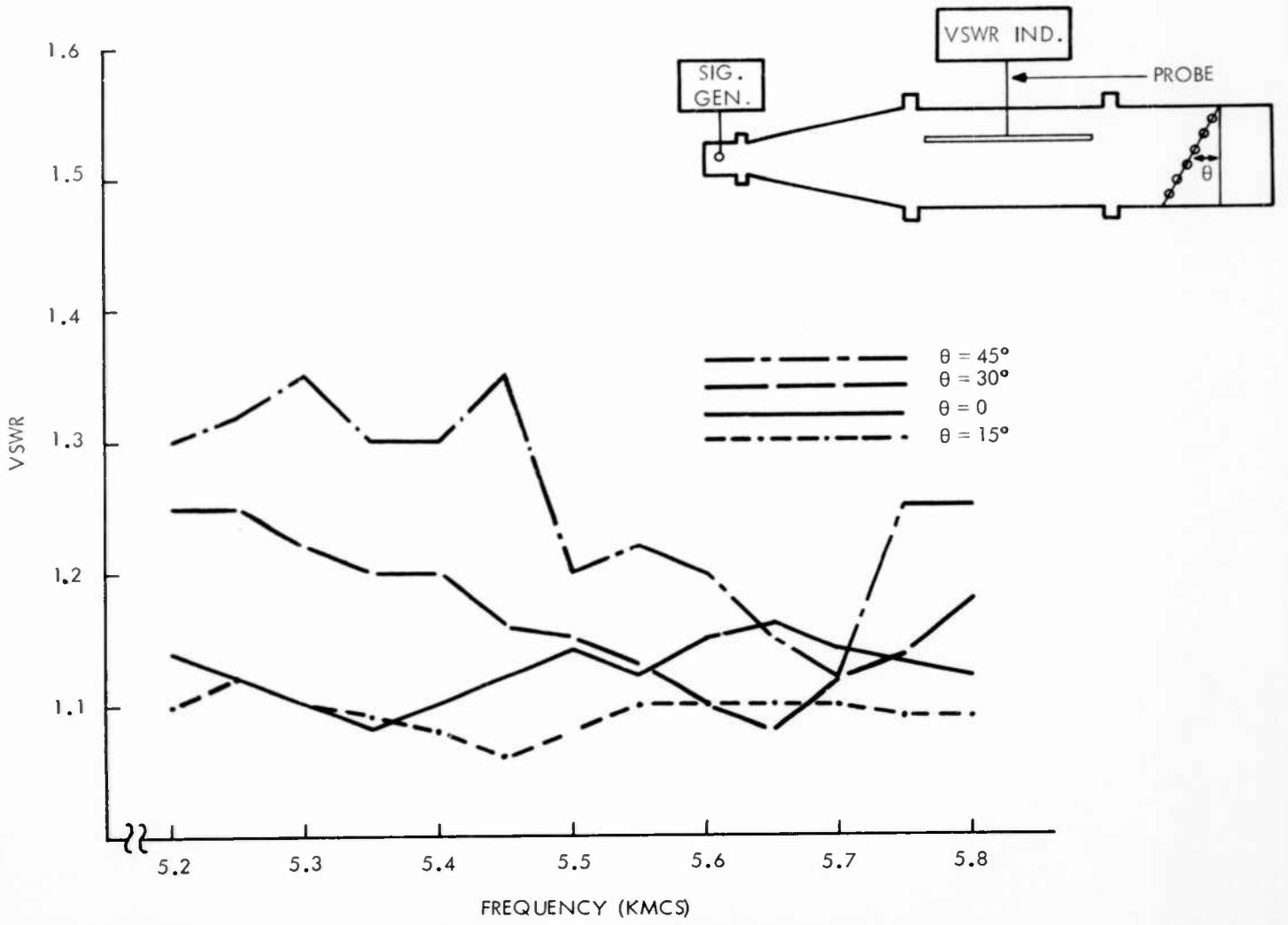

Figure 6-3. VSWR of Terminated Probe Array in Double Width Guide

The fore mentioned technique differs from the usual method of measuring from the "probe end" with the adjacent probes terminated, but it was felt that this method more nearly approached the conditions existing in the parallel plate region. For large angles of incidence the validity of this method may be questioned since a portion of the waveguide is beyond cut-off, by virtue of the fact that the probe array effectively acts as the waveguide wall which gradually tapers into a cut-off waveguide. Data taken on the phase and amplitude characteristics of the probes in the double width guide (see Figures 6-4 and 6-5) appear to indicate that this cut-off condition does exist in the guide which simulated the 45-degree angle of incidence. This condition was not used as a basis for the probe design, however, since they were matched at normal incidence and subsequently checked at the various angles indicated. Since this cut-off condition does not exist in the parallel plate line and because of the encouraging results at smaller angles of incidence, the probe design was considered adequate.

This probe design was also used in the scanner transition region, but due to mechanical difficulties in attaching the cables, the scanner probes were designed with a right angle bend. Figure 6-6 shows both of these probes. The probe dimensions and the spacing from the back wall are shown in Figure 6-7. These dimensions apply to the particular probes designed for the MUBIS lens system in the frequency range of 5250 MCS to 5750 MCS with a probe-to-probe spacing of 0.3λ.

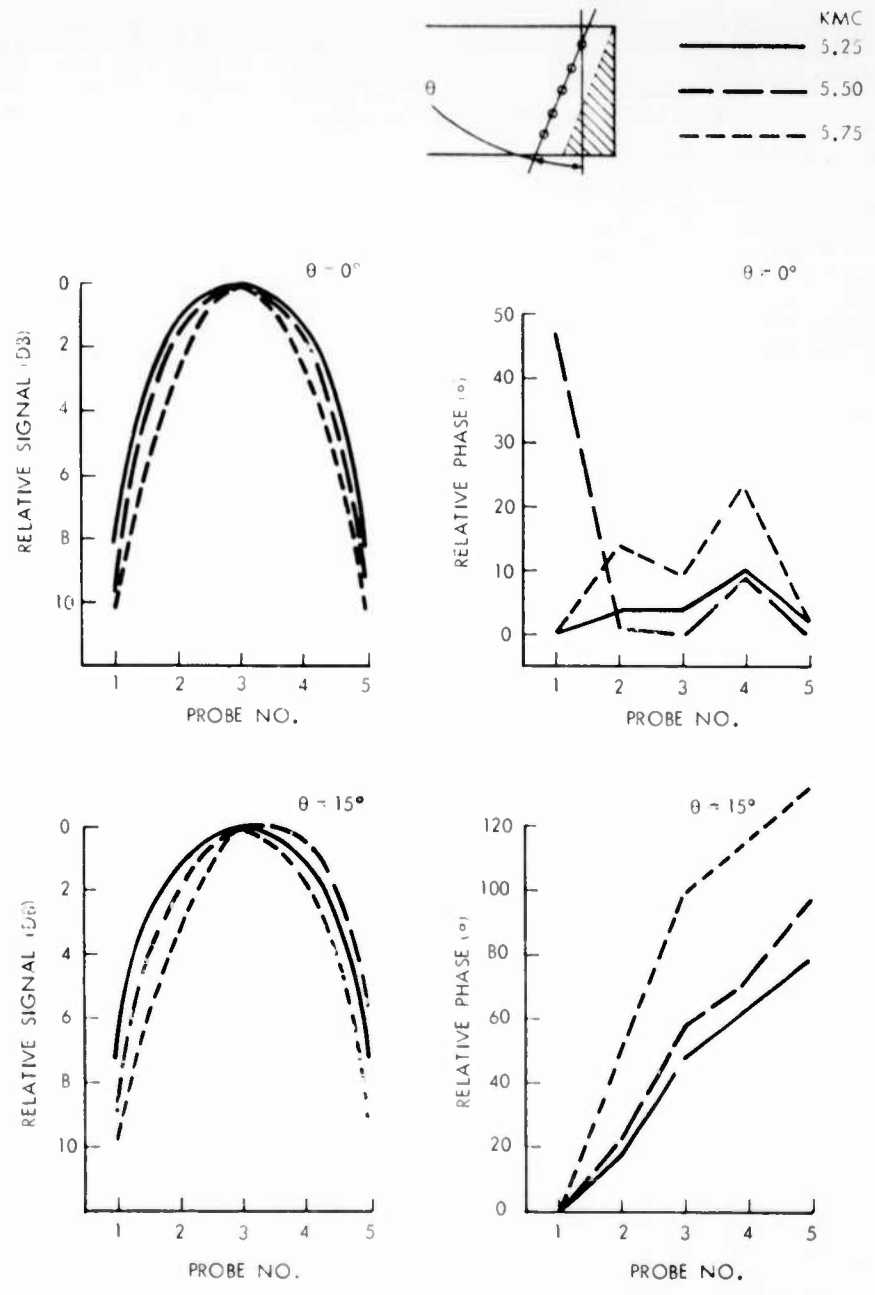

Figure 6-4. Phase and Amplitude Characteristics of Probes in Double Width Guide
$\theta = 0°$, $\theta = 15°$

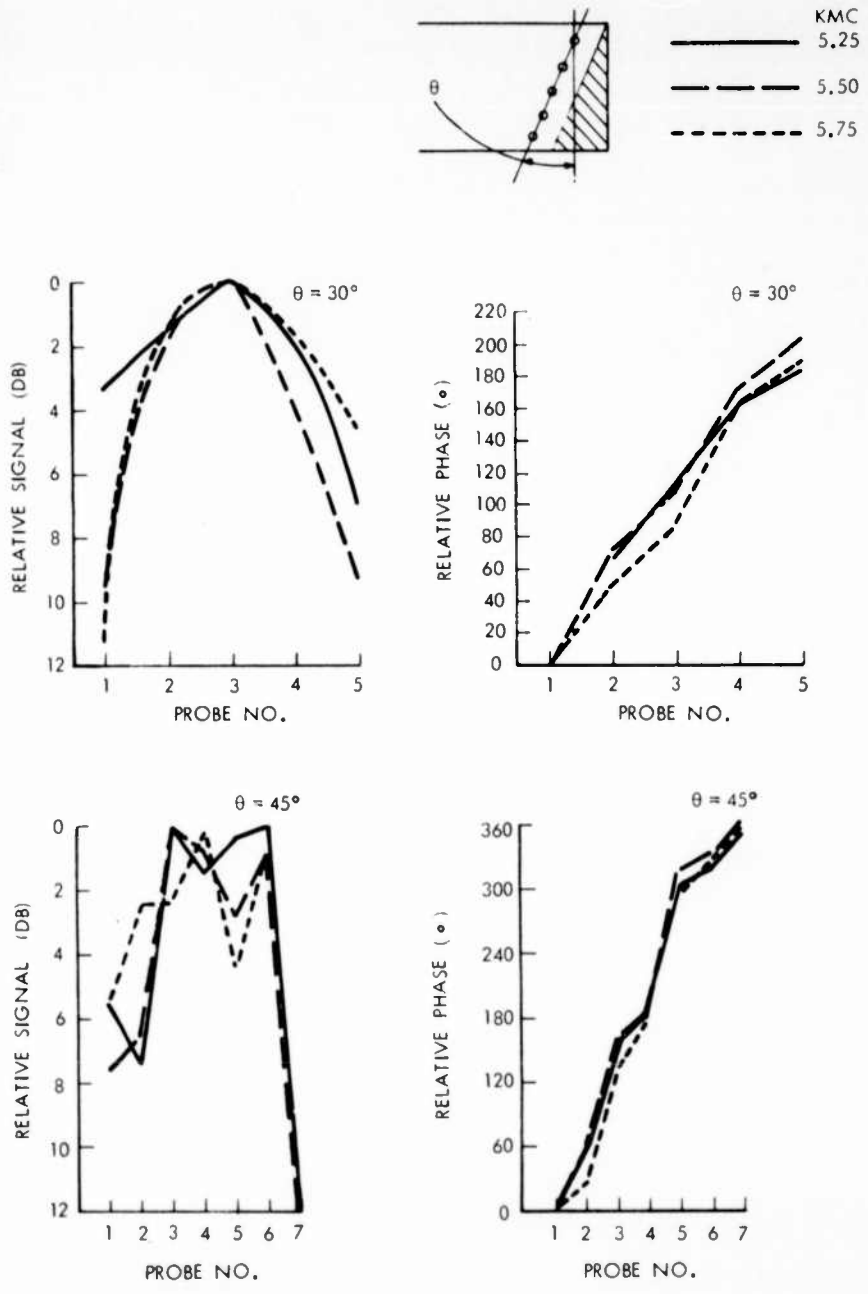

Figure 6-5. Phase and Amplitude Characteristics of Probes in Double Width Guide θ = 30°, θ = 45°

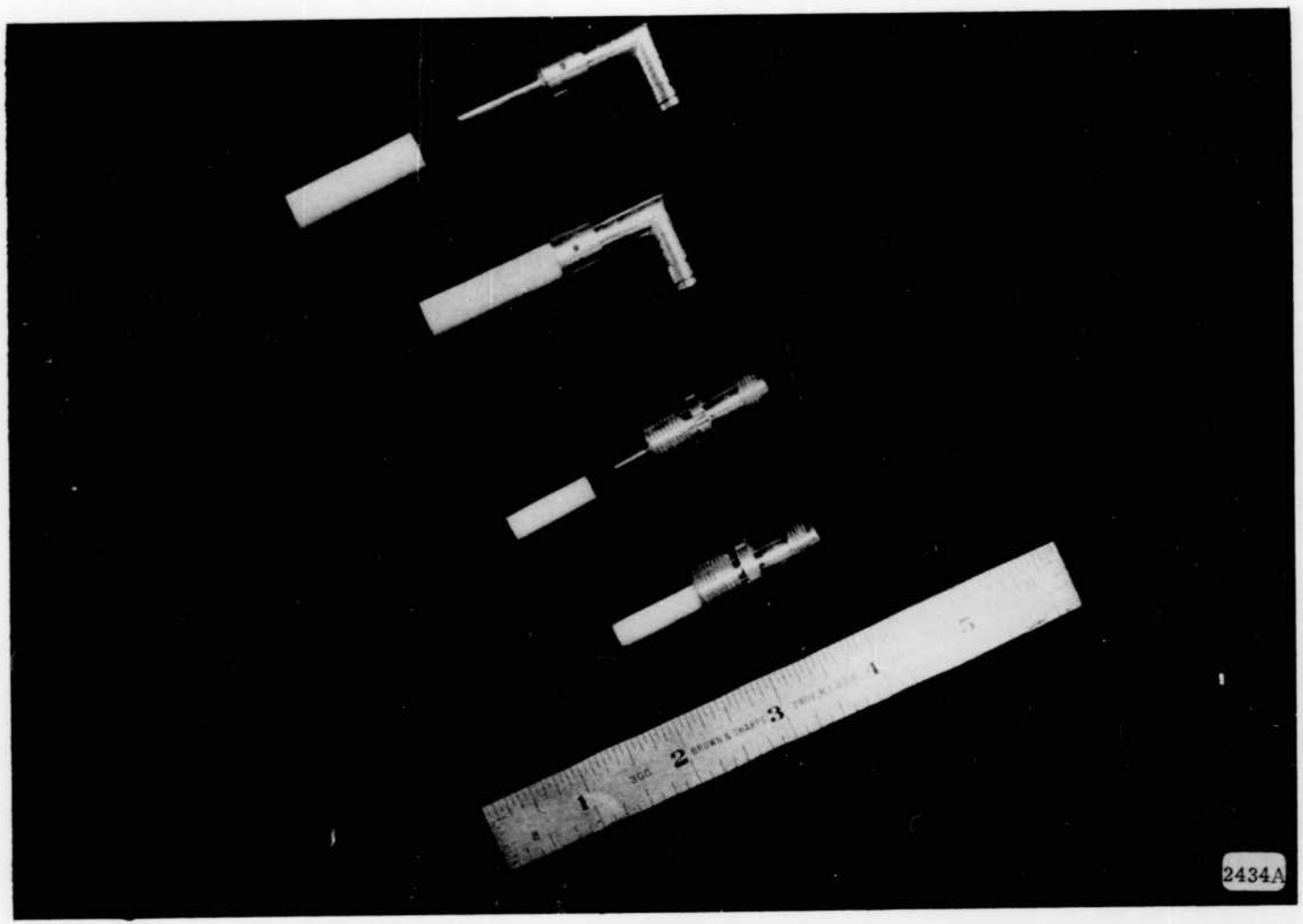

Figure 6-6. Probes Used in The MUBIS System

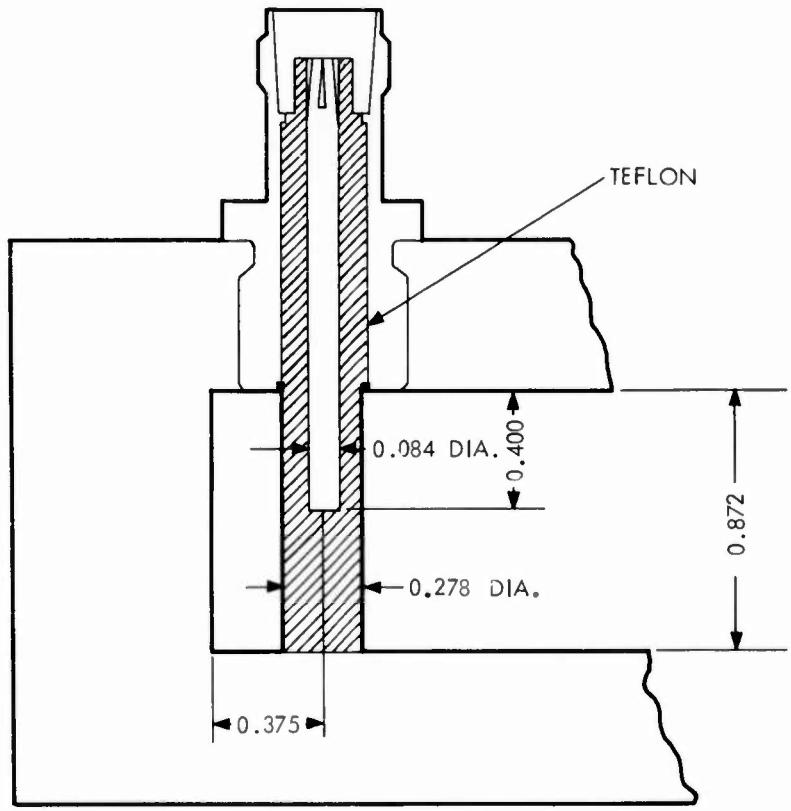

Figure 6-7. Probe Dimensions in Parallel Plate Transmission Lines

SECTION 7

COAXIAL CABLES

In the MUBIS lens system, coaxial cables determine the performance of the system: they connect the scanner to the focal arc and, as the lens elements, also connect the two surfaces Σ_1 and Σ_2. In both of these functions the lengths of the coaxial cable assemblies must be accurately controlled. Once these cables have been assembled it is desirable that they retain their electrical length relative to each other. This implies a cable which is stable with time and temperature or a set of cable assemblies whose characteristics, although not stable, will change uniformly so that the net change between cables will approach zero.

Since phase stable cables were not available, it was felt that "Aljak" an aluminum jacketed cable afforded the best compromise. The rigidity of the aluminum outer conductor would minimize unnecessary flexing of the cable which tends to aggravate the stability problem. However when the probe design was changed and the probe spacing was decreased from 0.6λ to 0.3λ the Aljak could not be used. The diameter of the connector used with this cable exceeded the probe spacing. As a result RG-5B/U flexible cable had to be used. This also posed a slight problem since the standard TNC connector used with this cable was still too large. It was necessary therefore, to have a special slim connector made for this particular application. A number of connector manufacturers were contacted and the problem was finally given to FXR-Amphenol who offered to assemble the cables as well as design the connector. To facilitate the phasing of the cables, they would incorporate a short line stretcher section into the connector so that the electrical length of the cable assembly could be easily adjusted. Their engineers felt that in the relatively narrow bandwidth of the system (5250 Mcs to 5750 Mcs) the connector could be designed to a VSWR of 1.2 to 1 and that the connector with the phasing section could be designed to a VSWR of 1.25 to 1. A photograph of the connectors is shown in Figure 7-1.

The problem turned out to be somewhat more difficult than had been anticipated and the resultant cable assemblies, after late delivery, had relatively high VSWR's, in some instances as high as 3.5 to 1. The cables

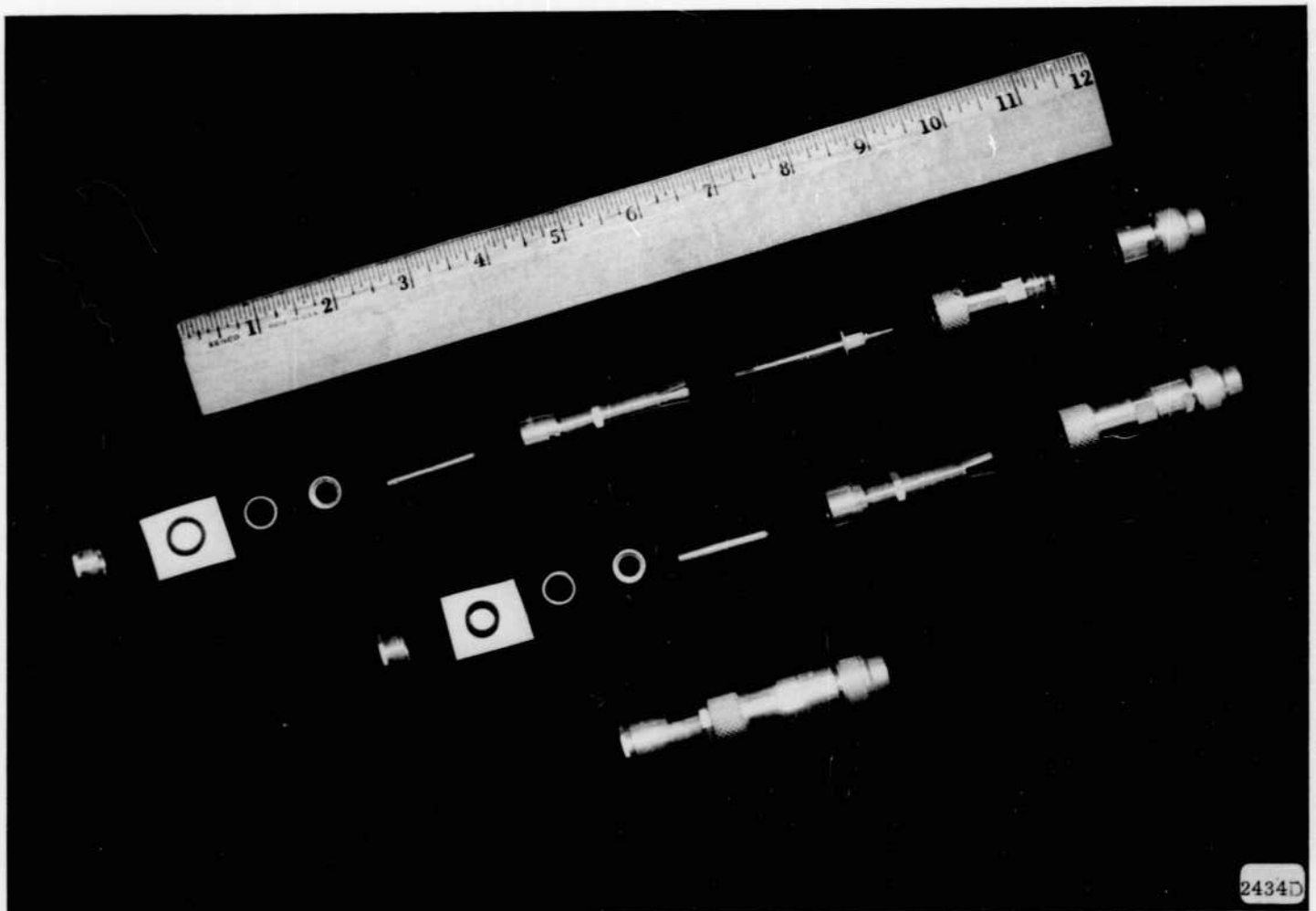

Figure 7-1. Assembled And Exploded Views of Special Connector And Phasing Section

were re-worked and some slight modifications were made on the connectors at Sylvania. This improved the VSWR of the cables but only to the extent of reducing it so that the maximum measured VSWR did not exceed 1. 8 to 1.

SECTION 8

COAXIAL ORGAN PIPE SCANNER

8.1 GENERAL DISCUSSION

In an organ pipe scanner, RF energy is transferred from a rotating horn through a transition region to a radiating aperture. The transition region is usually arranged in the form of a circle and is connected to the aperture by means of equal length transmission lines. From Figure 8-1 it can be seen that at any instant of time, the horn energizes a relatively small number of transmission lines, and therefore, only a small section of the aperture radiates. As the horn rotates the transmission lines are energized in a sequential manner such that the radiating section is moved along the total aperture. A lateral displacement of the radiating portion can, therefore, be obtained from the more easily produced rotary motion of the horn. This lateral motion of the radiating aperture can be effectively used in scanning antennas where a physical displacement of the phase center of the primary feed is reouired in order to scan the beam in space.

An organ pipe scanner of this type is particularly useful in a lens type of antenna system, in which the lens consists of a parallel plate transmission line operating in the TEM mode. The Luneberg Geodesic lens and the MUBIS lens are typical of this type. In these lenses, far field motion of the beam is produced by physically moving a radiating source along a focal arc. (Figure 2-2). By placing the scanner transmission lines sequentially along the focal arc of the lens so that the organ pipe aperture radiates into the lens, beam motion is produced as the scanner horn rotates (Figure 2-3).

The foregoing discussion precluded any consideration regarding the horn pattern and assumed that the transition regions and the

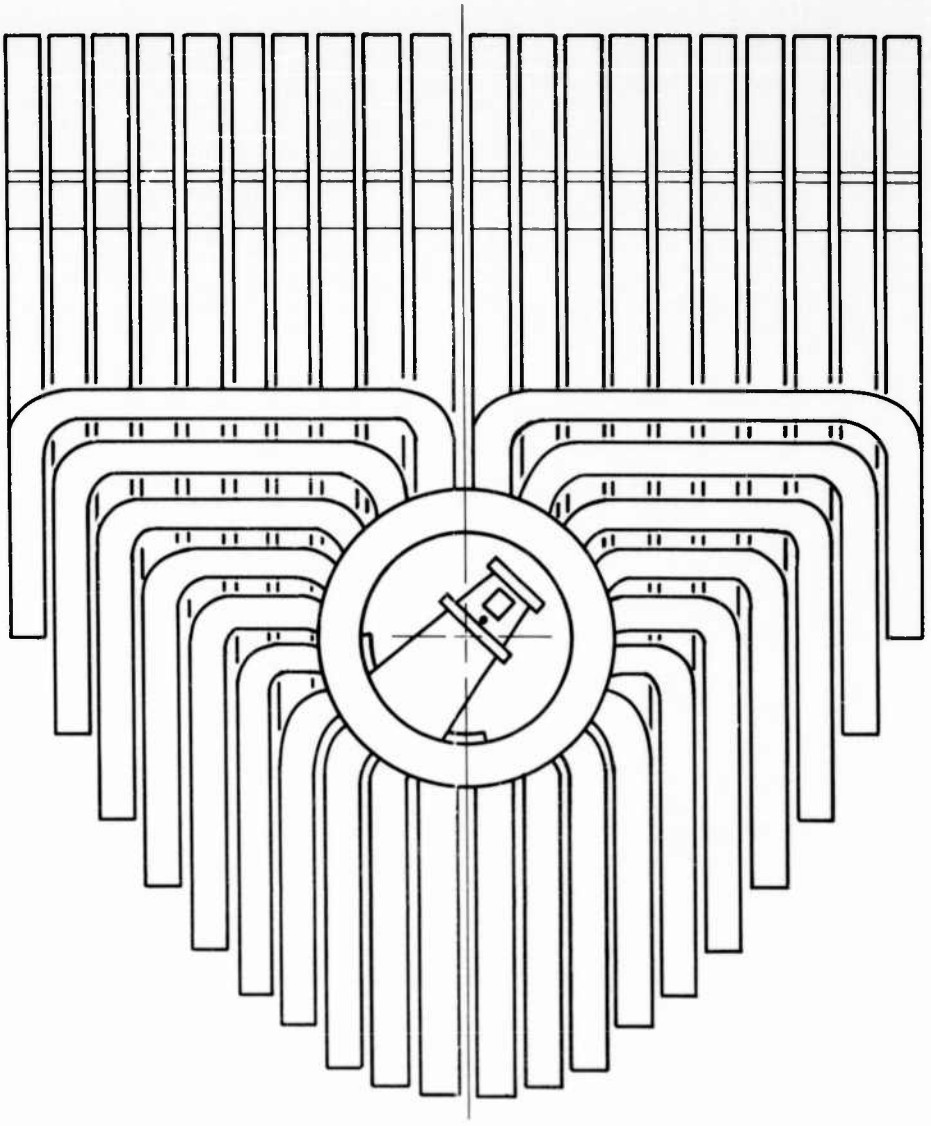

Figure 8-1. Organ Pipe Scanner

transmission lines accurately transferred to the focal arc, the amplitude and phase distribution of the field existing in the horn aperture. However, a conventional organ pipe scanner which uses rectangular transmission lines gives rise to beam pattern granularities as a function of scan angle which make its use impractical for monopulse operation. These granularities arise from the fact that the resultant illumination appearing at the focal arc of the lens is not the continuous distribution that exists in the scanner horn aperture, but rather a sampled representation of it. Consequently, as the horn rotates and the number of lines excited changes from N to N-1, the reconstituted aperture distribution is not always the same as the original horn distribution. From Figure 8-2 it can be seen that as the feed horn in the organ pipe scanner moves along the waveguides, the amplitude taper for different waveguide combinations will be proportional to the portion of the waveguide intercepted by the horn. Since the scan angle is proportional to the energy center of gravity, it can be seen that at points where the waveguides are excited in an asymmetrical manner as in case (b) and case (d) in Figure 8-2, there will be a deviation between the scan angle and the feed horn center line (indicated scan angle). This boresight shift or error in indicated scan angle is a periodic function of horn position and is referred to as "cogging". The maximum value of this cogging error can be reduced by increasing the number of waveguides intercepted by the feed horn. This is not feasible because the number of waveguides possible for a given horn aperture is fixed by the cutoff frequency of the guide. Increasing the horn aperture so that it can intercept a larger number of waveguides is also not feasible because as the aperture size is increased the resultant narrower beamwidth causes an improper lens illumination.

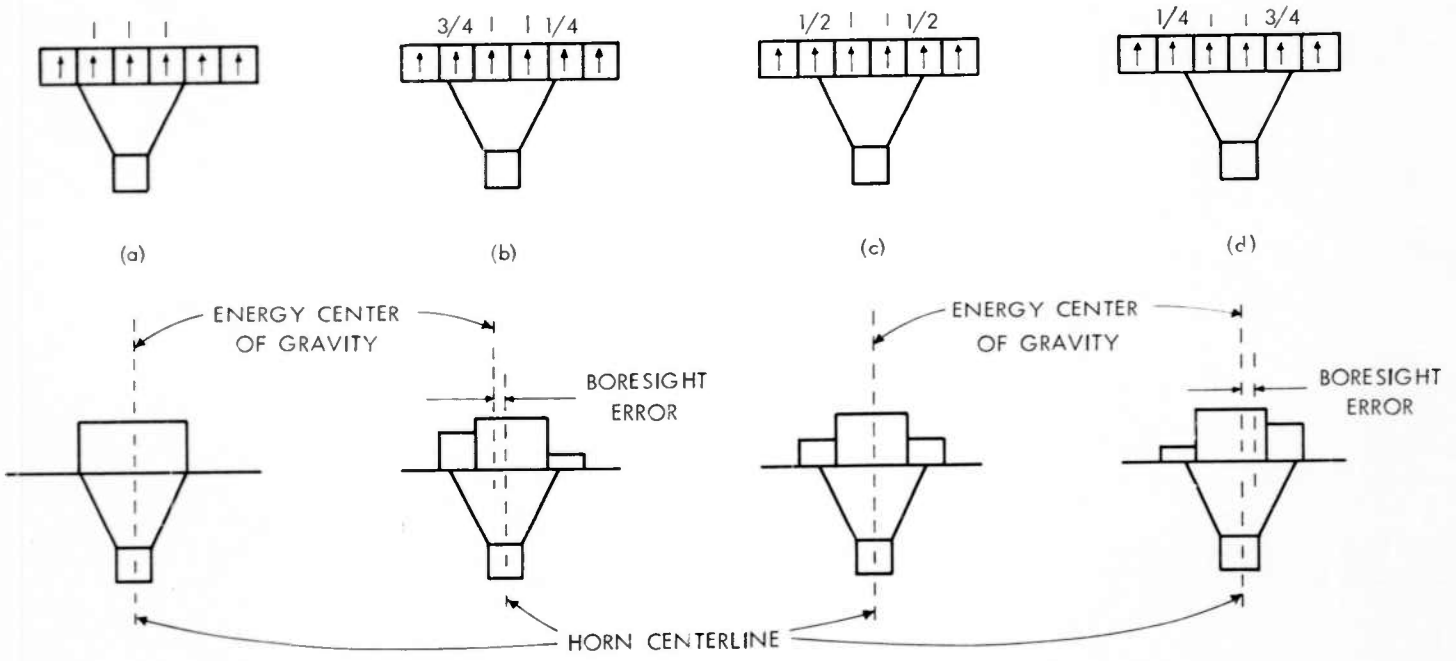

Figure 8-2. Symmetrical And Asymmetrical Waveguide Excitation Showing Resultant Boresight Shift Due to Cogging

A superior method designed by Sylvania for reducing the "cogging effects", while still maintaining a reasonable size horn aperture for proper lens illumination is the use of a coaxial probe monopulse organ pipe scanner conceived by R. Rubin and D. Ferrante. In this scanner coaxial probes are placed in the circular transition region and the waveguides are replaced by coaxial cables which connect the probes in the scanner with a similar set of probes on the focal arc of the lens. The energy appearing at the horn aperture is coupled out of the transition region by these probes and transferred by means of the coaxial cables to the focal arc probes which radiate into the lens. The relatively smaller size of the probe and cable assemblies allows a greater number of elements to be used in transferring the energy from the scanner to the focal arc. This results in a smoother, and more continuous scan, which reduces the "cogging" and allows the more efficient use of a monopulse scanning capability.

8. 2 DESIGN CONSIDERATIONS

The design of a coaxial probe monopulse organ pipe scanner for use with a lens is usually determined by the lens parameters. A single axis coaxial probe monopulse organ pipe scanner consists of a transition region, a monopulse comparator assembly and two rotary joints, all contained in a housing which has provisions for supporting and rotating the comparator assembly. Once the lens has been specified, the scanner must be designed to follow the general constraints imposed principally by the lens aperture and the focal length. The field appearing at the focal arc of the lens is shaped by the scanner horn and transferred from the transition region to the focal arc by means of probes and coaxial cables. The probes radiate into the parallel plate transmission line and illuminate the output probes which form the rear lens surface. Some granularities may exist in the radiation pattern due to the fact that the aperture on the focal arc is made up of a finite number of probes whose value alternates between n and n - 1 as the scanner rotates. However, the changes in the radiation pattern caused by these become extremely small for values of n approaching 10 and consequently may be neglected when computing the aperture on the focal arc required to properly illuminate the lens surface. A continuous aperture moving along the focal arc is, therefore, assumed and the horn aperture is designed as if it were physically placed along the focal arc.

The lens specifications derived from the general system requirements were as follows:

Frequency: C-Band 5250 Mcs - 5750 Mcs

Aperture: 40λ

N′ (where $\frac{f}{d} = \frac{1}{2N'}$) = 0.6

Off Axis Focal Points ±30°

On Axis Focal Length g′ = 1.137

The lens contour is uniquely determined once the positions of the three focal points have been specified. The f/d ratio fixes the aperture size with respeet to the focal length of the lens and is determined by specifying N′. In Figure 8-3 is shown a set of curves which relate the angle subtended at the focal are by the lens aperture as a function of N′ for 3 different scan angles. It must be remembered that these curves only apply to the lens mentioned above (i.e., off axis focal point = ±30° and on axis focal length g = 1.137). For the lens design considered a value of N′ = 0.6 was selected in order to insure that the "off foc s" aberrations be small for large angles of scan (Reference 1).

Once the desired beamwidth in the parallel plate region is known, the design of the scanner horn required to properly illuminate the lens aperture may appear to be straightforward. However, for monopulse operation this is not the case. In an amplitude comparison type of monopulse system, which is the type used with the lens for azimuth scan, the aperture requirements for the difference mode are that it be about twiee as wide as for the sum mode. This appears necessary in order to maintain the optimum gain and side lobe level in the two difference patterns as exist in the sum pattern. Since both modes of operation use the same horn aperture, independent control of the respeetive radiation patterns cannot be achieved by merely adjusting the physical size of the aperture. If the feed is optimized for the difference mode, the aperture becomes too large for the sum mode. This causes a more directive sum pattern in parallel plate region which would result in "wasted" lens aperture. Optimizing for the sum mode would result in two broad lobe patterns for the difference mode with high illumination at the lens edges and consequent high side lobes. Furthermore, due to mechanical construction the "spillover" at the lens edges would be reflected from the side walls and perturb the field in the lens aperture with resultant "null fill in" of the difference pattern. Even if it were possible to utilize an aperture size that would

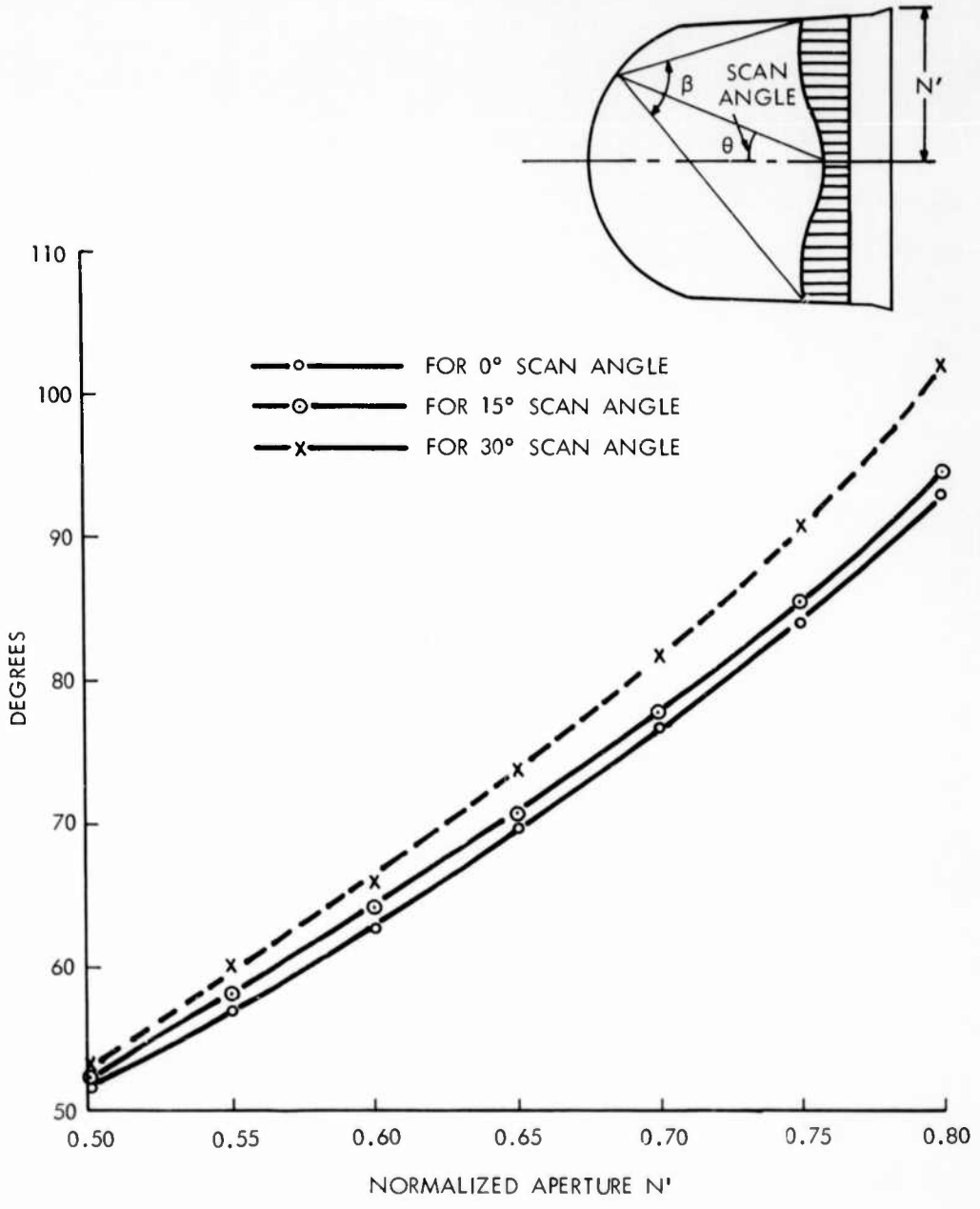

Figure 8-3. Angle at The Focal Arc Subtended by The Lens Surface for Several Scan Angles

effect a compromise between optimum sum mode and optimum difference mode performance, its use may be precluded by the type of monopulse comparator that is used in the scanner assembly. This will be discussed in detail in Section 8.4 on the monopulse comparator assembly.

8.3 THE TRANSITION REGION

The scanner transition region is a slot machined around the inner wall of the cylindrical housing to form an annular cavity concentric with the housing axis. The rotating scanner horn radiates into this cavity which is lined with coaxial probes equally spaced around the circumference. These probes couple out the energy appearing in the horn aperture. In order to confine the fields to the group of probes in the immediate vicinity of the horn aperture, skirts are placed on the sides of the horn such that the cavity on either side of the aperture will appear as a waveguide beyond cut-off. A non-contacting choke is machined along the input lip of the cavity to keep the energy from escaping over the horn surface. Figure 8-4 is a photograph of the partially assembled scanner showing the probes cavity choke and skirts mentioned above.

8.4 COMPARATOR ASSEMBLY

The monopulse comparator assembly used in the organ pipe scanner consists of a folded H-Plane hybrid and a flared horn. The hybrid provides the sum and difference channels necessary for monopulse operation. The two output arms of the hybrid which are side by side are separated by a septum and provide the two closely spaced feeds which produce the two "squinted" beams in azimuth required in an amplitude sensing monopulse system. In reception, the two squinted beams are combined in the comparator to produce outputs at the sum and difference ports of the hybrid which are respectively proportional to the sum and difference of the amplitudes of these two beams. Conversely when each of these ports

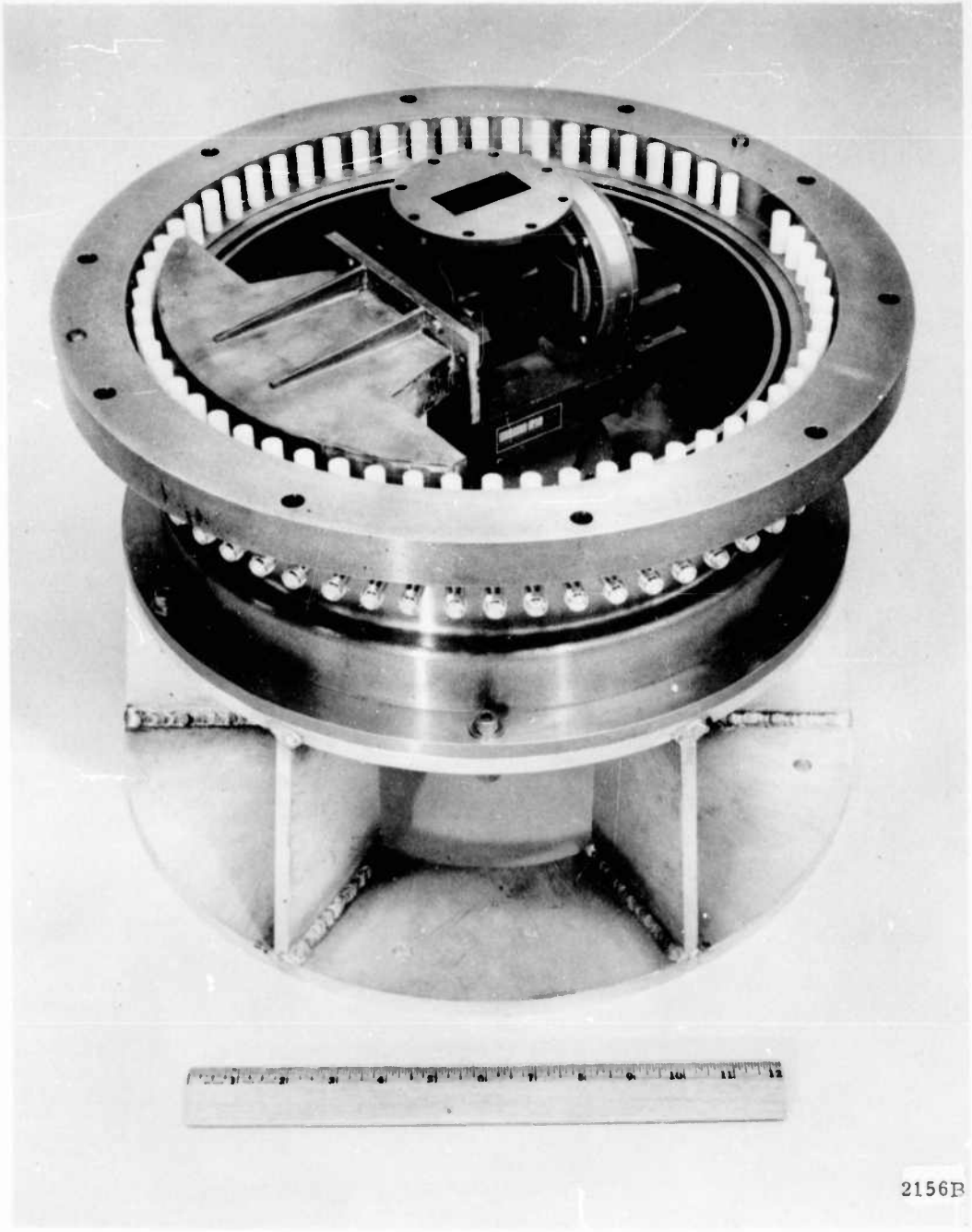

Figure 8-4. Partially Assembled Scanner

is separately energized the resultant radiation pattern is the sum or difference of these beams.

The horn which is attached to the output arms of the hybrid has no septum so that it forms a double width waveguide. This double width waveguide can support higher order TE_{m0} waveguide modes. The TE_{20} mode is excited when the difference port of the hybrid is energized. This mode is asymmetrical and is excited in the double width horn by virtue of the fact that the fields appearing in the two output arms of the hybrid are 180° out of phase with respect to each other.

When the sum port of the hybrid is energized the output arms are in phase and therefore the symmetrical TE_{10} mode is excited in the horn. In addition since the septum is abruptly terminated at the hybrid output higher order symmetrical modes are generated at the discontinuity. However, because of the dimensions of the double width guide only the TE_{30} mode will propagate, and at the discontinuity it is 180° out of phase with respect to the TE_{10} mode. Consequently when the sum port of the hybrid is energized, the field at any point in the horn is the vector sum of these two modes, and the TE_{30} mode can be used to provide aperture distribution shaping. Since the phase velocity is different for these two modes, the length of horn is adjusted in order that the two modes appearing in the horn aperture will have the proper phase so as to produce the desired aperture distribution. Additional control of the aperture distribution can be had by varying the amplitude of the TE_{30} mode with respect to the TE_{10} mode. This can be accomplished by placing irises in the double width region which will have different values of attenuation for each mode. Thus by adjusting the ratio of the amplitudes of the two modes and by taking advantage of the difference in their phase velocities, the sum mode aperture distribution can be varied independently without appreciably changing the difference mode aperture distribution. Conversely

it must be cautioned that in designing for the sum mode aperture distribution the effects of these higher order modes in the horn cannot be disregarded.

In the initial design of the MUBIS scanner, considerable attention was given to optimizing the sum mode aperture, by properly combining the TE_{10} and TE_{30} modes. This procedure involved adjusting the length of the horn so that the TE_{30} mode was 180° out of phase with the TE_{10} mode. The resultant distribution approached a uniform amplitude across the aperture and produced a measured radiation pattern in the parallel plate region shown in Figure 8-5. However, as can be seen from the curves the difference patterns were too broad and would result in an edge illumination in the difference mode which would be only about 1.5 db below the peak. This was undesirable since it would cause a large amount of energy to be reflected from the sidewalls of the lens and cause serious far field pattern deterioration. Since the only practical way of narrowing the difference pattern was by enlarging the aperture the horn was flared to 3.3λ. The resulting edge illumination of the lens for this aperture is indicated in Figure 8-6 which relates edge illumination to aperture size for a difference mode having a sin distribution and for a sum mode having a $\cos^2$ distribution. The shaded double curve for each distribution is given because the angle subtended by the lens surface varies as a function of scan angle. The shaded sections delineate the limits over which the edge illumination will vary as a result of the change of the subtended angle from 63° to 66.5°. A $\cos^2$ distribution was selected as a desirable sum mode aperture distribution because it allows the same aperture to be used for the sum and difference mode with reasonable edge illuminations for both modes, and could be approximated by proper combination of the TE_{10} and TE_{30} modes.

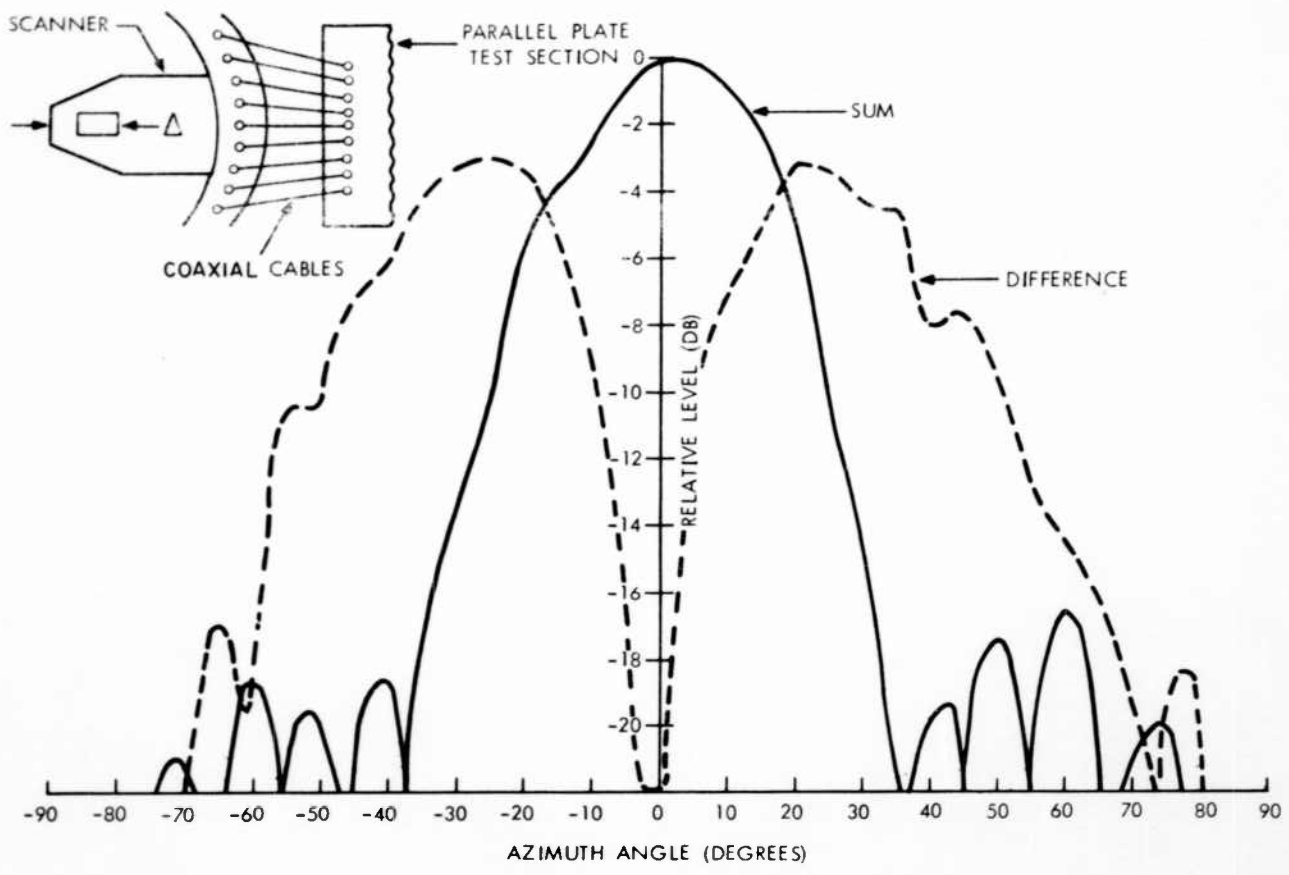

Figure 8-5. Measured Sum and Difference Patterns of Scanner at 5500 Mcs in the Parallel Plate Region

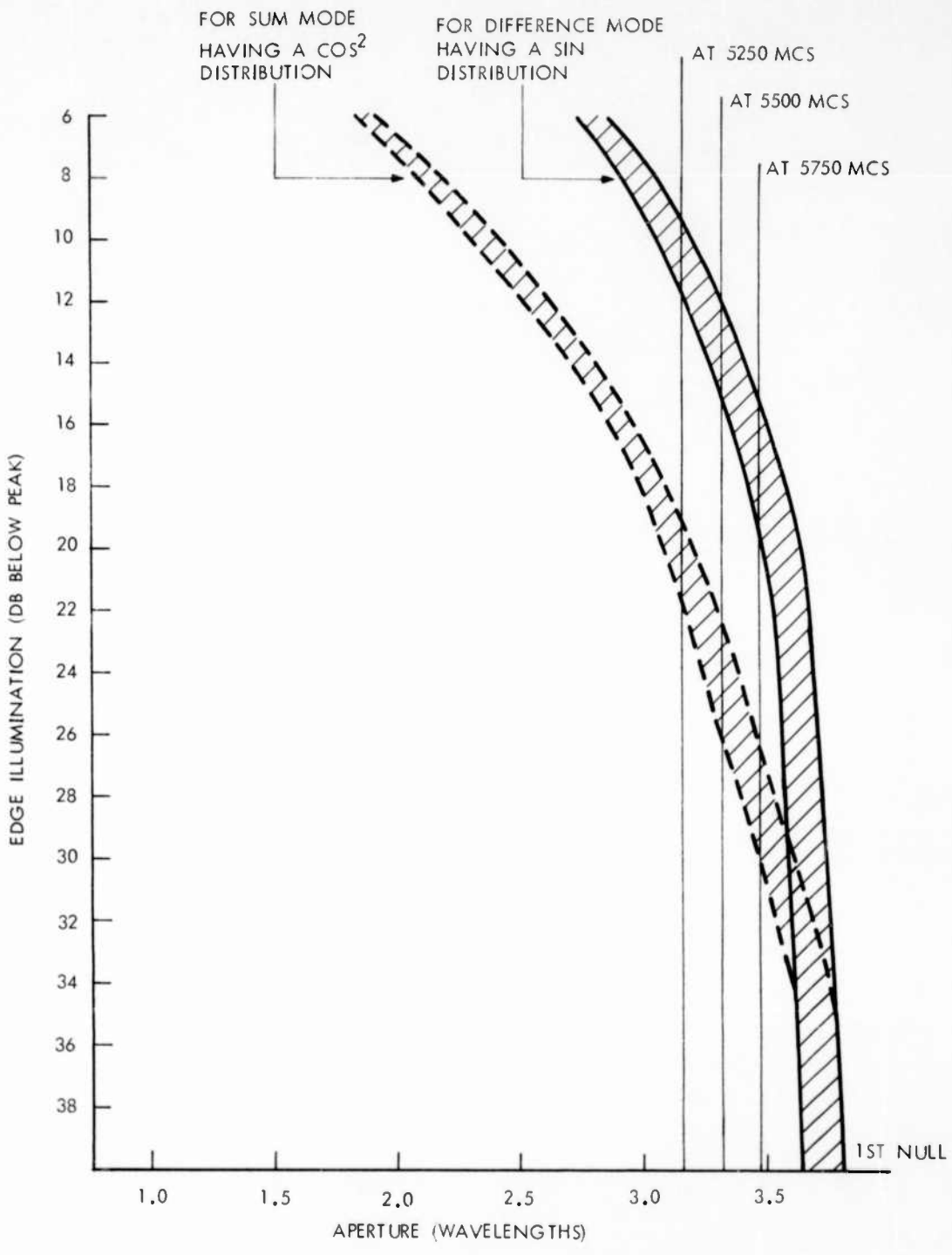

Figure 8-6. Calculated Edge Illumination of MUBIS Lens of N' = 0.60 versus Radiating Aperture on Focal Arc

Since the flared section could support additional higher order modes beyond TE_{30} the length of the flare required for the proper sum aperture distribution was calculated on the basis of the presence of the TE_{10} and TE_{30} modes only and then the radiation pattern in a parallel plate test section was checked experimentally. These results are summarized in Figures 8-7, 8-8 and 8-9.

Although there is only fair agreement between the predicted edge illumination and the measured, the results indicate that this method can be used for aperture shaping. Furthermore it is felt that if additional time were available better correlation could have been obtained.

In summary, the procedure to be followed in the design of the scanner comparator assembly should be:

1. Select an aperture size which will adequately illuminate the lens when the comparator is operating in the difference mode having a sin aperture distribution.
2. Adjust the amplitude distribution for the sum mode by properly combining the amplitudes and phase of the higher order symmetrical waveguide modes.

Completed views of the scanner are shown in Figures 8-10a and 8-10b.

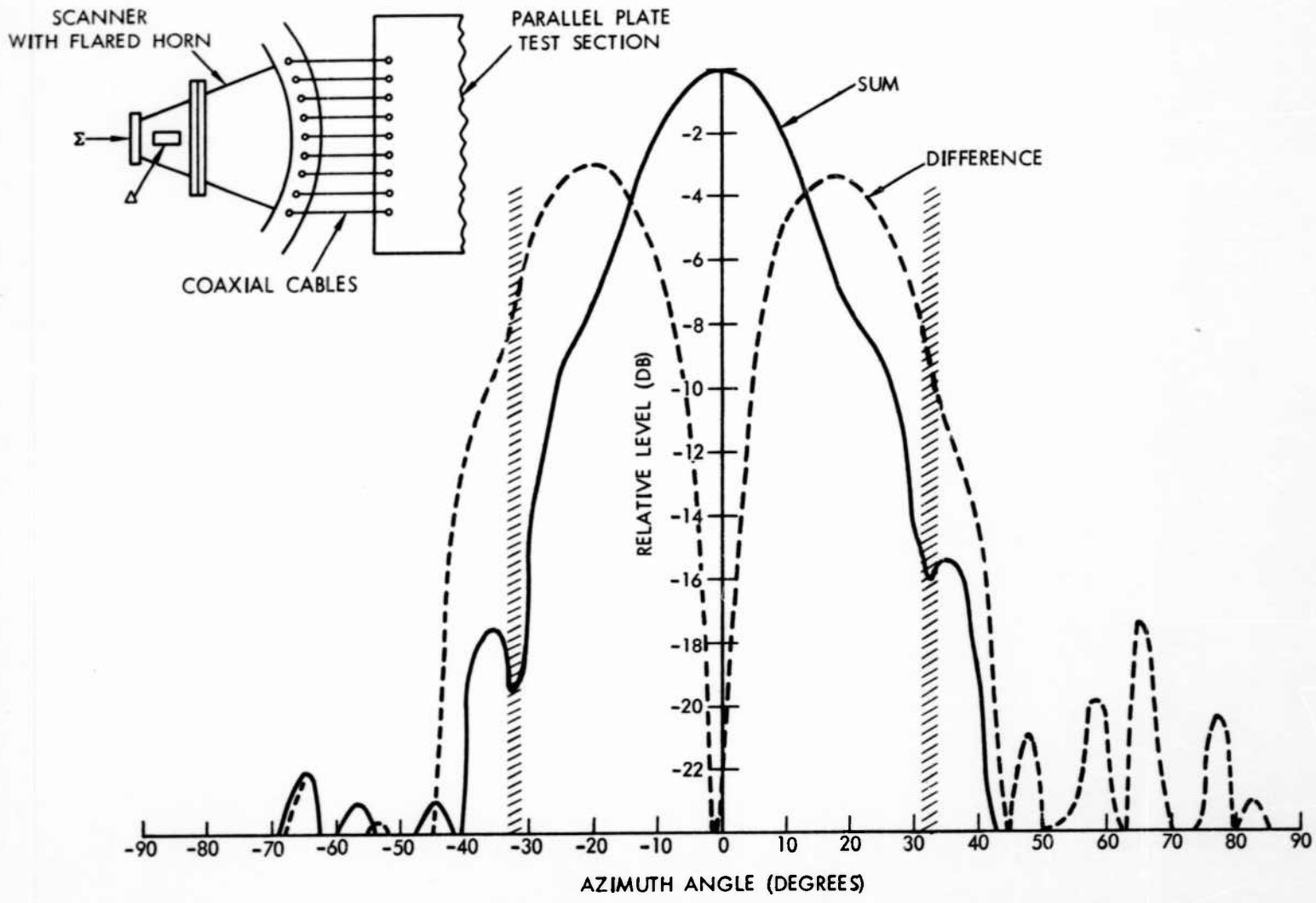

Figure 8-7. Measured Sum And Difference Patterns of Flared Scanner at 5250 Mcs in The Parallel Plate Region

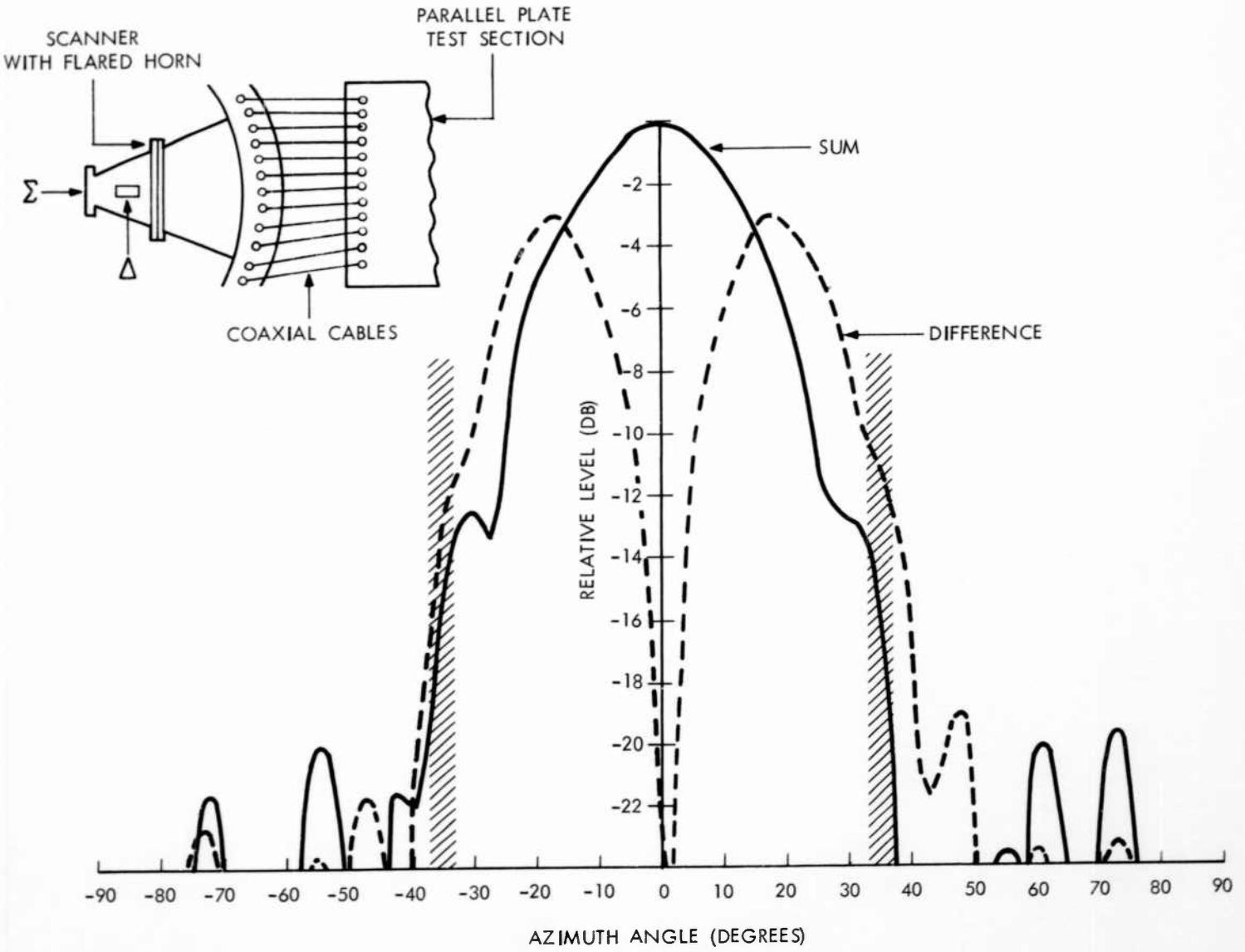

Figure 8-8. Measured Sum And Difference Patterns of Flared Scanner at 5500 Mcs in The Parallel Plate Region

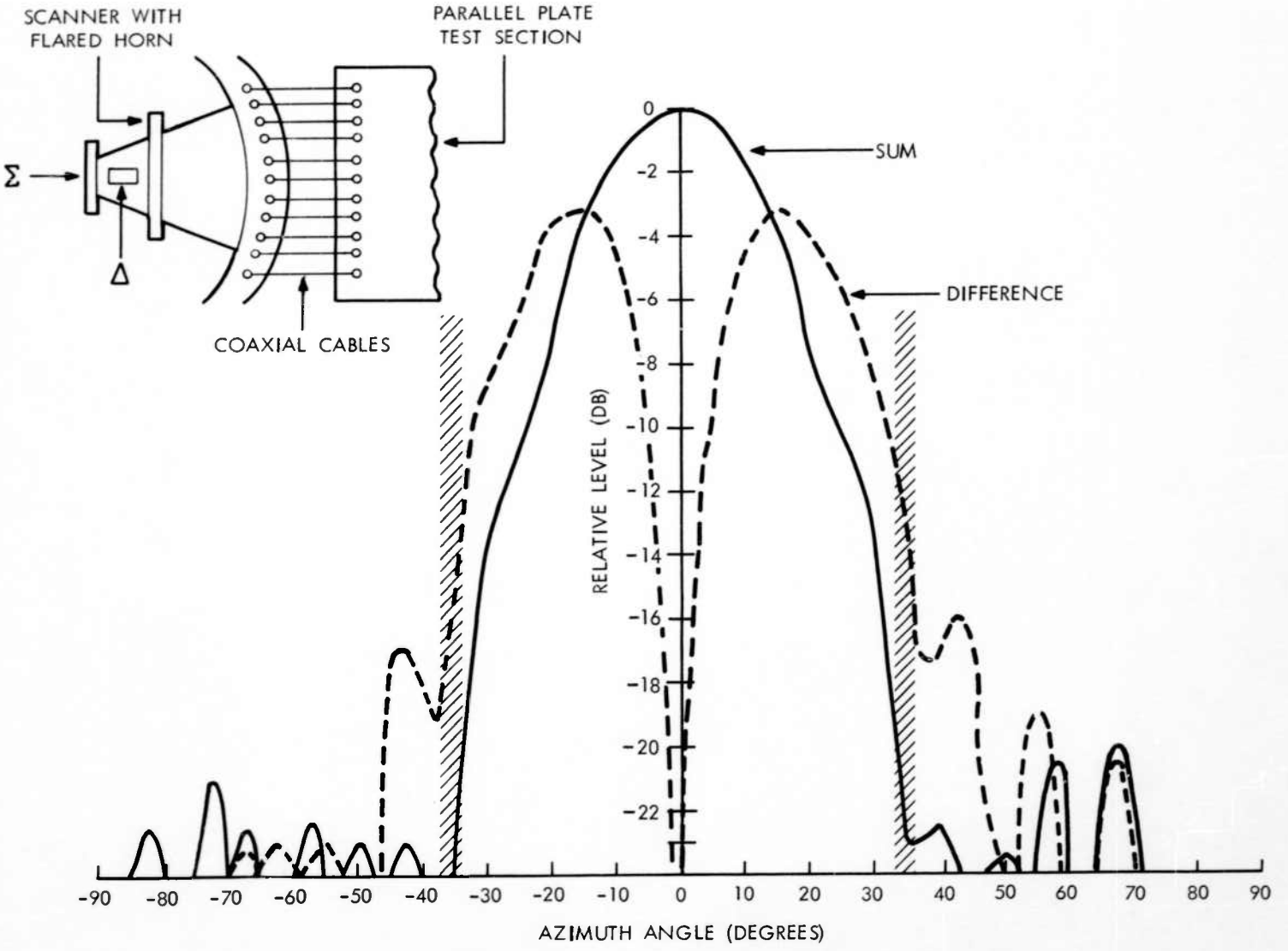

Figure 8-9. Measured Sum And Difference Patterns of Flared Scanner at 5750 Mcs in The Parallel Plate Region

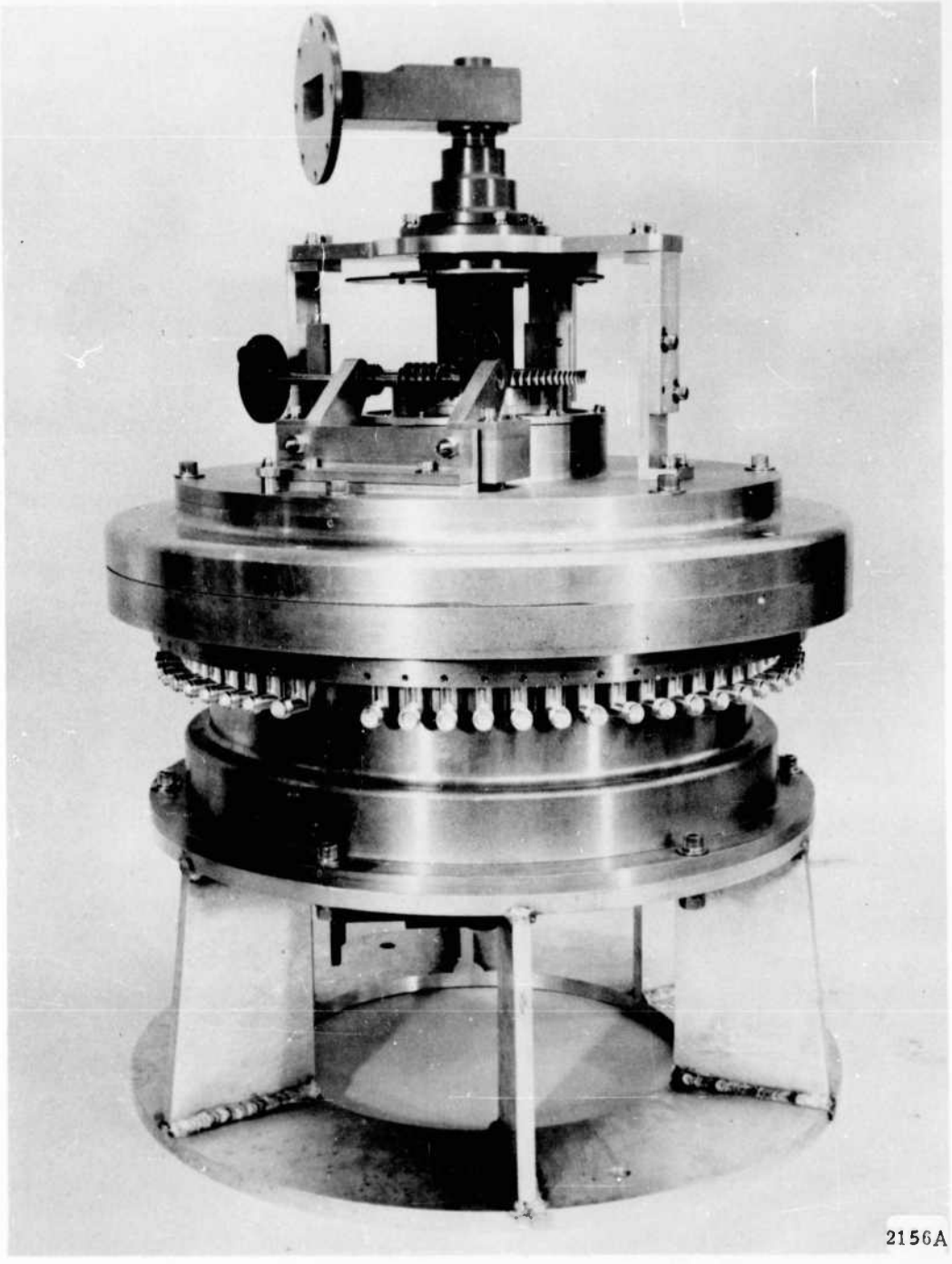

Figure 8-10a. View of Completed Scanner

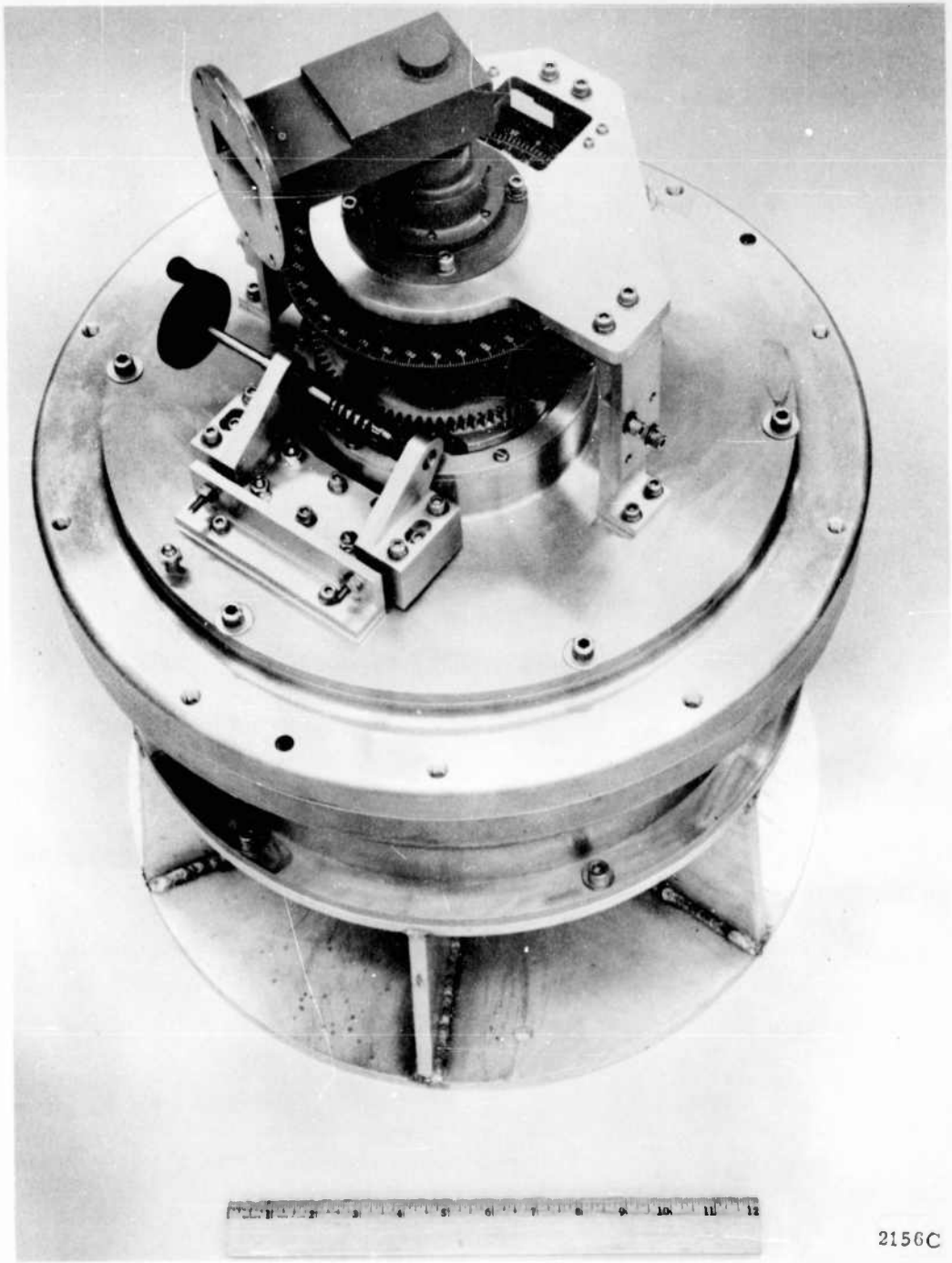

2156C

Figure 8-10b. View of Completed Scanner

SECTION 9

EXPERIMENTAL PROGRAM AND RESULTS

The first year of the program was chiefly concerned with the design and fabrication of the antenna system described in this report. Some difficulty was encountered during the course of the program in the design of a matched probe transition to the parallel plate transmission line. The technique of matching the probes in a setup approaching the TEM parallel plate line, described in Section 6, was not evolved until the conventional method of matching the probes was found to be inadequate for this application. Furthermore, the problem of the variation of probe impedance as a function of scan angle caused by a change in the mutual component of the probe impedance was not fully appreciated. As a result, the radiation patterns of this first antenna system showed marked deterioration of the monopulse sum and difference patterns. The magnitude of this deterioration varied in a random manner as the horn scanned the probes along the focal arc, and ranged from slight increases in sidelobe level to complete "break-up" of the main lobe of the sum pattern into two and even three equal lobes. The monopulse difference pattern deterioration ranged from slight "null fill in" to the merging of the two difference lobes into one main lobe on axis.

The reasons for this pattern break-up were not immediately obvious, but, based on the work done on a similar project, and a critical look at the existing design, it was felt that the probe design was the most probable cause of the problem. The system was redesigned as follows:

1) The probe-to-probe spacing was reduced from 0.6λ to 0.3λ throughout the system. This spacing was used on the line source, the parallel plate transmission line and the scanner transition region.

2) The probes were redesigned in accordance with the techniques described in Section 6.

3) New cables with adjustable phasing sections were installed throughout.

4) Since a new probe-to probe spacing was used, the coaxial probe monopulse organ pipe scanners were also redesigned.

Figures 9-1 and 9-2 show views of the redesigned antenna system on the turntable of the roof antenna range.

Prior to taking far field radiation patterns, the lens was checked using a sectoral horn in place of a group of probes, along the focal arc. Amplitude and phase were measured along the line source to make certain that the lens had been properly assembled, and that the output cable lengths had been properly phased. The measurements were taken with a microwave receiver using a small sampling probe to couple out a small amount of energy at each line source probe position. This was accomplished by drilling a small hole on the underside of the line source beneath each probe. The results of these measurements are shown in Figures 9-3 and 9-4. As can be seen in Figure 9-3 the measured phase variation along the line source was in very good agreement with the calculated phase taper, indicating proper operation of the lens. In Figure 9-4 the solid curve indicates the average of the measured amplitude points. The large variation of the points about the curve is due to the nature of the measuring technique. Since the amplitude of the energy coupled out is very sensitive to the position and the depth of penetration of the sampling probe, any slight variations in these two parameters when making repeated measurements results in large excursions in the data. The curve does serve to show a fairly low edge illumination for the aperture used. Additional amplitude measurements were made and all exhibited these large excursions of the amplitude data.

Radiation pattern measurements were subsequently taken on the roof range. Complete sets of patterns were taken at 5250 Mcs, 5500 Mcs, and 5750 Mcs. The patterns taken were the monopulse sum and difference patterns out to the limits of scan ±36 degrees at 1/2-degree intervals. Typical patterns are shown in Figures 9-5 through 9-18. The results of the complete set of patterns are summarized in Figures 9-19, 9-20, and 9-21. The summaries indicate variations in beamwidth, and sidelobe level for the sum mode and null fill in for the difference mode. In addition, difference mode patterns exhibited unequal lobes. These variations which appear almost random in nature can be ascribed to the VSWR's of both the input and output cable assemblies. Because of the long path lengths

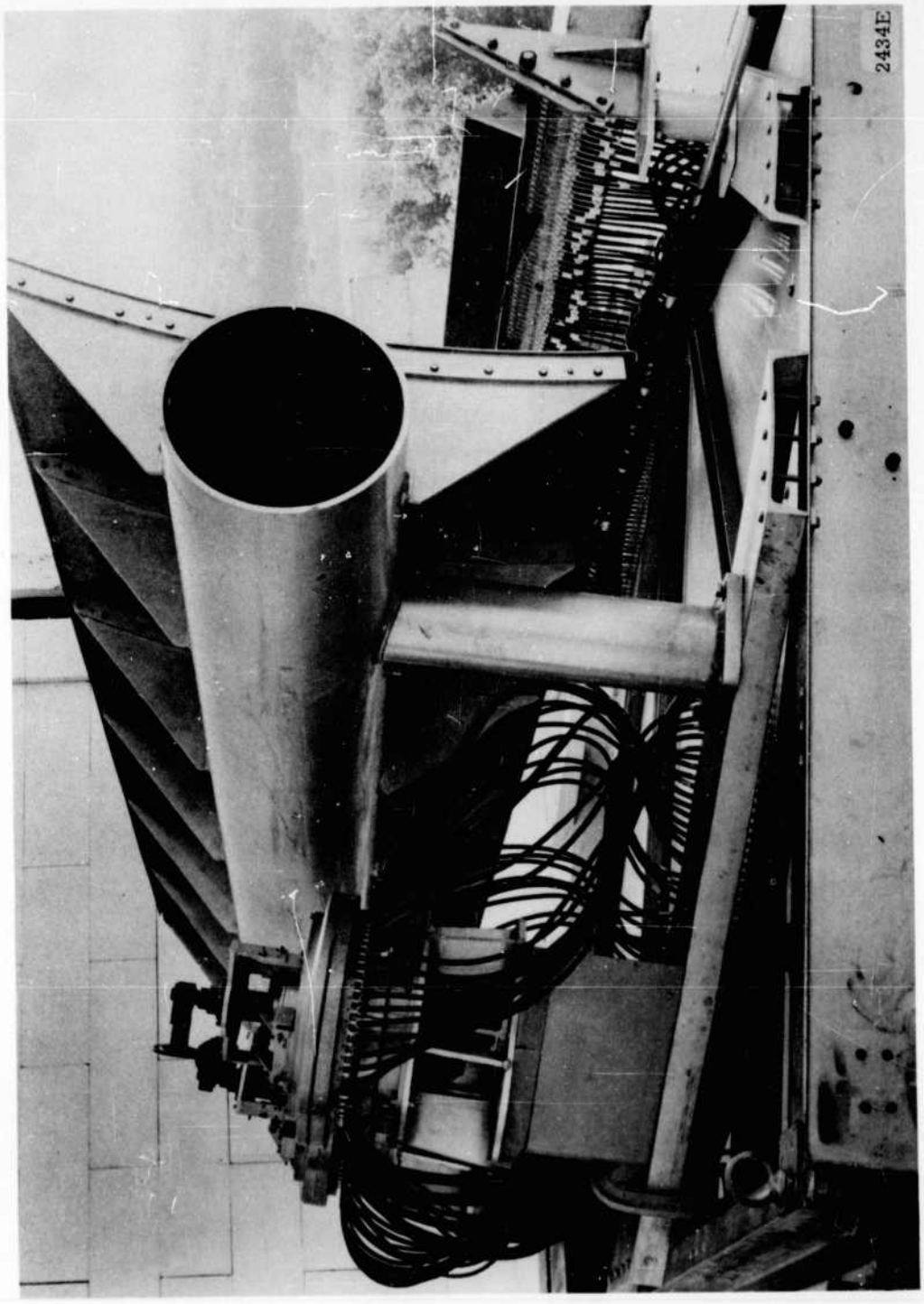

Figure 9-1. Rear View of Completed MUBIS Antenna System

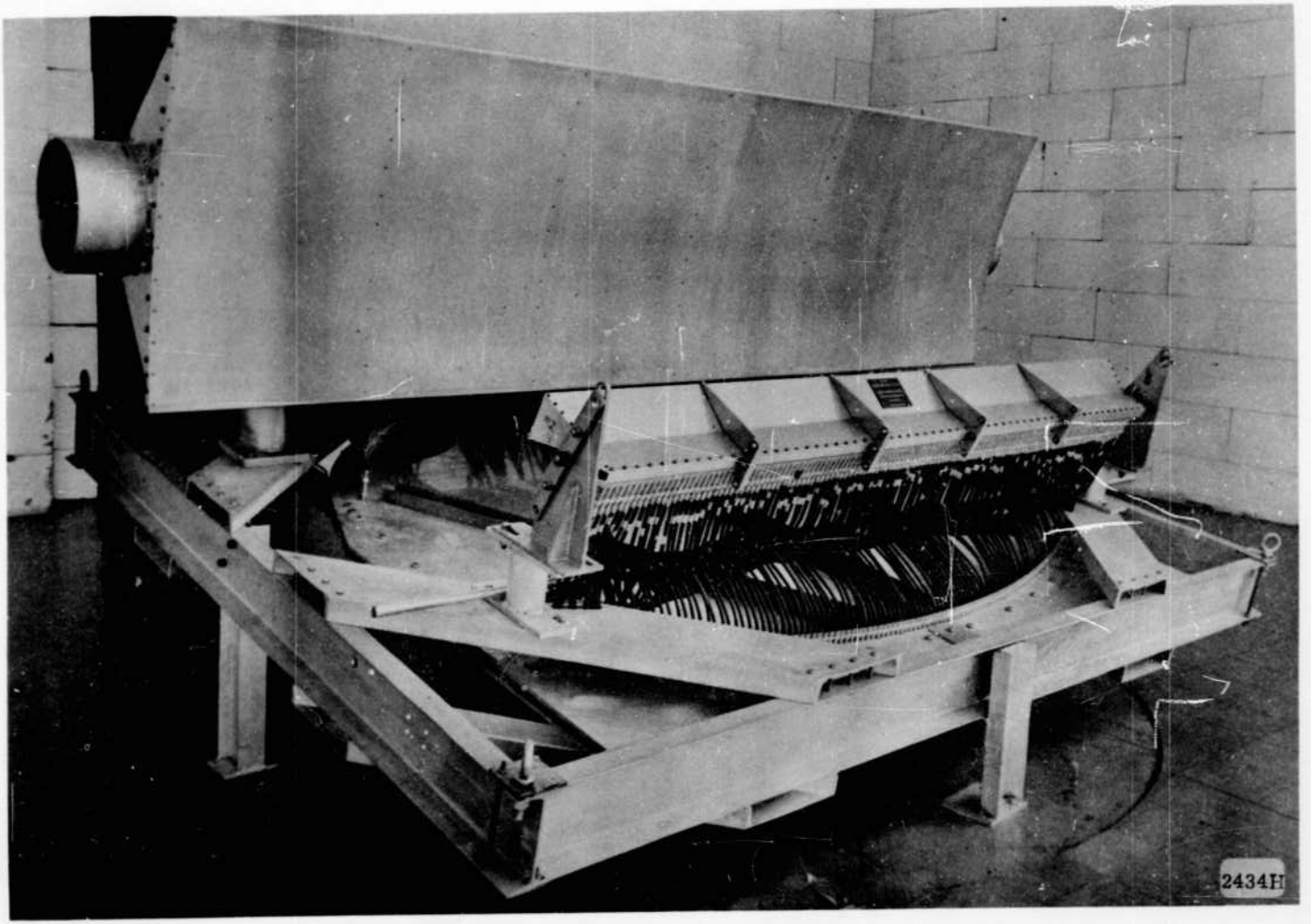

Figure 9-2. Front View of Completed MUBIS Antenna System

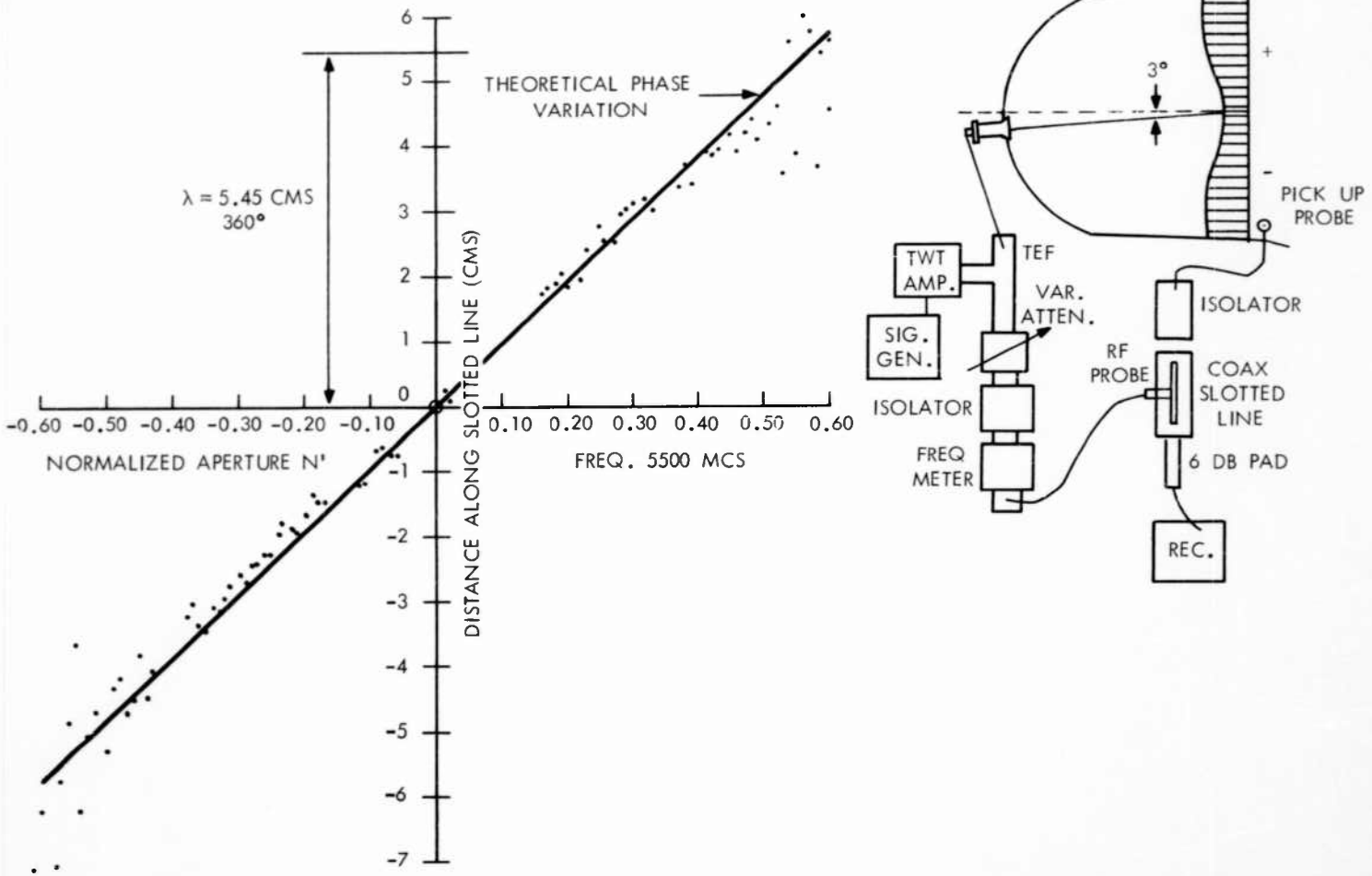

Figure 9-3. Measured Phase Variation Along Line Source

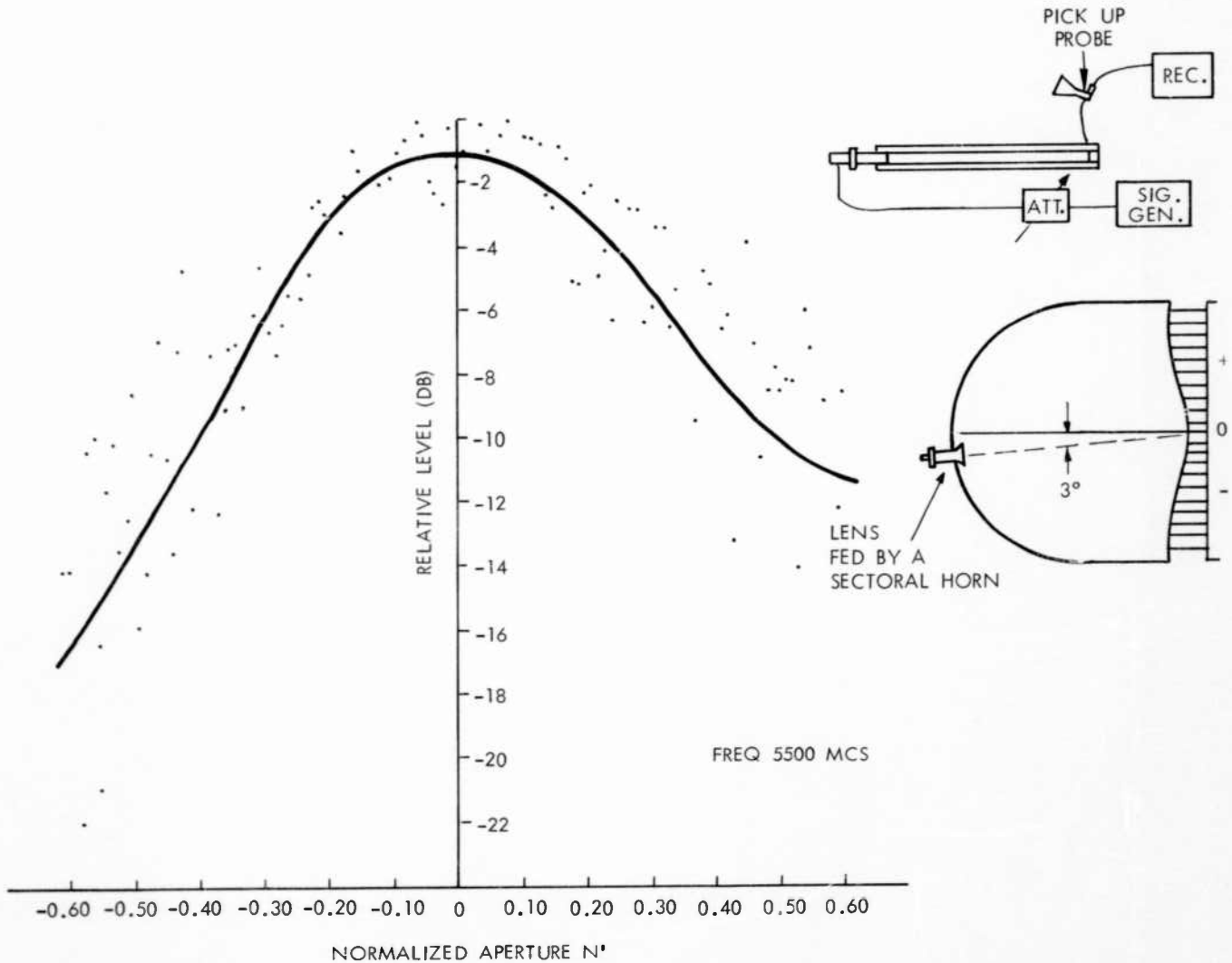

Figure 9-4. Measured Amplitude Distribution Along Line Source

Degrees Shown for Scale Purposes Only
Peak of Sum Beam at Azimuth Scan Angle: -35°
Frequency: 5250 Mcs

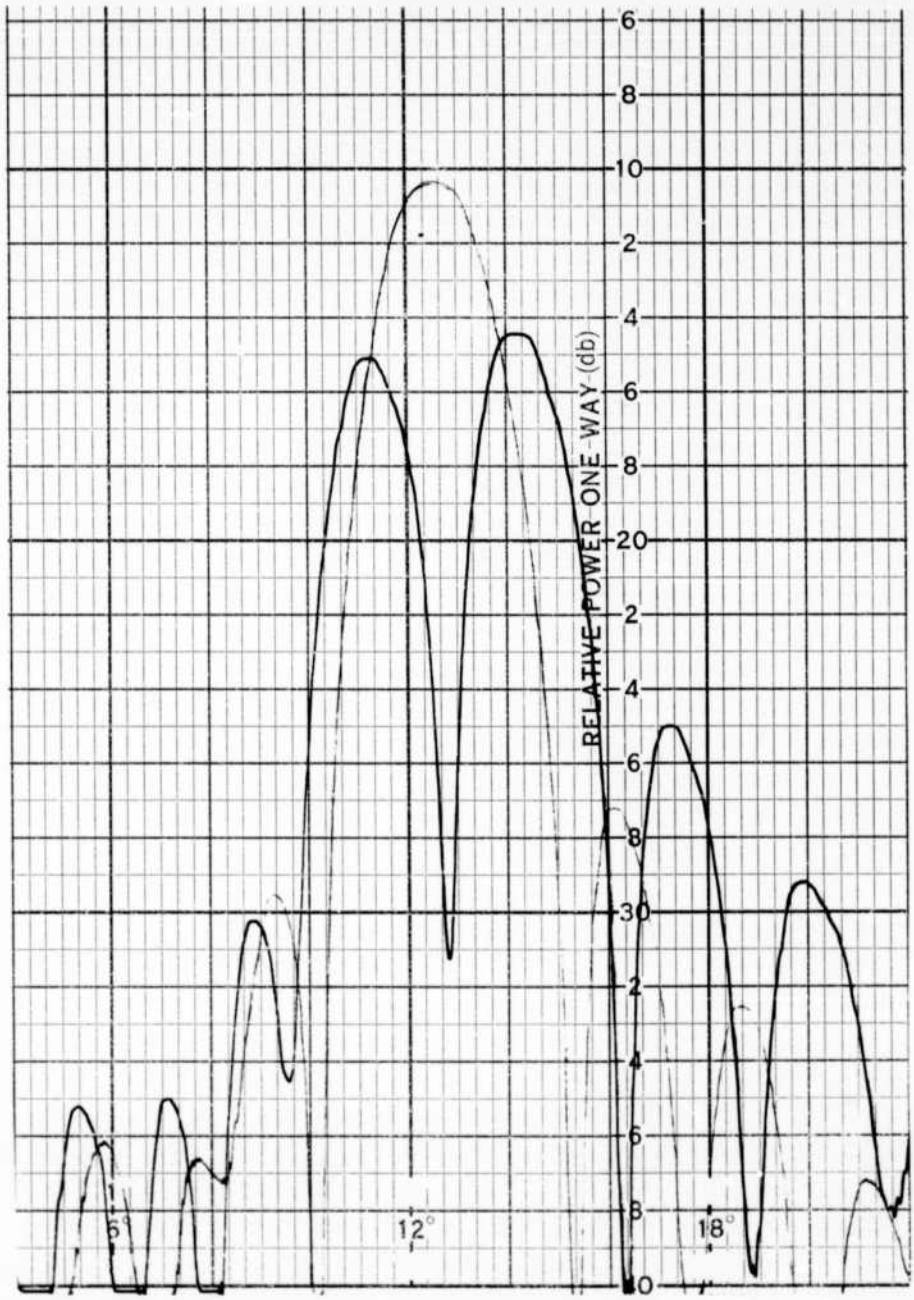

Figure 9-5. Typical Sum And Difference Patterns

Degrees Shawn for Scale Purpases Only
Peak af Sum Beam at Azimuth Scan Angle: -14.5°
Frequency: 5250 Mcs

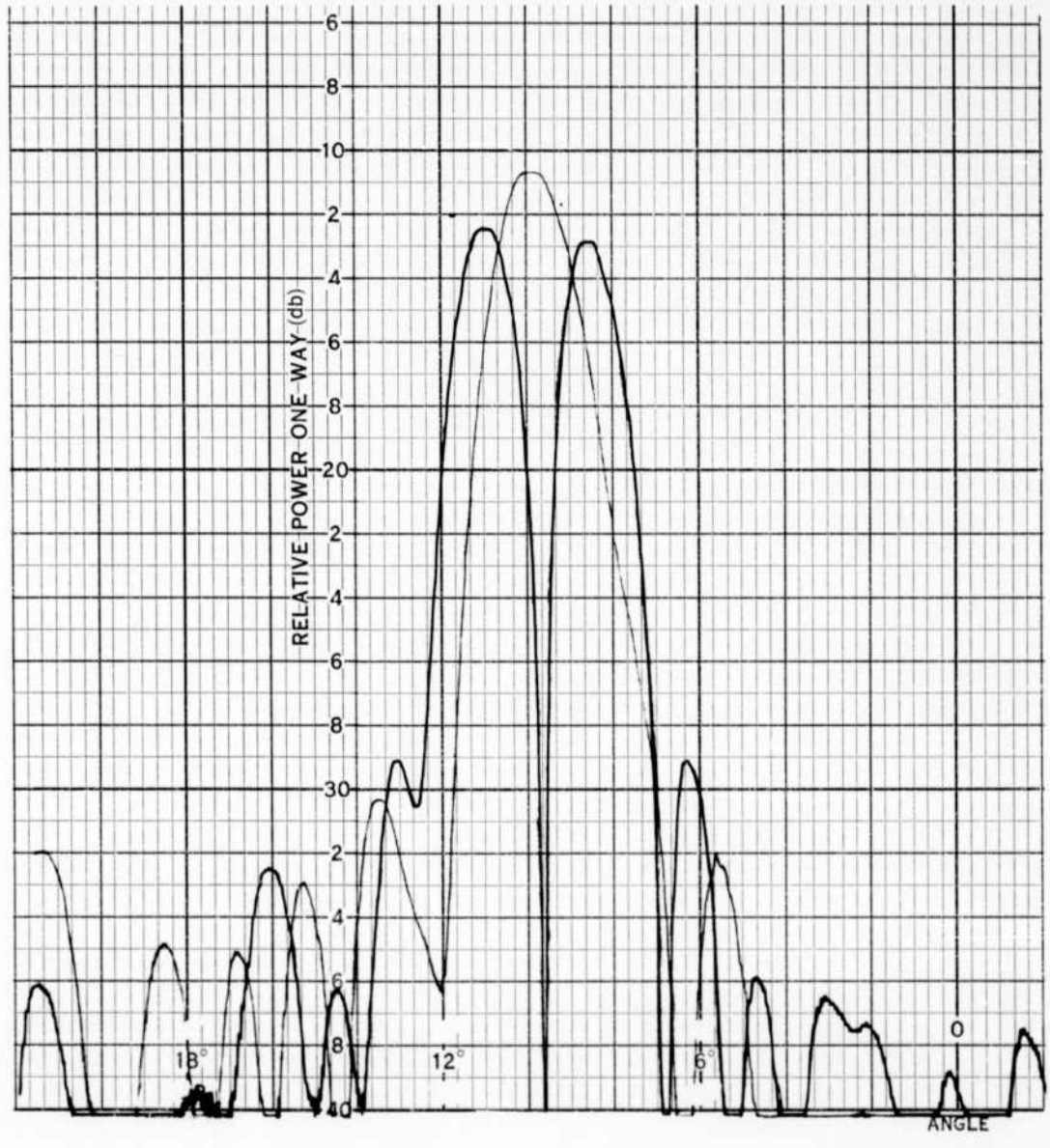

Figure 9-6. Typical Sum And Difference Pattems

Degrees Shown far Scale Purposes Only
Peak of Sum Beam at Azimuth Scan Angle: 0°
Frequency: 5250 Mcs

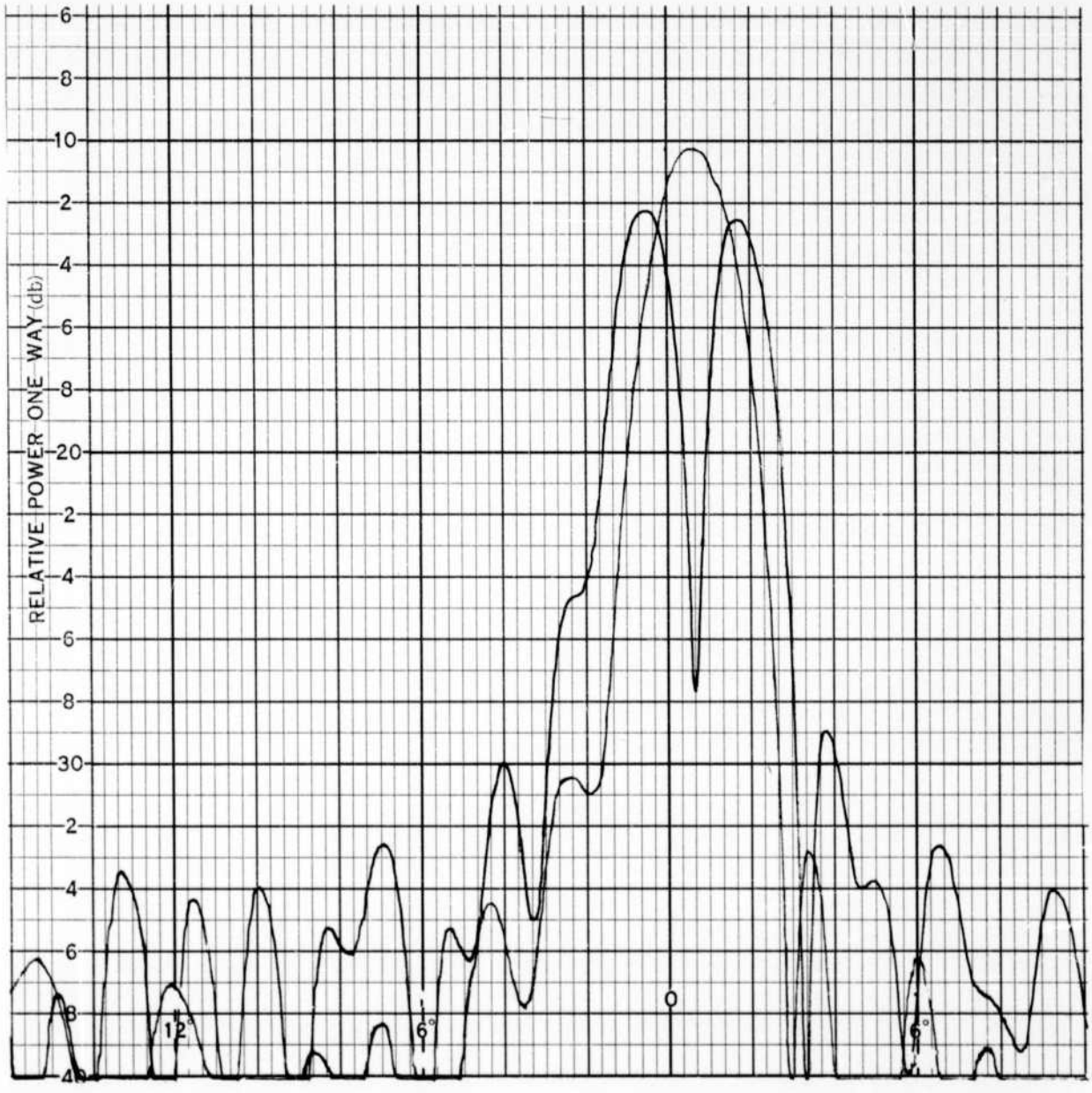

Figure 9-7. Typical Sum And Difference Patterns

Degrees Shawn for Scale Purposes Only
Peak of Sum Beam at Azimuth Scan Angle: +16°
Frequency: 5250 Mcs

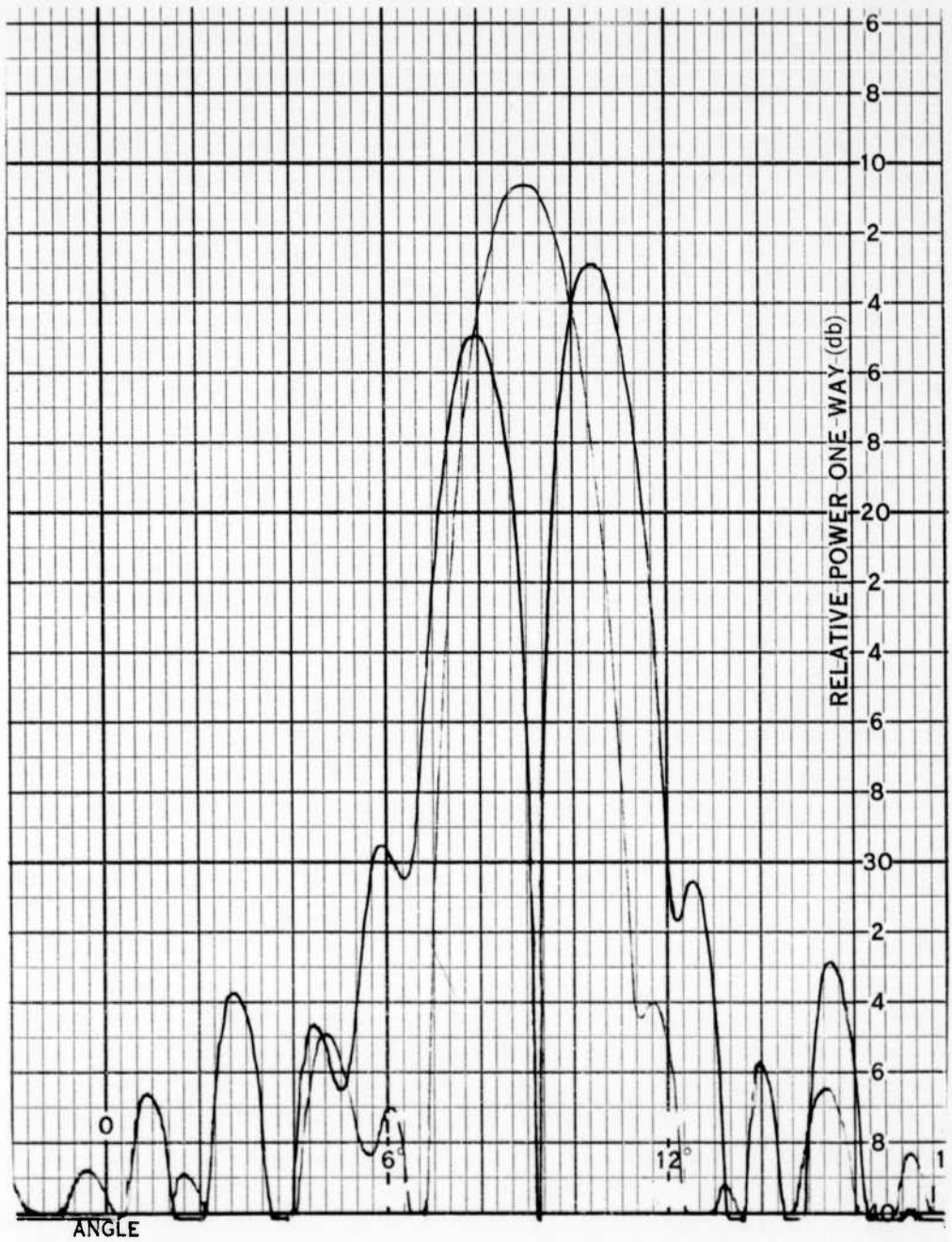

Figure 9-8. Typical Sum And Difference Patterns

Degrees Shown for Scole Purposes Only
Peak of Sum Beam ot Azimuth Scan Angle: +36°
Frequency: 5250 Mcs

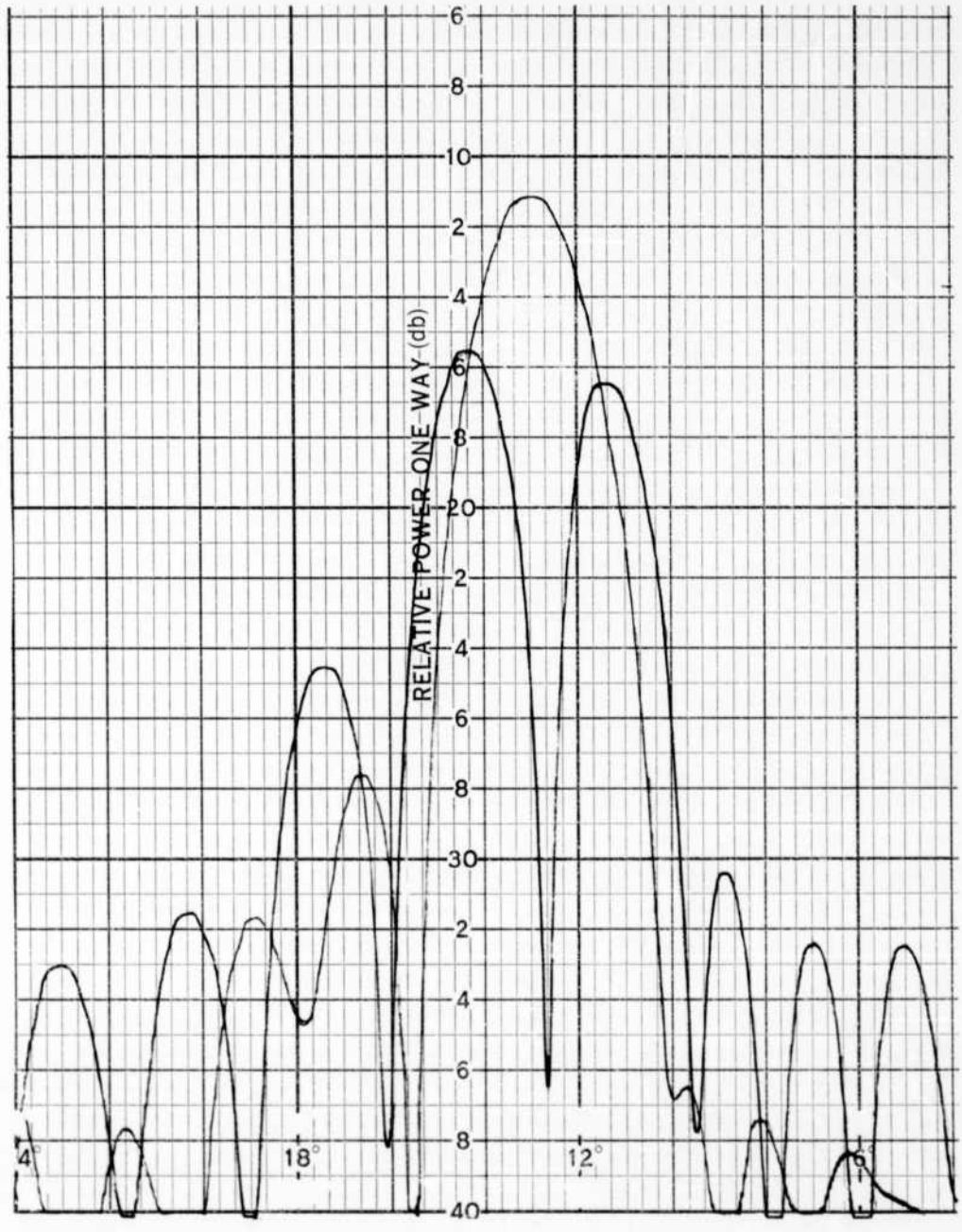

Figure 9-9. Typical Sum And Difference Pottems

Degrees Shown for Scale Purposes Only
Peak of Sum Beam at Azimuth Scan Angle: -15°
Frequency: 5500 Mcs

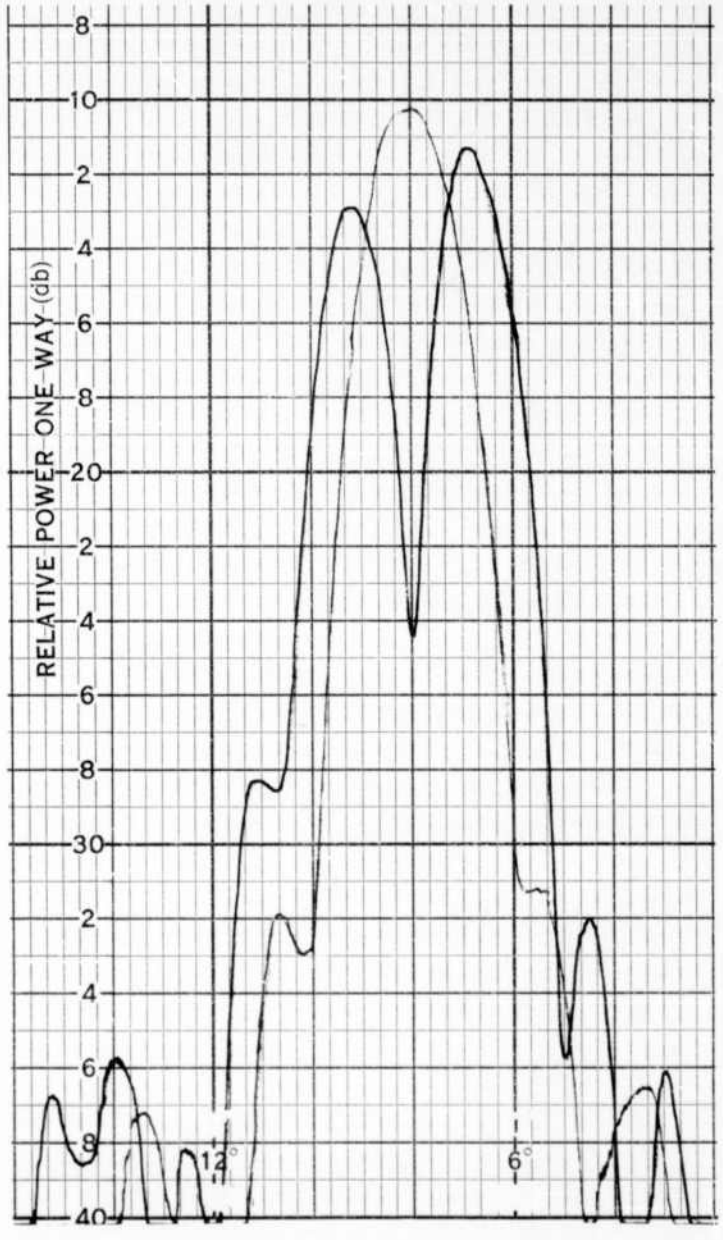

Figure 9-10. Typical Sum And Difference Patterns

Degrees Shown for Scale Purposes Only
Peak of Sum Beam at Azimuth Scan Angle: -2.5°
Frequency: 5500 Mcs

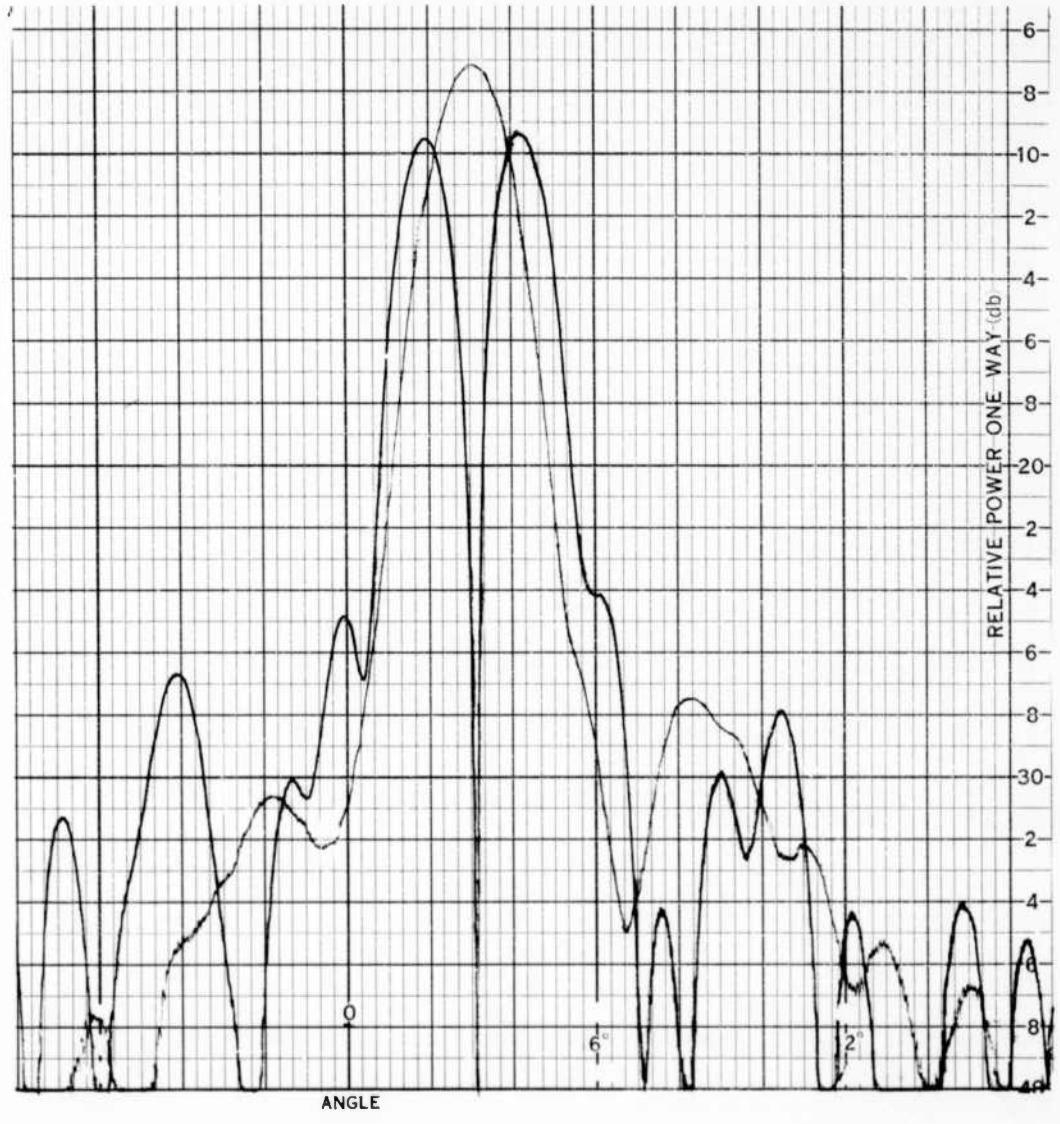

Figure 9-11. Typical Sum And Difference Patterns

Degrees Shawn far Scale Purposes Only
Peak af Sum Beam at Azimuth Scan Angle: +16°
Frequency: 5500 Mcs

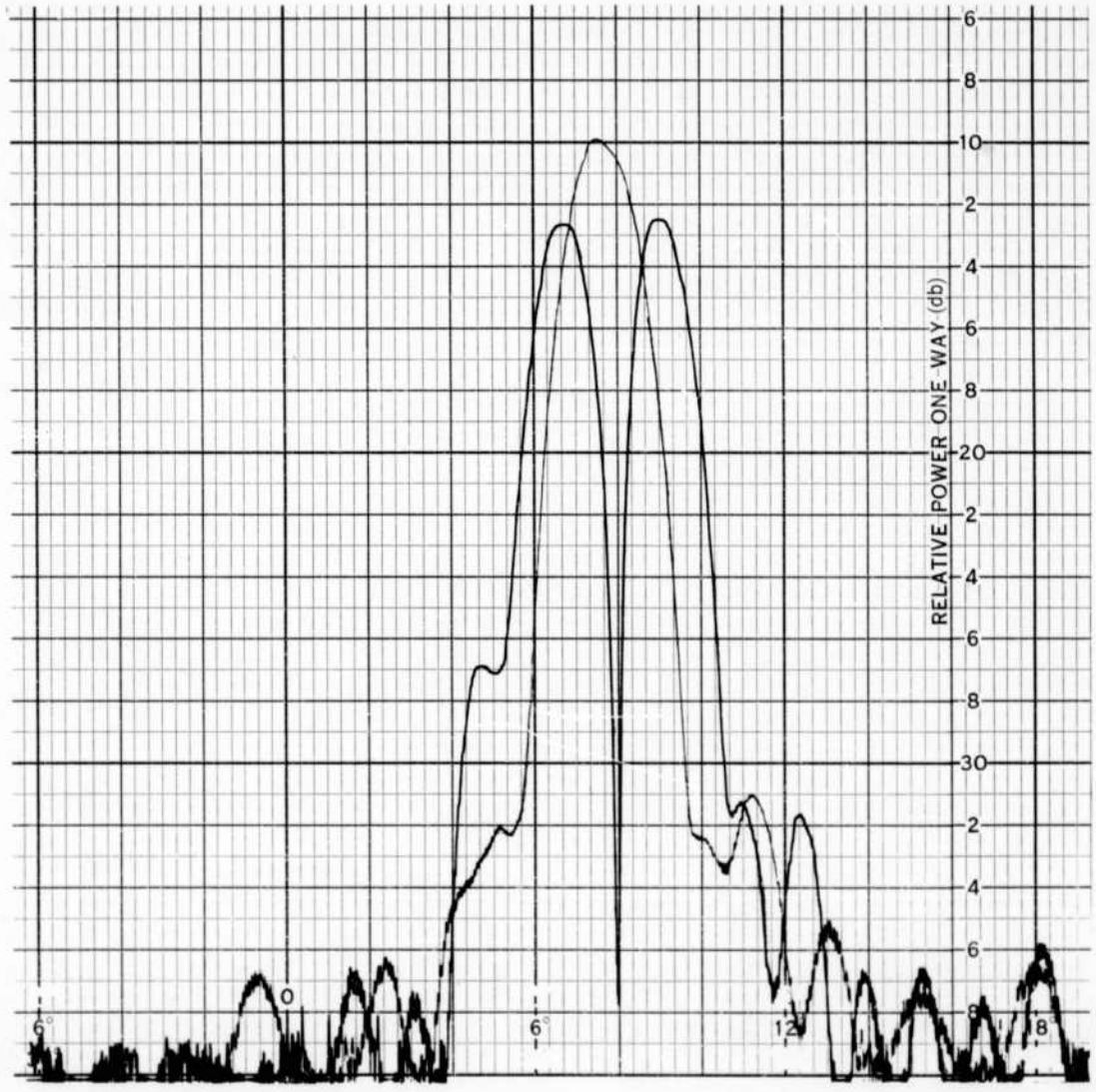

Figure 9-12. Typical Sum And Difference Patterns

Degrees Shown for Scale Purposes Only
Peak of Sum Beam at Azimuth Scan Angle: +35°
Frequency: 5500 Mcs

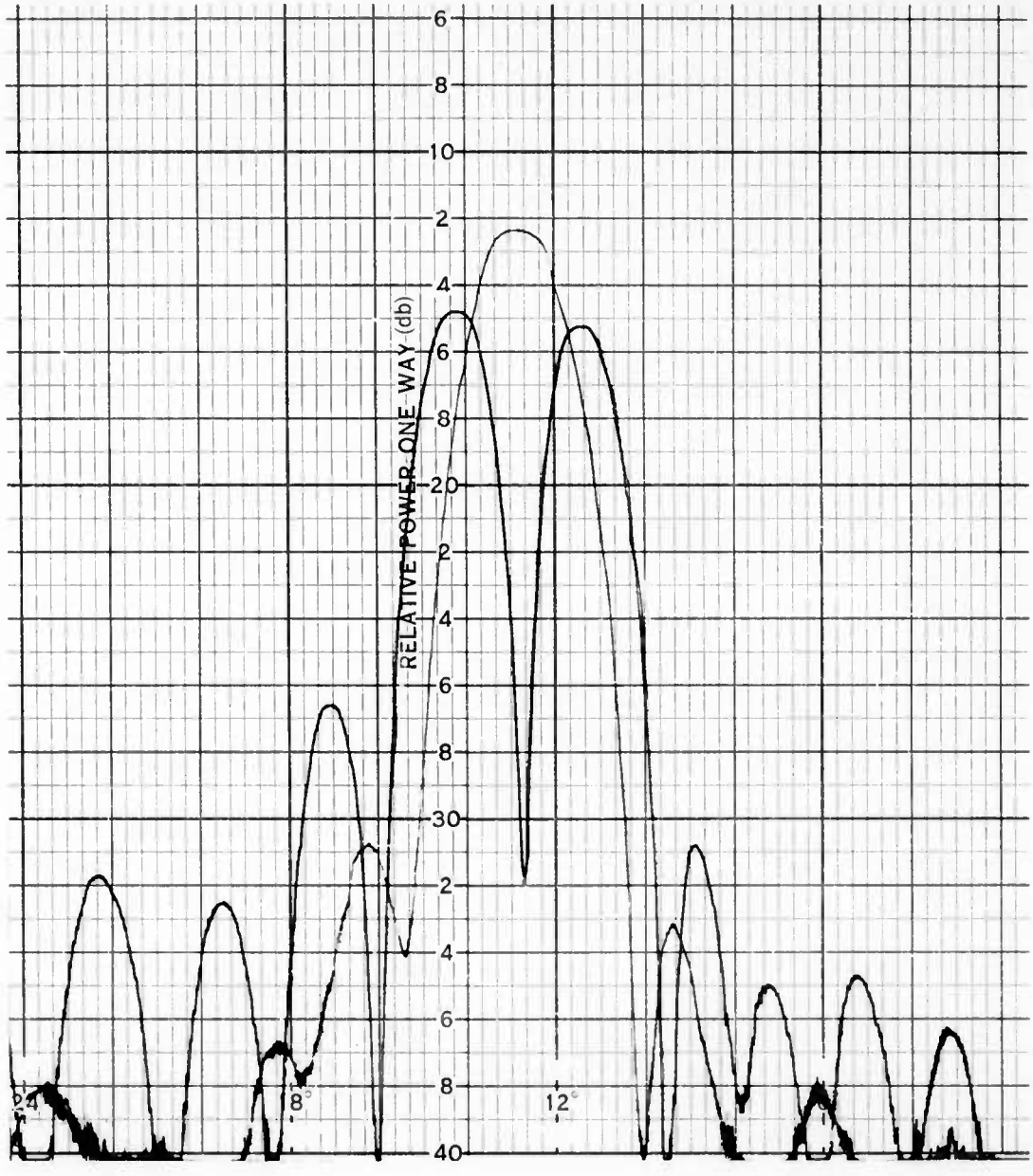

Figure 9-13. Typical Sum And Difference Patterns

Degrees Shown for Scale Purposes Only
Peak of Sum Beam at Azimuth Scan Angle: -35°
Frequency: 5750 Mcs

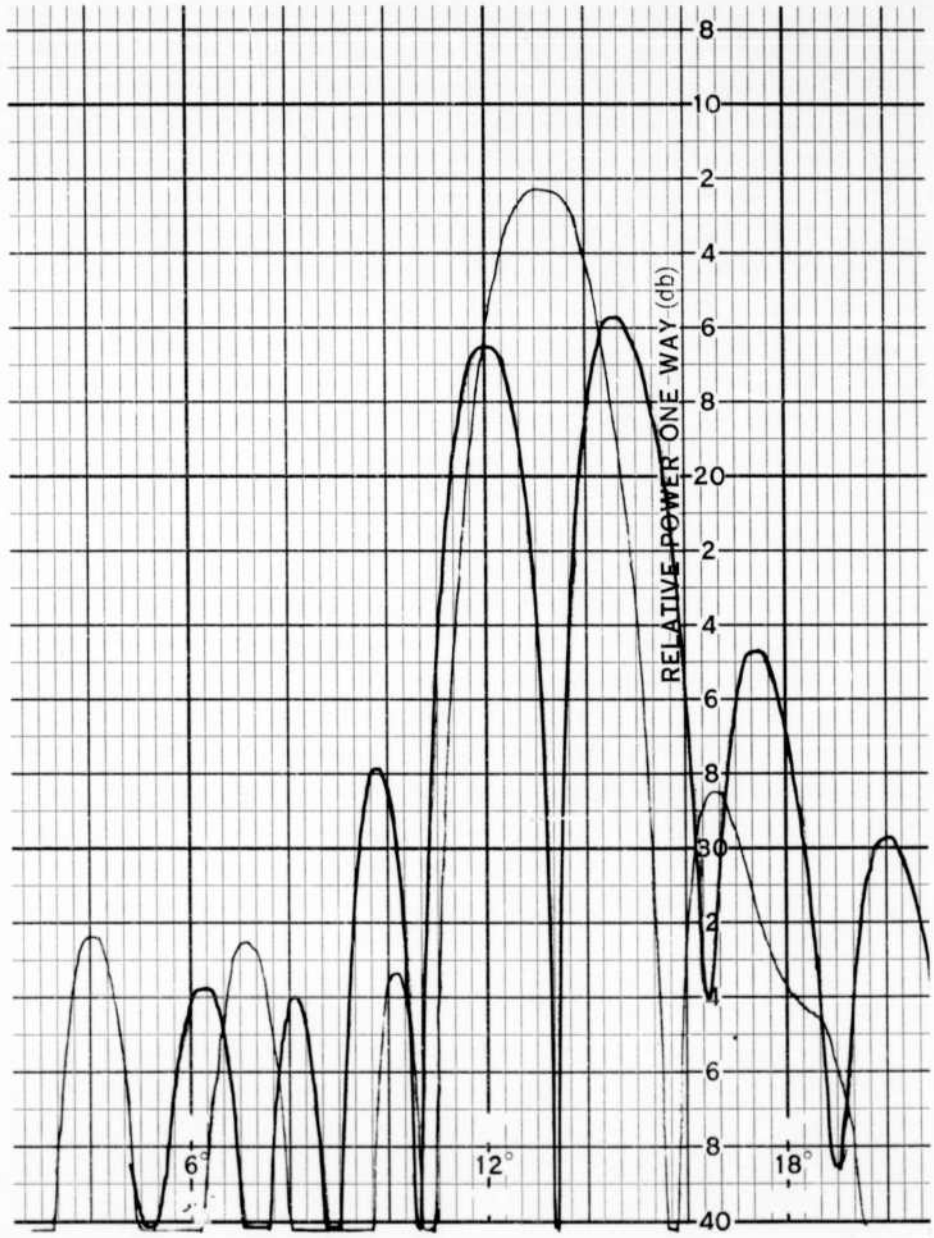

Figure 9-14. Typical Sum And Difference Patterns

Degrees Shown for Scale Purposes Only
Peak of Sum Beam at Azimuth Scan Angle: -14.5°
Frequency: 5750 Mcs

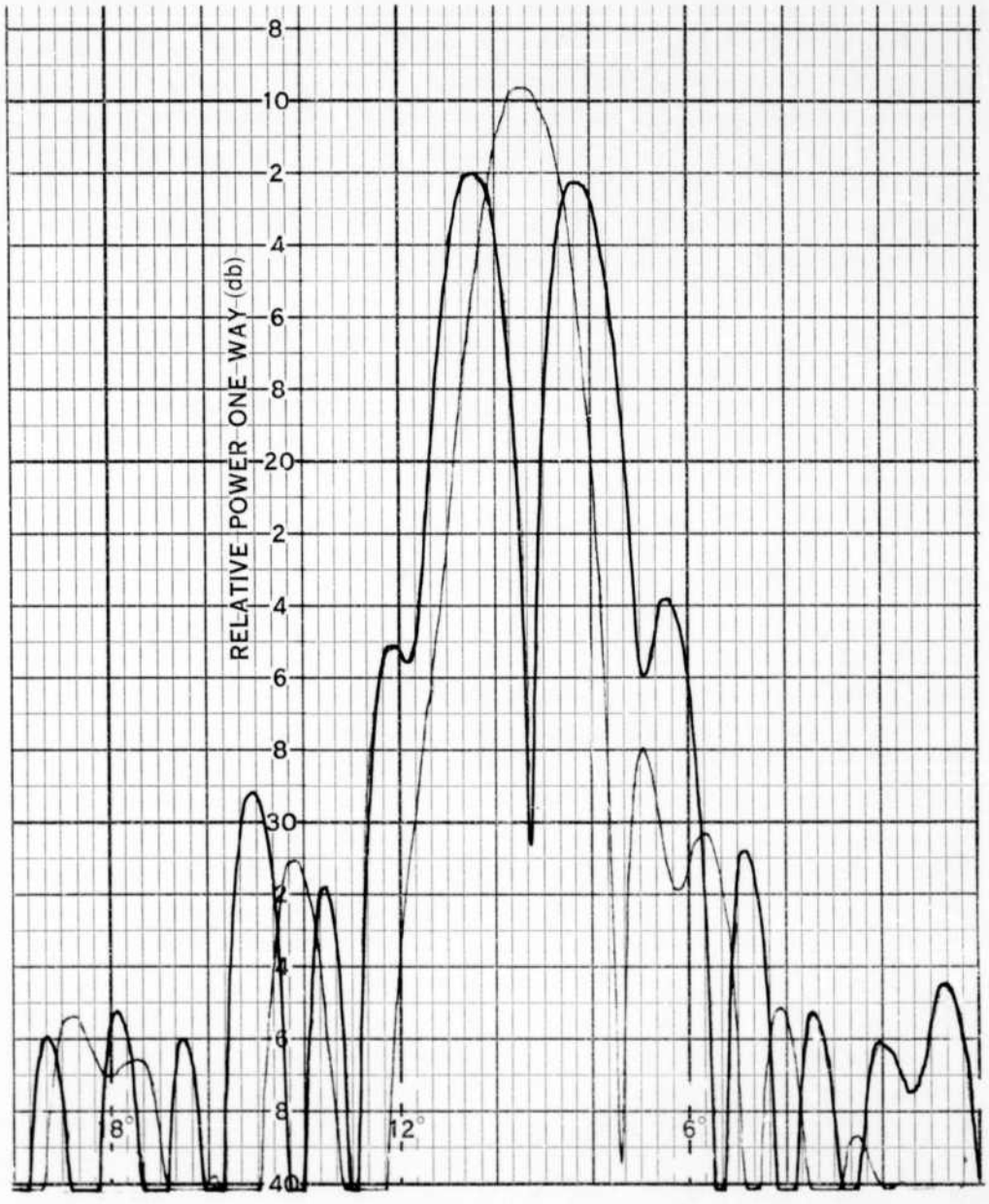

Figure 9-15. Typical Sum And Difference Patterns

Degrees Shown far Scale Purposes Only
Peak of Sum Beam at Azimuth Scan Angle: 0°
Frequency: 5750 Mcs

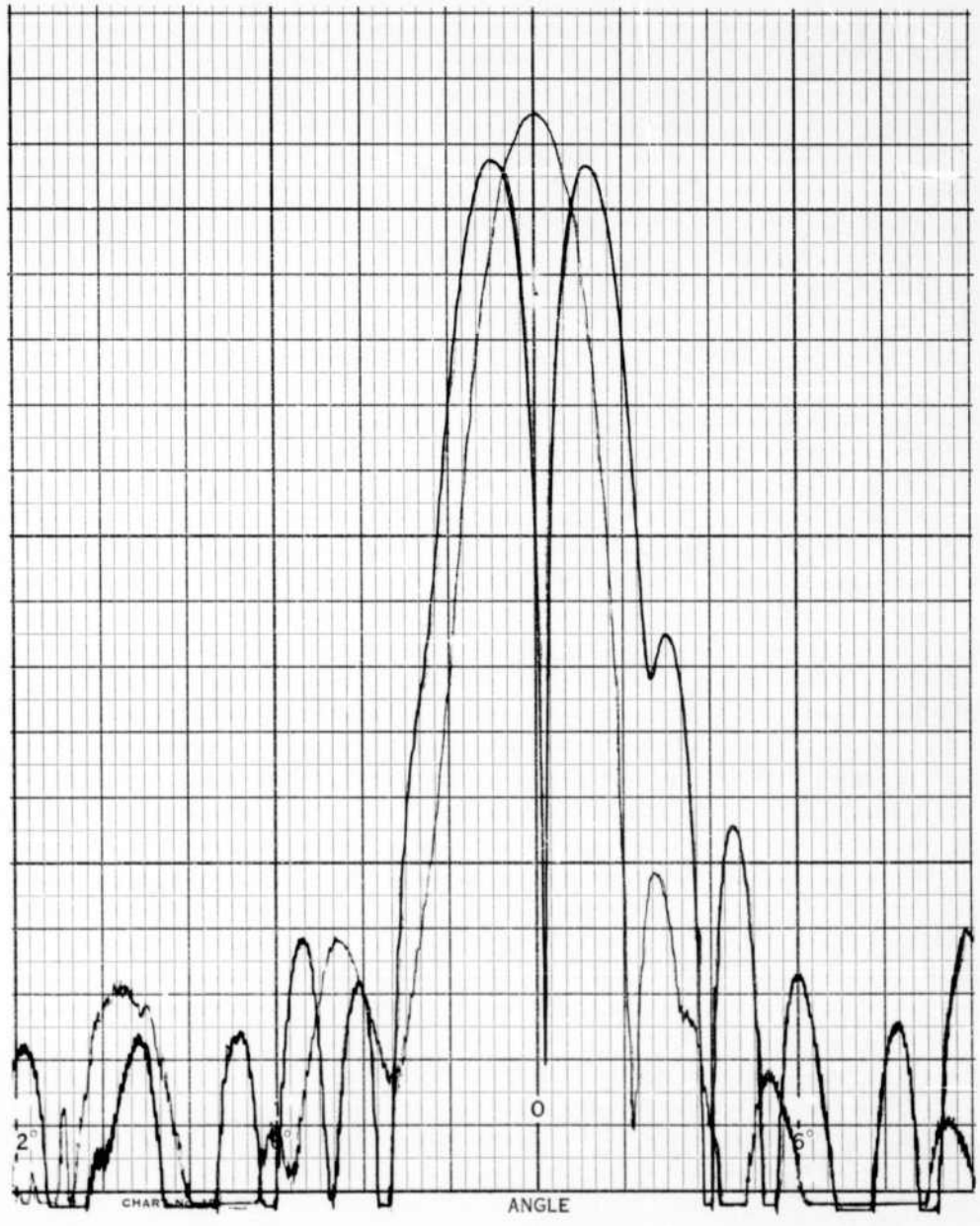

Figure 9-16. Typical Sum And Difference Patterns

Degrees Shown for Scale Purpose Only
Peak of Sum Beam at Azimuth Scan Angle: +16°
Frequency: 5750 Mcs

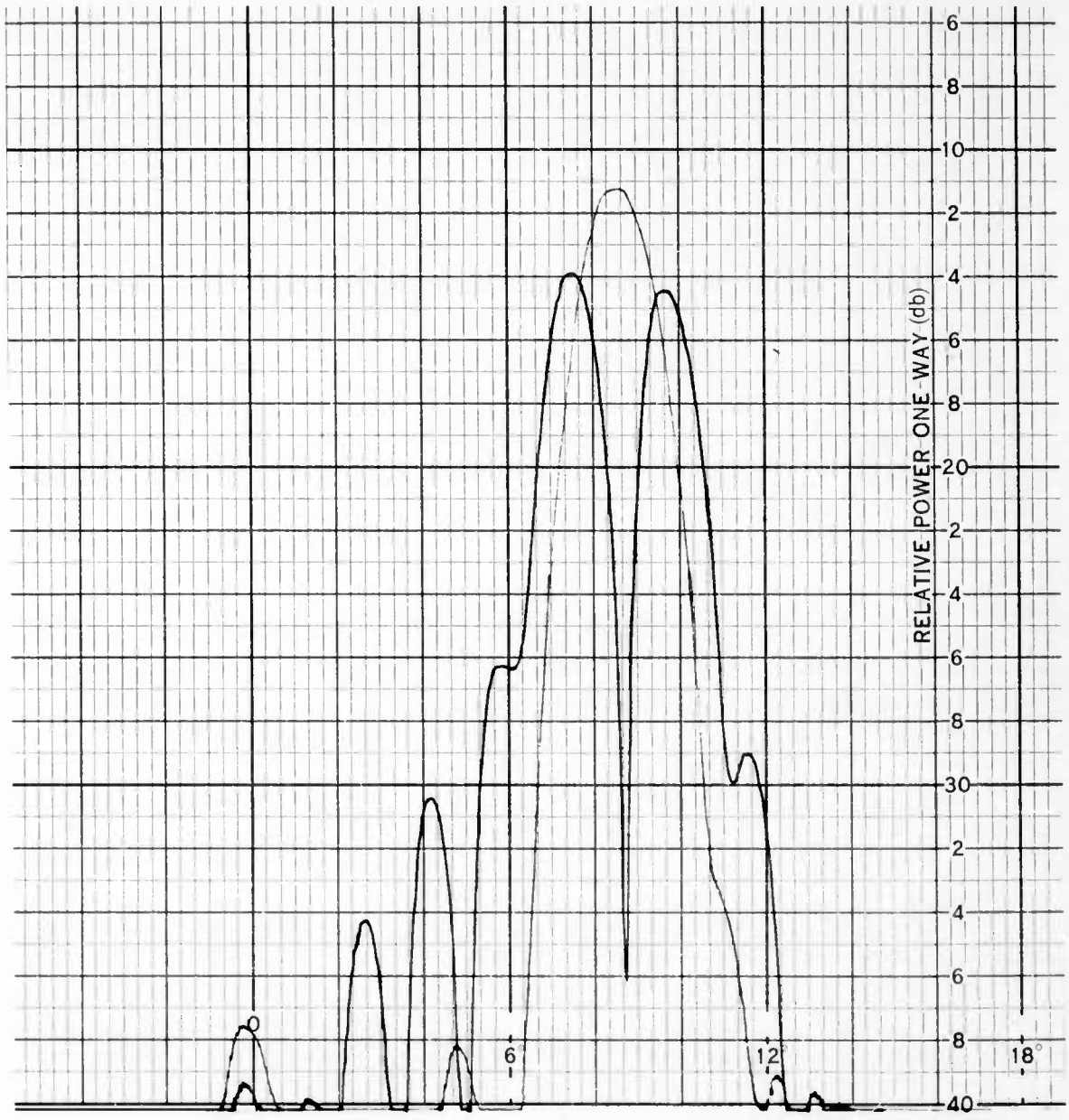

Figure 9-17. Typical Sum And Difference Pottems

Degrees Shown for Scale Purposes Only
Peok of Sum Beam at Azimuth Scon Angle: +35°
Frequency: 5750 Mcs

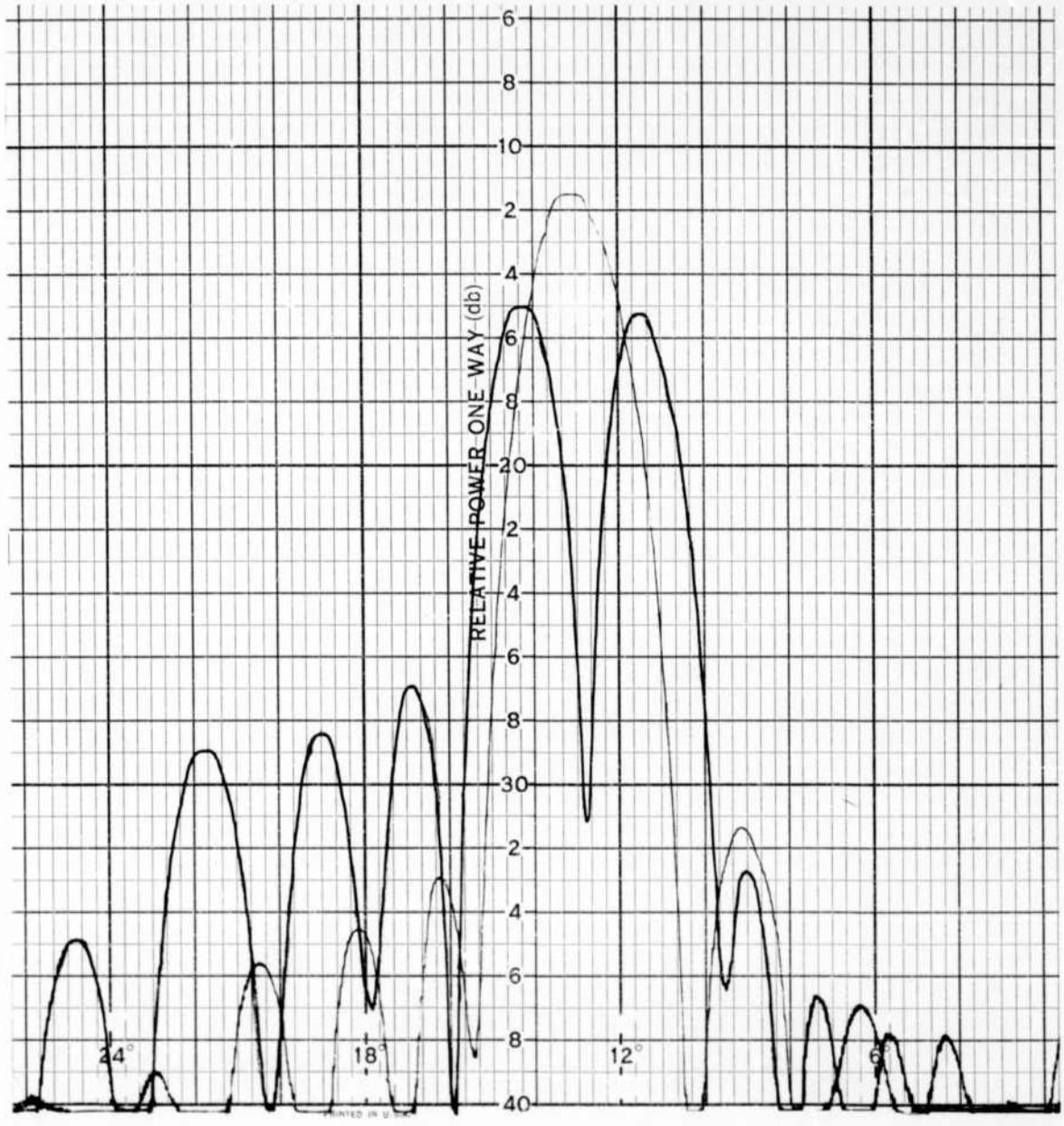

Figure 9-18. Typicol Sum And Difference Patterns

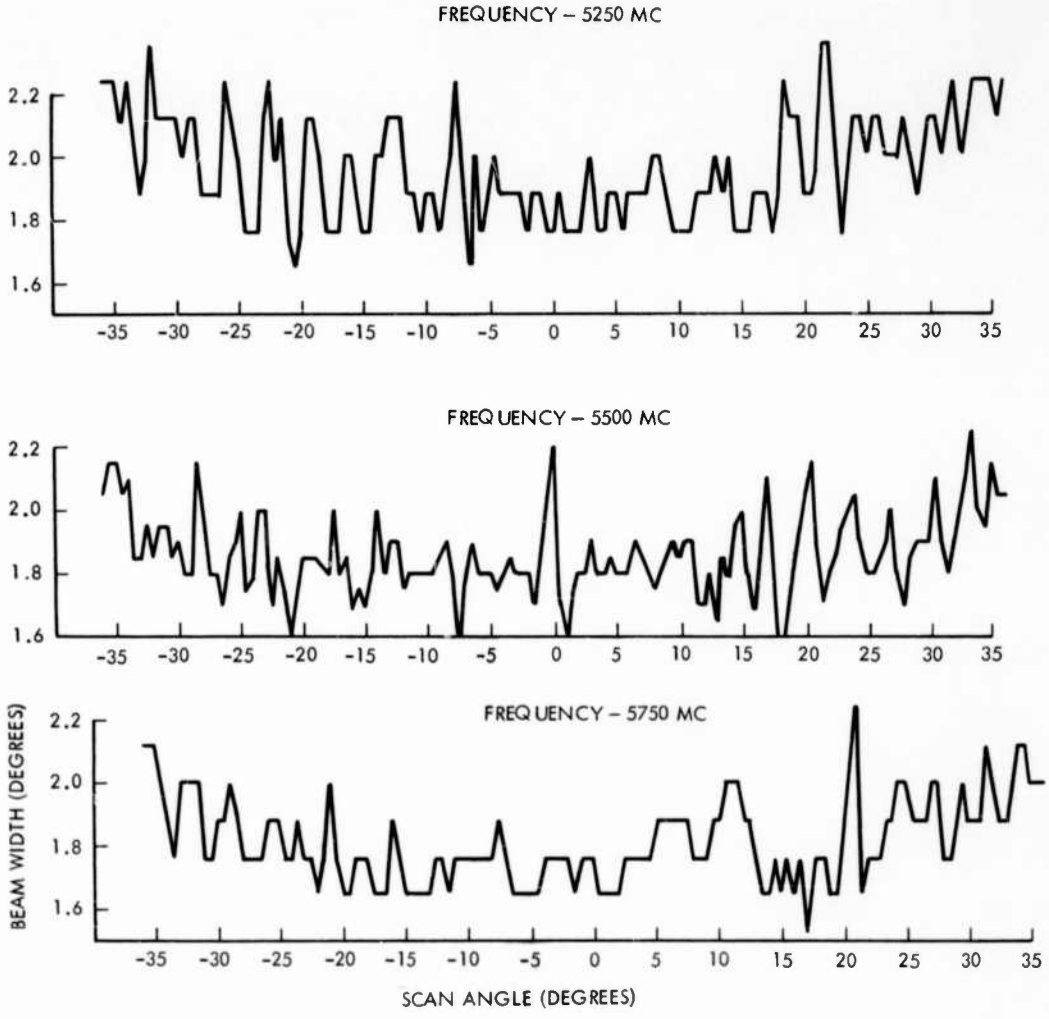

Figure 9-19. Sum Pattern Beamwidth Variation with Scan Angle

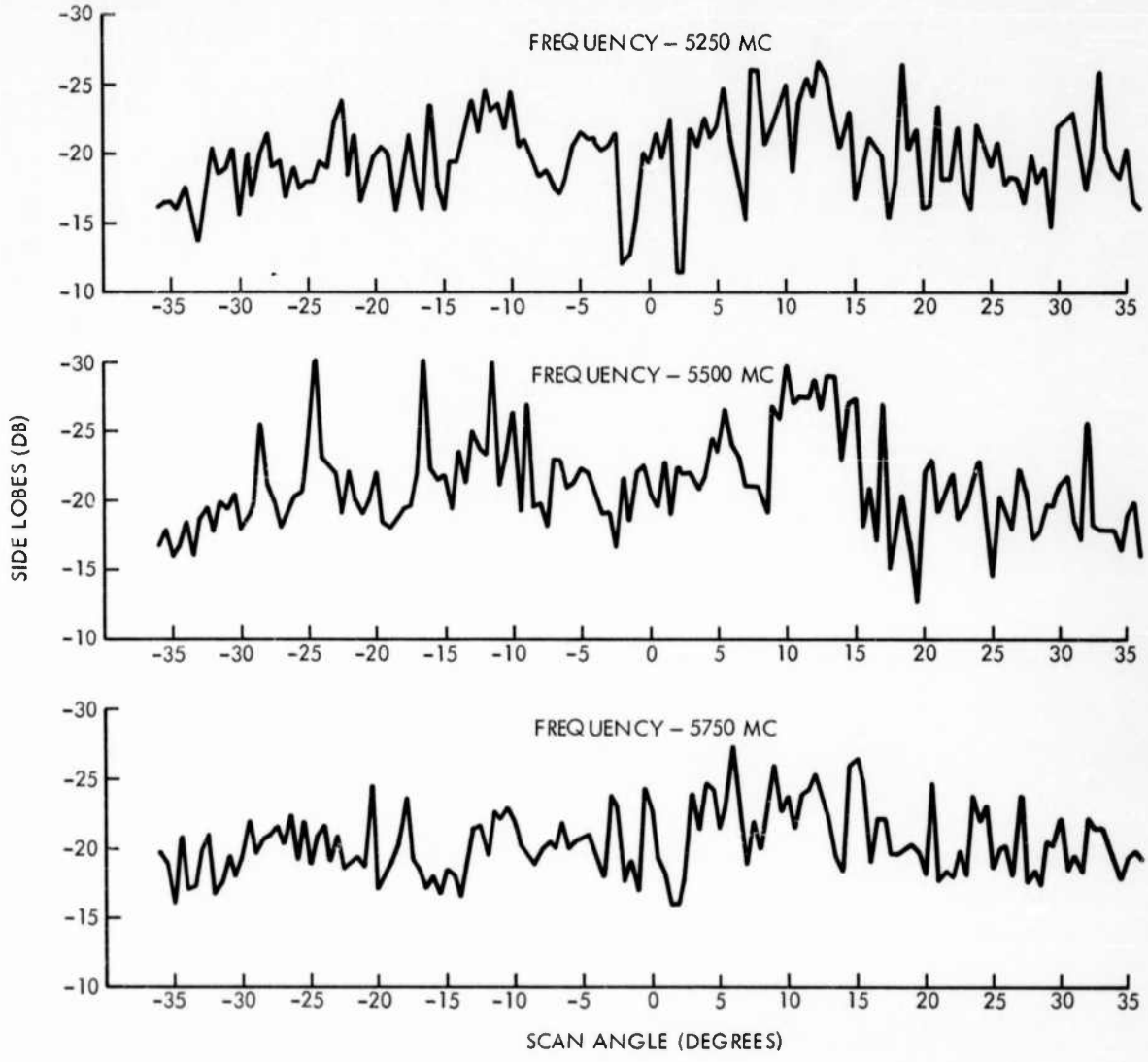

Figure 9-20. Sum Pattern Side Lobe Level Variation with Scan Angle

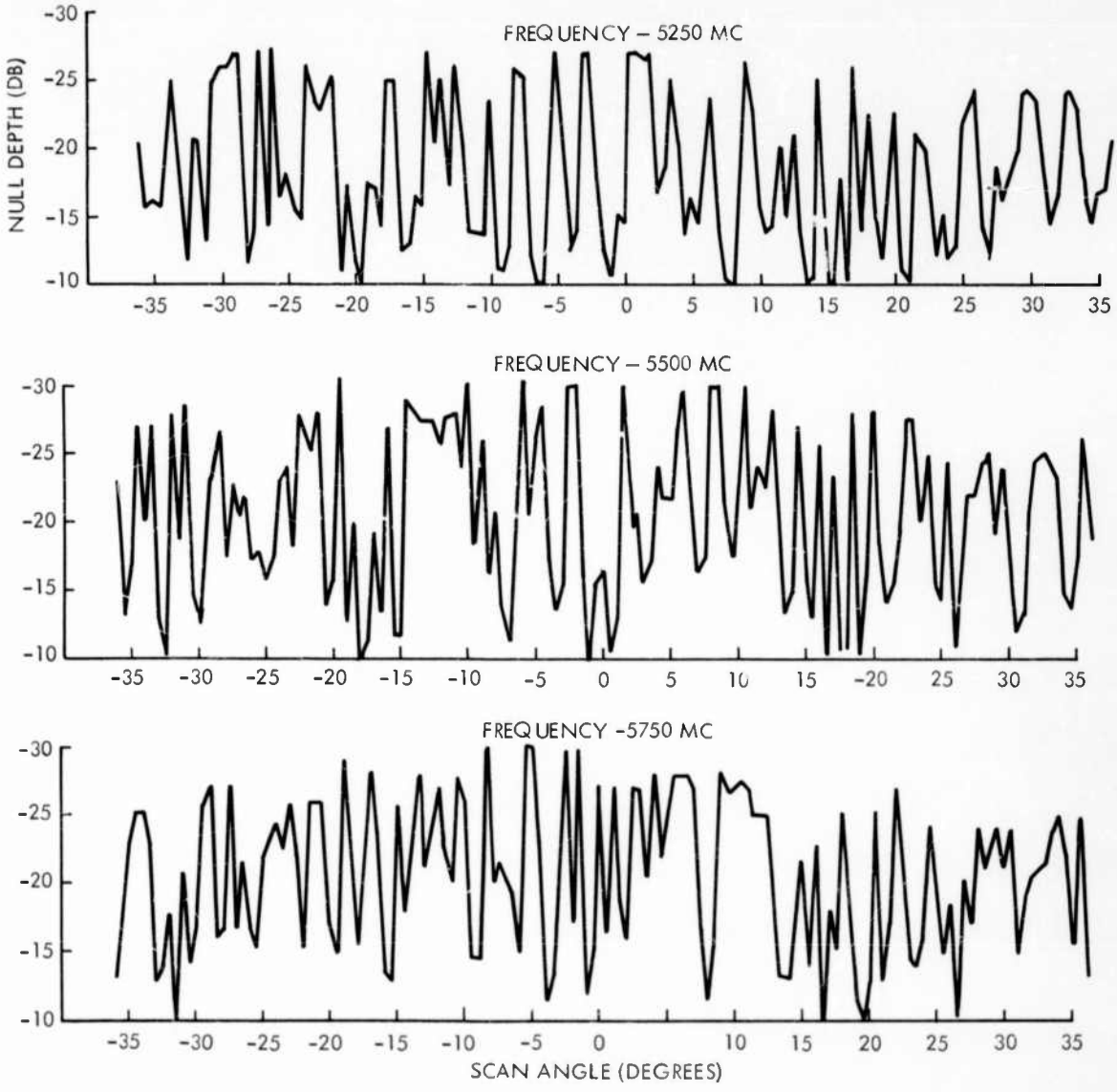

Figure 9-21. Difference Pattern Null Depth Variation with Scan Angle

Degrees Shown for Scale Purposes Only
Azimuth Position: -5°
Scon Limits: -4.5° to -5.5°
Frequency: 5500 Mcs

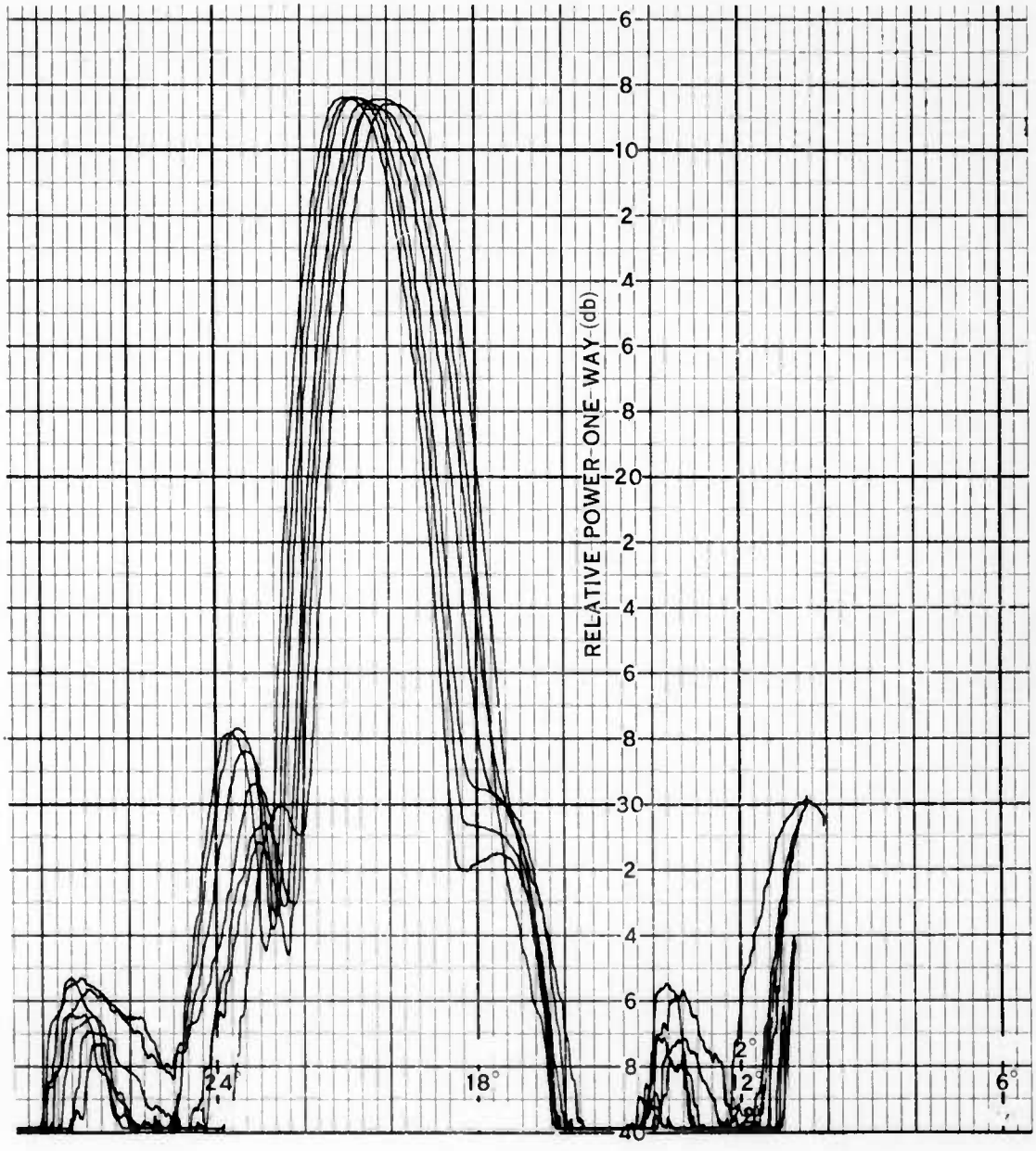

Figure 9-22. Voriotion of Sum Mode Radiotion Pattems with Scon Angle

Degrees Shown for Scale Purposes Only
Azimuth Position: -5°
Scan Limits: -4.5° to -5.5°
Frequency: 5500 Mcs

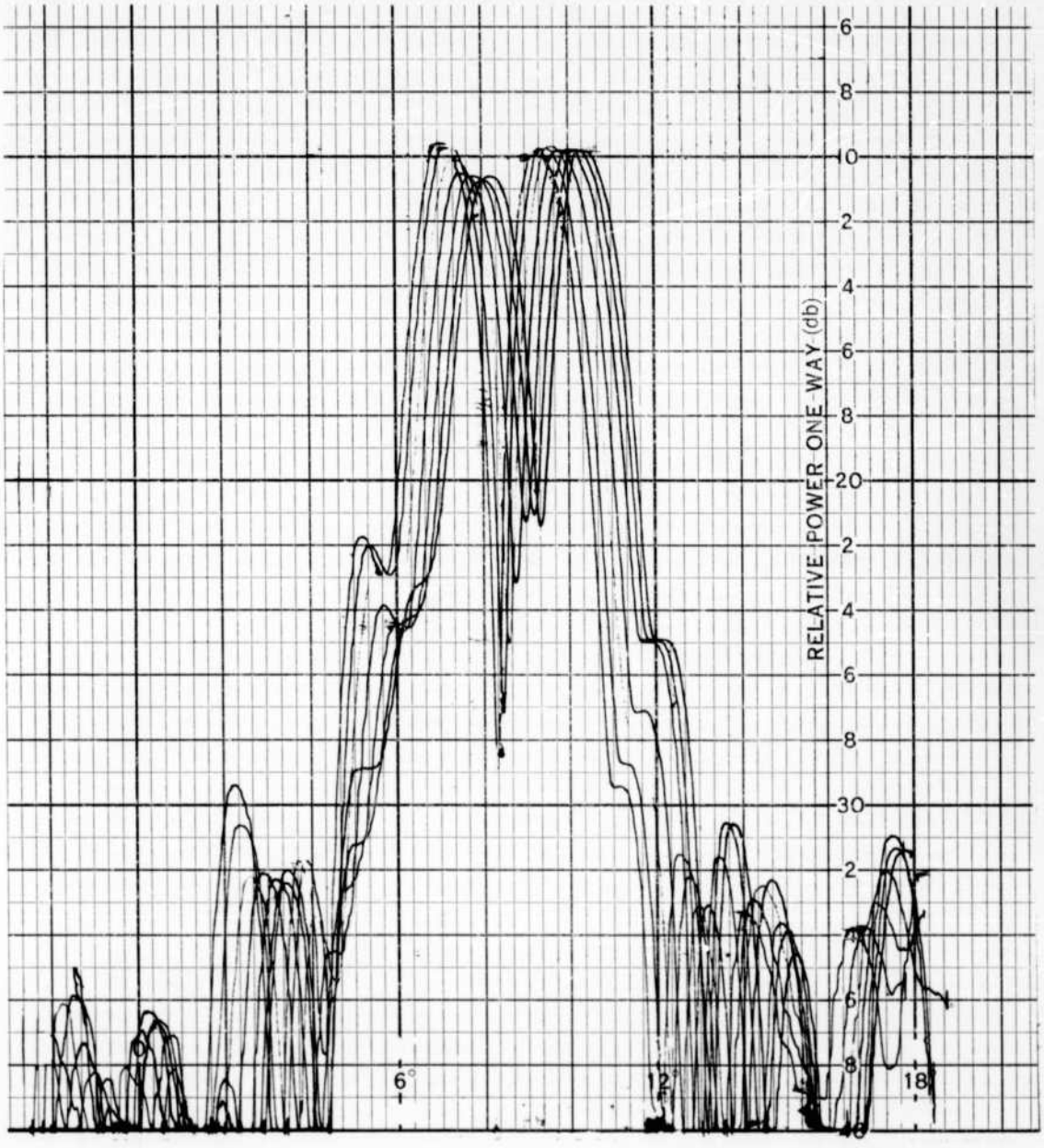

Figure 9-23. Variation of Difference Mode Patterns with Scan Angle

involved, the phases of the reflections caused by the output cable mismatches as seen at the focal arc change very rapidly with position and at some points can amount to phase differences as great as 30 degrees between adjacent probes. With cable VSWR's as high as 1.8 to 1, the resultant excitation appearing at each probe is altered from its original desired value. Since the scanner horn intercepts either 10 or 11 probes on the focal arc, the resultant amplitude and phase distribution appearing across this 10 or 11-probe aperture can be appreciably perturbed. This perturbation is further aggravated because the aperture is fed from the scanner through the additional mismatches of the input cables and is also affected by the mutual coupling between the probes. Therefore, the variations in the radiation pattern characteristics can occur very rapidly as a function of scan because the path lengths through cables and parallel plate transmission lines are usually on the order of 60λ to 80λ and the mismatches at each scan position occur at different points along these paths. Figures 9-22 and 9-23 indicate the rapid variation that can occur as a function of scan. The sum pattern, Figure 9-22, shows a definite increase in sidelobe level and slight variations in beam width. Each pattern represents a change in scan angle of 1/6 degree, and the series of patterns represents a total scan of only 1 degree. Variations of the difference pattern null depth and sidelobe level is shown in Figure 9-23 for the same scan interval and at the same scan position. In addition, there can also be seen in this figure a difference in the relative levels between the two difference lobe peaks. This difference also varied with scan angle and indicated an amplitude unbalance as well as a phase asymmetry in the two signals appearing in the ports of the monopulse hybrid. In an amplitude monopulse system, this branch amplitude asymmetry causes a boresight shift, which is an error in the indicated target angle. A branch phase asymmetry causes incomplete cancellation of the signals appearing in the two arms of the monopulse comparator and consequently prevents the difference signal from going to zero. By itself a branch phase asymmetry does not cause a boresight shift. However, the combination of a branch phase asymmetry β and a channel phase difference ϕ does produce a boresight shift. A channel phase difference ϕ may be defined as the relative phase shift of the difference channel output with respect to the sum channel output. The effect of these two asymmetries on the

accuracy of the idealized MUBIS antenna is shown in Figure 9-24. This shows a plot of the error factor curves for the idealized MUBIS system for both types of asymmetries. Since the maximum observed unbalance of the difference signal as observed in the radiation patterns amounted to about 2. 5 db, the boresight shift expected is about 0. 115 degrees. Since the channel phase difference and the magnitude of the branch phase asymmetry are not known, no estimate of the boresight shift due to these asymmetries could be made.

The overall experimental program proved very fruitful and indicated that the combination of a coaxial probe monopulse organ pipe scanner and a two-dimensional constrained lens is feasible. The sensitivity of the system to cable mismatches precluded the experimental investigation, of the effect of "cogging errors" or the "shaping factor" on the far field radiation pattern. In considering the possible future development of such a system, the need for a stable coaxial cable assembly having a low VSWR cannot be over emphasized.

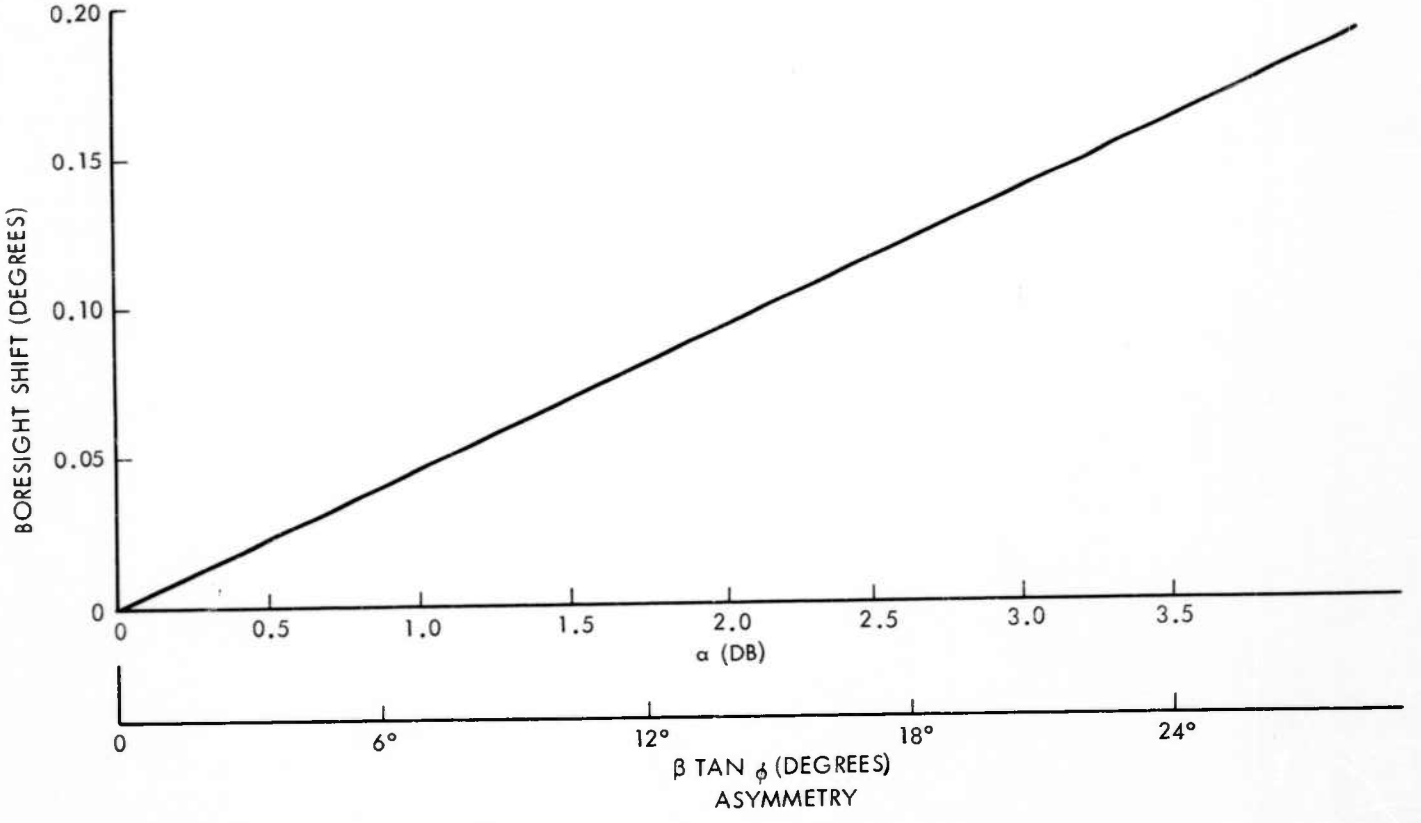

Figure 9-24. Error Factor for Idealized MUBIS System